

Universidade Estadual de Campinas

Instituto de Biologia



Gabriela Vaz Meirelles

**ESTUDOS ESTRUTURAIS E FUNCIONAIS
DAS PROTEÍNAS CINASES HUMANAS
NEK1 E NEK6**

Este exemplar corresponde à redação final
da tese defendida pelo(a) candidato (a)
GABRIELA VAZ MEIRELLES
Jörg Kobarg
Aprovada pela Comissão Julgadora.

Tese apresentada ao Instituto de Biologia da
Universidade Estadual de Campinas para a
obtenção do Título de Doutor em Biologia
Funcional e Molecular, na área de Bioquímica

Orientador: Prof. Dr. Jörg Kobarg

Campinas, 2011

**FICHA CATALOGRÁFICA ELABORADA PELA
BIBLIOTECA DO INSTITUTO DE BIOLOGIA – UNICAMP**

M478e	<p>Meirelles, Gabriela Vaz Estudos estruturais e funcionais das proteínas cinases humanas Nek1 e Nek6 / Gabriela Vaz Meirelles. – Campinas, SP: [s.n.], 2011.</p> <p>Orientador: Jörg Kobarg. Tese (doutorado) – Universidade Estadual de Campinas, Instituto de Biologia.</p> <p>1. Proteínas quinases. 2. Espalhamento a baixo ângulo. 3. Proteínas hub. 4. Redes de interações. 5. Sinalização celular. 6. Centrossomos. 7. Carcinogênese. I. Kobarg, Jörg. II. Universidade Estadual de Campinas. Instituto de Biologia. III. Título.</p> <p style="text-align: right;">(rcdt/ib)</p>
--------------	---

Título em inglês: Structural and functional studies of Nek1 and Nek6 protein kinases.

Palavras-chave em inglês: Protein kinases; Small angle scattering; Hub proteins; Protein networks; Signal transduction; Centrosomes; Carcinogenesis.

Área de concentração: Bioquímica.

Titulação: Doutor em Biologia Funcional e Molecular.

Banca examinadora: Jörg Kobarg, Carmen Veríssima Ferreira, Claudio Chrysostomo Werneck, Deborah Schechtman, Adriane Regina Todeschini.

Data da defesa: 04/03/2011.

Programa de Pós-Graduação: Biologia Funcional e Molecular.

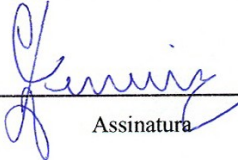
Campinas, 04 de março de 2011

BANCA EXAMINADORA

Prof. Dr. Jörg Kobarg (Orientador)


Assinatura

Profa. Dra. Carmen Veríssima Ferreira


Assinatura

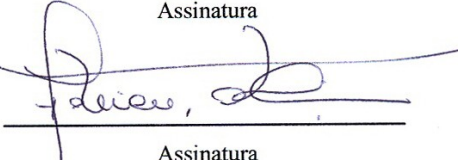
Prof. Dr. Cláudio Chrysostomo Werneck


Assinatura

Profa. Dra. Deborah Schechtman


Assinatura

Profa. Dra. Adriane Regina Todeschini


Assinatura

Prof. Dr. Ricardo José Giordano

Assinatura

Profa. Dra. Ana Carolina de Mattos Zeri

Assinatura

Prof. Dr. Celso Eduardo Benedetti

Assinatura

Aos meus pais, Joaquim e Maria de Lourdes, e ao meu irmão, Tiago, pelo incentivo, apoio e amor absolutos.

AGRADECIMENTOS

Ao Prof. Dr. Jörg Kobarg, em primeiro lugar, por ter acreditado na minha capacidade, ter me proporcionado essa grande oportunidade e, após esses quatro anos, continuar apostando no meu potencial como pesquisadora. Obrigada pelas tantas palavras de incentivo, por estar sempre disponível, por me direcionar nos momentos de dúvida, pela paciência, apoio às minhas idéias e pela liberdade oferecida na execução deste projeto. Obrigada ainda pela amizade, pelo forró e por gostar de rock!

À Eugênia, pelo imenso cuidado com a organização do laboratório e de todo o nosso grupo de pesquisa, pela amizade e por me ajudar em todos os momentos que precisei.

A todos os técnicos do LNBio, Givanil Garrido, Adriana Alves, Tereza Lima, Thaís Dombroski, Bianca Pauletti, Sami Yokoo, Jackeline Zanella, Caroline Bondarik, Jaqueline Silva, Andréia Meza, Celisa Tonoli, Renata Rocha, Lilian Pino, Wanderley Pedroso, Zildene Corrêa, Gabriela Reis e Elaine Teixeira, sempre muito solícitos, responsáveis por manter nosso laboratório sempre funcionando.

Aos colaboradores, Prof. Dr. Guido Lenz, Prof. Dr. Kleber Gomes Franchini, Profa. Dra. Adriana Franco Paes Leme, Profa. Dra. Íris Torriani, Dr. Júlio César Silva, Prof. Dr. Carlos Henrique de Inácio Ramos, Prof. Dr. Mário Tyago Murakami, Prof. Dr. João Alexandre Barbosa, Profa. Dra. Sara Saad e Dra. Carla Judice, pelas discussões, ensinamentos, troca de reagentes, uso de equipamentos e suporte na execução de experimentos, de extrema importância para a realização deste trabalho. A todos os demais pesquisadores do LNBio, pela enriquecedora convivência e discussões.

À Profa. Dra. Ana Carolina de Mattos Zeri, ao Prof. Dr. Cláudio Chrysostomo Werneck e à Profa. Dra. Deborah Schechtman, pela disponibilidade e pela valiosa contribuição na minha qualificação.

Aos membros da banca, Profa. Dra. Carmen Veríssima Ferreira, Prof. Dr. Cláudio Chrysostomo Werneck, Profa. Dra. Deborah Schechtman, Profa. Dra. Adriane Regina Todeschini, Prof. Dr. Ricardo José Giordano, Profa. Dra. Ana Carolina de Mattos Zeri e Prof. Dr. Celso Eduardo Benedetti, por terem aceitado participar da avaliação deste trabalho.

Aos meus queridos amigos do grupo BMO, Kaliandra, Marcos Alborghetti, Daniel Lanza, Daniel M. T. (Oráculo), Gustavo Bressan, Alexandre e Marcel, que me

receberam tão bem e me ajudaram tanto desde o início, e aos novos amigos do grupo, Priscila Zenatti, Marcos (Toty), Ariane, Ângela, Germanna, Deivid, Daniel Saito, Camila, Felipe e Gustavo Camacho, pela grande amizade e troca de idéias. Lanza, obrigada pela parceria científica tão inspiradora (e produtiva)! Marcão, obrigada por ter sido a minha dupla dinâmica em tantos desafios no laboratório (e pelo enorme apoio e incontáveis histórias)! E como não poderia deixar de agradecer, ao Eduardo, Edmárcia, Fernanda, Mayra, Priscila Ferreira e Diogo, meus queridos “pupilos” e novos amigos integrantes do grupo das Neks!

À Jéssica, minha excelente aluna de iniciação científica, pelo tamanho esforço e dedicação a um projeto de tamanha dificuldade. Obrigada pela paciência, pelo grande empenho e pela nossa amizade!

Aos demais amigos do LNBio e Unicamp, Yuri, André, Tiago, Mariane, Maria Luiza (Malu), Adriana Soprano, Bruna, Andres, Fabiana, Fábio, Tatiana, Nádia, José Geraldo, Carolina Perez, Vanessa, Priscila Oliveira, Camila dos Santos, Carla, Joice, Patrícia, Andrey, Leandro, Aline Sampaio, Beatriz, Juliana Smetana, Juliana Oliveira, Carlos Paier, Aline dos Santos, Alisson, Ana Helena, Jorge, Gustavo Arruda (Ceará), Luís Gustavo (Guga), Marília, Fernando, Rafael, Veruska, Marcelo, Ramon, Pedro Araújo, Sônia Rodrigues, Lisandra, Júlio Borges, Daniel Corrêa, Danieli, Karina, Thiago Seraphim, Thiago Cagliari, Melissa, Ana Olívia, Letícia, Isabel e Viviane, pelas conversas, troca de experiência, amizade e ótimo convívio. Ao Pedro e Kali, novamente, pelos ótimos dias que passamos em Ubatuba!

Aos meus queridos amigos “mg_talkianos” Aline, Tati, Nádia, Carol, Yuri, Marcos, André, Tiago, Gustavo, Guga e Fábio, pelos memoráveis encontros, ótimas discussões científicas e, principalmente, por serem meus amigos!

Ao Yuri, em especial, pelos tantos anos de convivência e por me apoiar em todos os momentos da minha vida!

Aos meus sempre companheiros de almoço, Priscila e André, pelas inestimáveis (e inesquecíveis) conversas! Obrigada pelas risadas, pela grande amizade e por poder contar com vocês sempre!

Aos meus amigos forrozeiros, Kali, Edmárcia, André, Ariane, Eduardo, Vinicius, Marry, Salvador, Jessica, Cassandra, Guilherme, Vornei e Jhony, pela dança, pelas aulas, pelas risadas, pelos encontros depois das aulas, pelos domingos no Rudá, pelo apoio e pelos momentos de distração que, com certeza, tornaram os meus dias muito mais leves e felizes nessa fase trabalhosa de conclusão do doutorado. Ao

Vinicius, em especial, pela amizade, pelo grande apoio, pela atenção e por me ajudar a corrigir o português da minha tese!

Aos meus grandes amigos, Ana Guerreiro, Carlos Stein, Ricardo Perini, Kainara Cunha e Mariana Moreira, por estarem ao meu lado nos melhores momentos e também nos mais difíceis. Obrigada pela amizade eterna!

Aos queridos Renata Soares e Fabrizzio Lacerda, pelos anos de amizade desde a minha iniciação científica na UFG e por terem me acolhido em Campinas num momento de importante decisão na minha vida, juntamente com os amigos Rodrigo e Michele, que também foram peças-chave na minha mudança à Campinas, me incentivando ao doutorado e me passando o contato do Jörg! Obrigada, em especial, à Renata, pelos meus primeiros ensinamentos na área de Biologia Molecular, pelo total apoio no meu doutorado, por ser meu exemplo de competência e garra, e por sempre fazer parte da minha vida profissional e pessoal.

À Fundação de Amparo à Pesquisa do Estado de São Paulo, FAPESP, pelo apoio financeiro.

Ao Laboratório Nacional de Biociências, LNBio, e Laboratório Nacional de Luz Síncrotron, LNLS, pela excelente infra-estrutura para a pesquisa.

E, principalmente, à minha amada família. Aos meus pais, meus maiores ídolos e fãs, meus grandes exemplos de amor, honestidade, força, coragem e persistência pra enfrentar e aproveitar a vida e, ao mesmo tempo, aqueles que mais acreditam em mim e têm orgulho de tudo o que posso ser. Ao meu irmão, parte de mim, que me faz lembrar todos os dias do valor de uma amizade incondicional, inteiramente verdadeira. À minha querida madrinha Mônica (Dinda) e meu afilhadinho Victor, que sempre me deram suporte e me acompanham sorrindo por todos os momentos da minha vida. Aos meus avós, tios e primos, que são a minha alegria e meus exemplos de amor.

Meus sinceros agradecimentos a todos vocês que fazem parte da minha vida e que me fazem querer ser uma pessoa cada dia melhor. E a ter esperanças no futuro!

*“You say you want a revolution
Well, you know
We all want to change the world”
The Beatles*

ÍNDICE

AGRADECIMENTOS	v
LISTA DE FIGURAS E TABELAS	x
LISTA DE ABREVIACÕES E SIGLAS	xi
RESUMO	xiv
ABSTRACT	xv
I. INTRODUÇÃO	1
1. A Proteína NIMA de <i>Aspergillus nidulans</i>	1
2. As Proteínas da Família Nek em Mamíferos	3
2.1. Estrutura Primária: Quais Características Fazem de uma Nek uma Nek?	4
2.2. Estrutura Secundária e Terciária: Cristais de Nek2 e Nek7	5
2.3. Nek1 e Nek8: Cílios, Ciclo Celular e Rins Policísticos	12
2.4. Nek6 e Nek7: Simplicidade Estrutural e Cascata de Sinalização na Mitose	13
2.5. Nek9: Regulador de Nek6 e Nek7 na Mitose?	14
3. Neks: Alvos de Inibidores em Terapias Anti-Câncer	15
II. OBJETIVOS	17
1. Objetivo Geral	17
2. Objetivos Específicos	17
III. RESULTADOS	18
1. Artigo I: <i>Characterization of hNek6 interactome reveals an important role for its short N-terminal domain and colocalizations with proteins at the centrosome</i>	18
2. Artigo II: <i>Human Nek6 is a monomeric mostly globular kinase with an unfolded short N-terminal domain</i>	50
3. Artigo III: <i>FEZ1 interacts with CLASP2 and NEK1 through coiled-coil regions and their cellular colocalization suggests centrosomal functions and regulation by PKC</i>	66

IV. CONCLUSÕES E PERSPECTIVAS	80
V. REFERÊNCIAS BIBLIOGRÁFICAS	86

LISTA DE FIGURAS E TABELAS

Figura 1. A extensa família Nek (<i>NIMA-related kinase</i>).	5
Figura 2. A conformação cataliticamente ativa do domínio de cinase.	7
Figura 3. Estrutura do domínio de cinase da hNek2 em complexo com o inibidor SU11652.	9
Figura 4. O motivo DFG e o loop de ativação adotam diferentes conformações dependentes do ligante.	10
Figura 5. A estrutura cristalográfica da Nek7 mostra uma conformação auto-inibitória que sugere um mecanismo regulatório ainda não descrito para cinases.	11
Figura 6. Possíveis vias de sinalização para a hNek6.	82
Tabela 1. Funções propostas para as Neks de mamíferos.	3

LISTA DE ABREVIACÕES E SIGLAS

Abl: *Abelson murine leukemia*

ADP: Adenosina difosfato

AMP: Adenosina monofosfato

Asn: asparagina

Asp: aspartato

ATP: Adenosina trifosfato

ATP γ S: Adenosina-(γ -3-tiotrifosfato)

Bcr-Abl: *Abelson murine leukemia-Breakpoint cluster region*

Bicd2: *Bicaudal D homolog 2*

BioGRID: *Database of Protein and Genetic Interactions*

Cdc2: *Cell division control protein 2*

Cdk: *Cyclin-dependent kinase*

Clasp2: *Clip associated protein 2*

C-Nap1: *Centrosomal Nek2-associated protein 1*

COS-7: *cell line CV-1 in Origin, carrying SV40 genetic material*

DFG: aspartato, fenilalanina, glicina

DLG: aspartato, leucina, glicina

DNA: *Deoxyribonucleic acid*

FACT: *Facilitates chromatin transcription complex*

Fez1: *Fasciculation and elongation protein zeta 1*

Fin1: *Filaments in between nuclei protein 1*

Glu: glutamato

GST: Glutathione S-transferase

HEK293: *Human Embryonic Kidney 293 cell line*

HeLa: *Human epithelial cervical cancer cell line*

HRD: histidina, arginina, aspartato

IL-1: interleucina-1

IRK: *Insulin Receptor Kinase*

jck: *juvenile cystic kidney*

kDa: *kiloDalton*

KIF3A: *Kinesin family member 3A*

KOMP: *Knockout Mouse Project Repository*

Leu: leucina

Lys: lisina

Mg⁺²: íon magnésio

mRNA: RNA mensageiro

MTOC: *Microtubule-Organising Centre*

Nek: *NIMA-related kinase*

Nercc1: *Never in mitosis A-related kinase 9*

NF-κB: *Nuclear Factor Kappa B*

Nim1: *G2-specific protein kinase nim-1*

NIMA: *Never In Mitosis, gene A*

Nlp: *Ninein-like protein*

PEST: prolina, glutamato, serina e treonina

Pfam: *Protein families database*

PKA: *Protein Kinase A*

PKC: *Protein Kinase C*

PKD: *Polycystic Kidney Disease*

PKI: *Protein Kinase Inhibitor*

Plk: *Polo-like kinases*

RanGEF: *Ran Guanine nucleotide Exchange Factor*

RCC1: *Regulator of Chromosome Condensation*

RNAi: *RNA de interferência*

SBP: *Spindle Pole Body*

Ser: *serina*

SH3: *SRC Homology 3 Domain*

THP1: *Human acute monocytic leukemia cell line*

TPX2: *Microtubule-associated, homolog*

Tyr: *tirosina*

U2OS: *Human osteosarcoma cell line*

γ -TuRC: *γ -Tubulin Ring Complex*

RESUMO

A proteína NIMA foi identificada e caracterizada funcionalmente em *Aspergillus nidulans* como sendo uma serina/treonina cinase crítica para a progressão do ciclo celular. As Neks (*NIMA-related kinases*) constituem uma família de cinases composta por 11 membros em mamíferos, que compartilham 40-45% de identidade com a proteína NIMA no domínio catalítico N-terminal. As Neks estão associadas a funções do ciclo celular e diversas patologias, o que as torna potenciais alvos quimioterápicos. Mutações no gene da Nek1 levam ao desenvolvimento da doença renal policística e ao aparecimento de diversos efeitos pleiotrópicos, sugerindo sua participação em vias reguladoras de vários processos celulares. A Nek6, por sua vez, é ativada durante a mitose, e a super-expressão de mutantes inativos ou a sua depleção por RNAi produz células exibindo defeitos no fuso, anormalidades nucleares, parada na metáfase e apoptose. A Nek6 humana foi recentemente associada à carcinogênese, mas, assim como para a maioria das Neks, sua estrutura molecular, parceiros de interação e vias de sinalização permanecem ainda desconhecidos. Nesse trabalho, introduzimos a hNek6 como uma hub no interactoma humano. Uma extensa comparação de bancos de dados baseada em análises de conectividade mostrou que o quinoma humano é enriquecido em hubs. Nossas redes de interação incluem um amplo espectro de novos parceiros de interação para a hNek6 identificados em *screenings* de duplo-híbrido em levedura, classificados em 18 categorias funcionais. Alguns novos parceiros de interação da hNek6 são também possíveis substratos e, ainda, colocalizam com a hNek6 e γ -tubulina em células humanas, apontando para uma possível interação centrossomal. Os diversos parceiros de interação conectam a hNek6 a novas vias, como a sinalização de Notch e a regulação do citoesqueleto de actina, ou fornecem novas pistas de como a hNek6 poderia regular vias previamente propostas, como ciclo celular, reparo de DNA e sinalização do NF- κ B. Além disso, obtivemos o primeiro modelo estrutural de baixa-resolução para a hNek6 a partir de SAXS. Análises estruturais revelaram que a hNek6 é um monômero em solução, apresentando uma conformação predominantemente globular, mas levemente alongada. Particularmente, a curta região N-terminal desordenada da hNek6 é importante para mediar as interações com seus parceiros. No caso da hNek1, observamos que ela interage com Fez1 e Clasp2 através de seus motivos *coiled-coil*, e colocaliza com essas proteínas em uma região candidata ao centrossomo.

ABSTRACT

NIMA was identified and functionally characterized in *Aspergillus nidulans* as a critical Ser/Thr kinase for cell cycle progression. The mammalian Neks (NIMA-related kinases) represent an evolutionarily conserved family of 11 serine/threonine kinases that share 40-45% identity with NIMA N-terminal domain. Neks are associated to cell cycle-related functions and diverse pathologies, which highlight them as potential chemotherapeutic targets. Nek1 gene mutations lead to the development of polycystic kidney disease and the emergence of several pleiotropic effects, suggesting its involvement in pathways regulating various cellular processes. Nek6, in turn, is activated during mitosis, and overexpression of inactive mutants or its depletion by iRNA produces cells exhibiting mitotic spindle defects, nuclear abnormalities, metaphase arrest and apoptosis. Human Nek6 was recently found to be linked to carcinogenesis, but as for the majority of Neks, the molecular structure, interacting partners and signaling pathways remain elusive. Here we introduce hNek6 as a hub kinase in the human interactome. We performed a broad databank comparison based on degree distribution analysis and found that the human kinome is enriched in hubs. Our networks include a large set of novel hNek6 interactors identified in our yeast two-hybrid screens, classified into 18 functional categories. Some novel interactors are also putative substrates and colocalized with hNek6 and γ -tubulin in human cells, pointing to a possible centrosomal interaction. The interacting proteins link hNek6 to novel pathways, e.g. Notch signaling and actin cytoskeleton regulation, or give new insights on how hNek6 may regulate previously proposed pathways such as cell cycle, DNA repair and NF- κ B signalings. Furthermore, we obtained the first low-resolution structural model of hNek6 by SAXS. Structural analysis revealed that hNek6 is a monomer in solution with a mostly globular, though slightly elongated conformation. Notably, we found that hNek6 unfolded short N-terminal region is important to mediate the interactions with its partners. In the case of hNek1, we found that it interacts with Fez1 and Clasp2 through coiled-coil motifs and colocalizes with these proteins in a candidate centrosomal region.

I. INTRODUÇÃO

A mitose é uma etapa crucial do ciclo celular onde uma célula se divide em duas através de uma reorganização massiva da arquitetura celular. O citoesqueleto é reorganizado para formar um fuso bipolar entre os centros organizadores de microtúbulos, previamente duplicados, os cromossomos são condensados e ligados ao fuso através de seus cinetócoros e, pela ação de múltiplos motores moleculares, os cromossomos são segregados em duas células-filhas. Durante a mitose, ocorre também uma substancial onda de fosforilações, controlando eventos de sinalização que coordenam os processos mitóticos e asseguram uma segregação cromossomal precisa.

A conservação dos mecanismos gerais e vias regulatórias que controlam a mitose nos eucariotos evidenciam o seu caráter antigo e sua importância. É esta conservação que tem possibilitado a identificação de um conjunto comum de reguladores mitóticos a partir da diversidade dos eucariotos, desde fungos até humanos. Vários reguladores mitóticos essenciais são proteínas serina/treonina cinases, responsáveis por modular a entrada e a progressão da mitose (O'Connell *et al.*, 2003).

1. A Proteína NIMA de *Aspergillus nidulans*

Em 1975, Ron Morris realizou um *screening* genético no fungo filamentoso *Aspergillus nidulans* para mutantes sensíveis à temperatura que fracassavam na progressão do ciclo celular (Morris, 1975). A análise dos mutantes resultantes levou à sua classificação em dois grupos: os mutantes *bim* (*blocked in mitosis*), que eram bloqueados na mitose mantendo a condensação dos cromossomos e o fuso mitótico; e os mutantes *nim* (*never in mitosis*), que nunca entravam em mitose, devido a uma parada na intérfase. Entre os genes classificados no grupo *bim*, estavam importantes genes envolvidos na mitose, como os componentes do complexo promotor da anáfase (APC), enquanto o grupo *nim* incluía genes que codificavam reguladores do ciclo celular, como a ciclina do tipo B, a fosfatase Cdc25 e DNA polimerases. Nesse grupo também estavam incluídos quatro alelos do gene *nimA*. Nos anos 80, ensaios de clonagem e expressão deste gene demonstraram que ele codifica uma serina/treonina cinase crítica para a progressão do ciclo celular, designada NIMA (*Never In Mitosis, gene A*) (Osmani *et al.*, 1987; Osmani *et al.*, 1988).

Entre as diversas famílias de proteínas cinases descritas, os membros da família das que se encontram relacionadas à NIMA são os menos caracterizados funcionalmente. A proteína NIMA foi identificada e caracterizada funcionalmente no fungo *Aspergillus nidulans*, sendo essencial para a entrada na mitose (Bergen *et al.*, 1984; Osmani *et al.*, 1991) e sua degradação necessária para a saída da mitose (Pu & Osmani, 1995). NIMA apresenta funções envolvidas na condensação da cromatina, organização do fuso mitótico e citocinese (O'Regan *et al.*, 2007). Mutantes de NIMA sensíveis à temperatura ou a superexpressão de formas dominante-negativas de NIMA causam interrupção do ciclo celular na fase G2, detectando-se DNA não-condensado e microtúbulos na forma encontrada em intérfase (Osmani *et al.*, 1991). Além disso, a superexpressão de NIMA em fungos e em células de mamíferos resultou no desencadeamento precoce de eventos relacionados à mitose, como a despolimerização dos microtúbulos e uma condensação prematura da cromatina (Lu & Hunter, 1995).

Mutações nesse gene, que resultam na perda de função, causam a parada do ciclo celular sem a interferência na ativação de p34-Cdc2, um importante regulador do ciclo celular, indicando que NIMA possui papel fundamental na transição G2/mitose (Osmani *et al.*, 1991). A iniciação da mitose em *A. nidulans* requer, portanto, a ativação tanto de p34-Cdc2, quanto de NIMA. Células com mutações no gene *nimX3*, que codifica a Cdc2, apresentaram parada do ciclo em G2 e ausência de ativação de NIMA, sugerindo que ativação da NIMA poderia ocorrer por meio de sua fosforilação direta pela Cdc2 (Ye *et al.*, 1995). NIMA é também necessária para a localização do complexo Cdc2/ciclina B no núcleo, durante a transição para a mitose (Wu *et al.*, 1998), especialmente no corpo polar do fuso mitótico (SBP, *Spindle Pole Body*), o principal centro de organização dos microtúbulos (MTOC) em fungos, equivalente ao centróssomo de eucariotos superiores. Nos mamíferos, Cdk1 (homóloga de Cdc2) é primeiramente ativada nos centróssomos, sugerindo que a concentração de reguladores do ciclo celular nos centróssomos/SBPs representa um mecanismo conservado de ativação do complexo Cdc2/ciclina B para o início da mitose (Jackman *et al.*, 2003). A habilidade de NIMA em regular a mitose em eucariotos superiores sugere a existência de vias de sinalização envolvendo proteínas homólogas à NIMA, conservadas durante a evolução.

2. As Proteínas da Família Nek em Mamíferos

As Neks (*NIMA-related kinases*) constituem uma família de proteínas cinases encontradas em mamíferos, composta por 11 membros que compartilham 40-45% de identidade com a proteína NIMA de *A. nidulans* no domínio catalítico N-terminal. A extremidade C-terminal constitui seu domínio regulatório e apresenta maior variabilidade, estando envolvida na determinação da especificidade por substratos e na interação com outras proteínas (O'Connell *et al.*, 2003). As Neks formam uma família altamente conservada de proteínas cinases, estando envolvidas na regulação do ciclo celular. Algumas Neks de mamíferos localizadas nos cílios, além de afetarem a progressão do ciclo, também se encontram relacionadas a funções ciliares (Quarmby & Mahjoub, 2005).

Em 1992, Letwin e colaboradores descreveram a primeira proteína cinase relacionada à NIMA em humanos, a Nek1. Posteriormente, outros trabalhos descrevendo membros dessa família foram publicados, mas nem todos possuem sua função caracterizada (Tabela 1).

Tabela 1. Funções propostas para as Neks de mamíferos.

Proteína	Função proposta	Referência
Nek1	Alterações no gene <i>nek1</i> em animais são modelos para a doença renal policística em humanos.	Upadhyia <i>et al.</i> , 2000
	Interage com proteínas envolvidas no ciclo celular e no reparo do DNA.	Surpili <i>et al.</i> , 2003
	Papel na resposta a dano ao DNA induzido por radiação ionizante.	Polci <i>et al.</i> , 2004
	É transportada através do núcleo e afeta tanto a ciliogênese quanto a estabilidade do centrôssomo.	White & Quarmby, 2008 e Hilton <i>et al.</i> , 2009
Nek2	Localizado em centrôssomos e cinetócoros.	Fry <i>et al.</i> , 1995 e 1999
	Fosforila a C-Nap1 e Nlp no centrôssomo.	Fry <i>et al.</i> , 2002
	Possível papel na regulação do fuso mitótico.	Chen <i>et al.</i> , 2002
	Regula a separação do centrôssomo na transição G2/mitose.	Rapley <i>et al.</i> , 2005
	Aumento da expressão em câncer de mama.	Tsunoda <i>et al.</i> , 2009
Nek3	Aumento da expressão em tumores de Ewing, linfomas de células B, colangiocarcinomas, adenocarcinomas de pulmão e seminomas testiculares.	Wai, 2002; de Vos, 2003; Kokuryo, 2010; Landi, 2008 e Barbagallo, 2009
	Modula a sinalização dos receptores de prolactina.	Miller <i>et al.</i> , 2005
Nek6	Aumento da expressão em câncer de mama.	McHale <i>et al.</i> , 2008
	Participa junto com as Neks 7 e 9 da mesma cascata de sinalização na mitose.	Belham <i>et al.</i> , 2003
	A super-expressão da Nek6 inativa reduz a taxa de crescimento de células humanas de câncer de mama.	Yin <i>et al.</i> , 2003
	A super-expressão de Nek6 correlaciona-se à super-expressão de Pin1 em 70% dos carcinomas de células hepáticas.	Chen <i>et al.</i> , 2006
	Aumento da expressão em linfomas não-Hodgkin e tumores de mama, laringe e colorretal.	Capra <i>et al.</i> , 2006
Aumento da expressão em câncer gástrico.	Takeno <i>et al.</i> , 2008	

	Seus níveis de transcrito, de proteína e de atividade de cinase estão elevados em tumores malignos e células de câncer.	Nassirpour <i>et al.</i> , 2010
Nek7	Localiza-se no centróssomo e é necessária para a montagem do fuso e progressão da mitose. Aumento da expressão em tumores de mama, laringe e colorretal.	Yissachar <i>et al.</i> , 2006 e Kim <i>et al.</i> , 2007 Capra <i>et al.</i> , 2006
Nek8	Alterações no gene <i>nek8</i> em animais estão associadas à doença renal policística. Aumento da expressão em câncer de mama.	Liu <i>et al.</i> , 2002 Bowers & Boylan, 2004
Nek9	Associação ao Bcd2 <i>in vivo</i> , fosforilação de Bcd2. Regula o alinhamento e a segregação dos cromossomos na mitose. Ativa a Nek6 durante a mitose. Regula a progressão de G1 e S através da interação com o complexo facilitador da transcrição da cromatina (FACT). Mediador da organização dos cromossomos e do centróssomo.	Holland <i>et al.</i> , 2002 Roig <i>et al.</i> , 2002 Belham <i>et al.</i> , 2003 Tan & Lee, 2004 Roig <i>et al.</i> , 2005
Nek10	Gene potencial causador de câncer de mama.	Ahmed <i>et al.</i> , 2009
Nek11	Cinase responsiva a estresse replicativo e a danos ao DNA. É ativada pela Nek2A em células com defeito na progressão do ciclo celular em G1/S.	Nogushi <i>et al.</i> , 2002 Nogushi <i>et al.</i> , 2004

Tabela modificada extraída de Quarmby & Mahjoud, 2005.

2.1. Estrutura Primária: Quais Características Fazem de uma Nek uma Nek?

A NIMA é uma proteína de 79 kDa composta por um domínio catalítico N-terminal, o qual apresenta a propriedade única de reconhecer preferencialmente um resíduo hidrofóbico N-terminal no substrato, com forte seletividade para uma fenilalanina na posição -3 (consenso F-R-R/K-S/T) (Songyang *et al.*, 1996). No domínio regulatório C-terminal, existe uma região *coiled-coil* predita, imediatamente após o domínio catalítico, que pode ser importante na formação de oligômeros de NIMA (Lu *et al.*, 1994), além de duas sequências PEST que direcionam a NIMA para a proteólise dependente de ubiquitina. Ambos os motivos são cruciais para a função *in vivo* e regulação de NIMA (Pu & Osmani, 1995) e, por essa razão, os homólogos de NIMA são preditos de apresentar uma organização similar de domínios.

Atualmente, as cinases são definidas como Neks, baseando-se na similaridade de sequência com o domínio catalítico de NIMA. Várias dessas proteínas apresentam o mesmo arranjo de motivos no domínio C-terminal e, portanto, parecem ser homólogos mais próximos de NIMA. Outras apresentam motivos adicionais ou a falta dessas sequências não-catalíticas essenciais (Figura 1). Nesses casos, é possível que o domínio catalítico de uma proteína NIMA ancestral tenha surgido em outras proteínas favorecendo funções adicionais ou possivelmente não-relacionadas, fora do contexto do controle da mitose (O'Connel *et al.*, 2003).

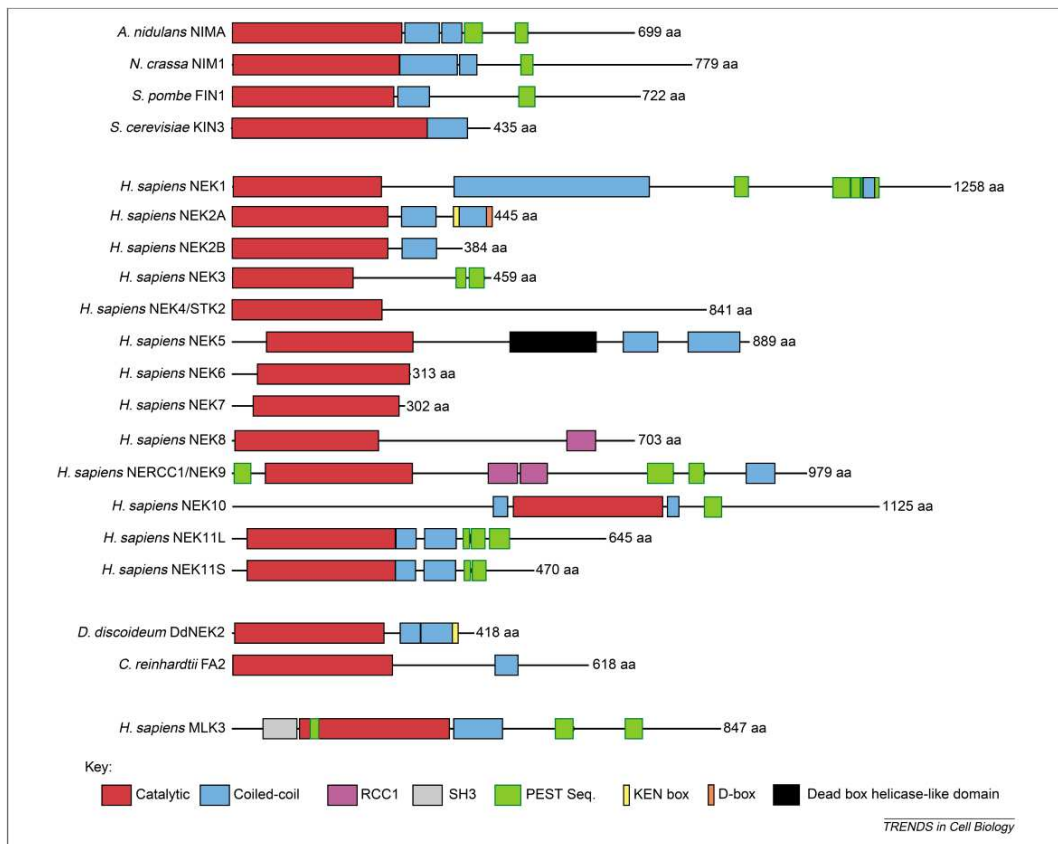


Figura 1. A extensa família Nek (*NIMA-related kinase*). Alinhamento de características estruturais importantes da família Nek, incluindo: sequências PEST (<http://embl.bcc.univie.ac.at/embnet/tools/bio/PESTfind/>); domínios *coiled-coil* (http://www.ch.embnet.org/software/COILS_form.html); domínios de cinase e outros (SH3/RCC1), utilizando o Pfam (<http://www.sanger.ac.uk/Software/Pfam/search.shtml>). As sequências completas de NEK1–NEK11 humanas foram obtidas de <http://www.kinase.com>. As NIMA cinases de fungos são mostradas no topo, demonstrando o arranjo clássico de domínio catalítico e sequências *coiled-coil* e PEST, essenciais para a atividade e regulação das proteínas NIMA de *A. nidulans*, Nim1 de *Neurospora crassa* e Fin1 de *Schizosaccharomyces pombe*. Abreviações: aa, aminoácido; *C. reinhardtii*, *Chlamydomonas reinhardtii*; *D. discoideum*, *Dictyostelium discoideum*; *S. cerevisiae*, *Saccharomyces cerevisiae*. Extraído de O’Connel *et al.*, 2003.

2.2. Estrutura Secundária e Terciária: Cristais de Nek2 e Nek7

Os primeiros estudos estruturais de cinases identificaram os resíduos que devem ser precisamente posicionados para a catálise e os motivos conservados dentro dos quais eles se encontram, revelando estruturas bastante similares no estado ativo em contraste com uma plasticidade conformacional exibida por diferentes cinases no estado inativo

(Figura 2) (Huse & Kuriyan, 2002). De modo geral, a estrutura das serina/treonina e tirosina cinases é bastante conservada, sendo dividida em dois domínios ou lobos: N-terminal, composto por cinco fitas- β e uma α -hélice proeminente (hélice αC), e C-terminal, sendo maior e constituído predominantemente por α -hélices. No estado ativo, por exemplo, uma lisina conservada na cavidade de ligação do nucleotídeo (Lys⁷² na PKA), entre os dois lobos, interage com os fosfatos α e β do ATP, segurando-os em posição de catálise e é, por sua vez, adequadamente posicionada através da formação de uma ligação iônica com um glutamato (Glu⁹¹ na PKA) na hélice αC . Além disso, um aspartato (Asp¹⁸⁴ na PKA) dentro do motivo conservado DFG (aspartato, fenilalanina, glicina) ou DLG (aspartato, leucina, glicina) ativa um cátion bivalente (Mg⁺², por ex.) associado com o γ -fosfato do ATP. O motivo DFG/DLG localiza-se na região N-terminal do *loop* de ativação que, em muitas cinases, deve ser fosforilado para formar uma plataforma ordenada de ligação ao substrato. A transferência do grupo fosfato do ATP para o substrato também requer um arranjo espacial preciso de vários resíduos catalíticos absolutamente conservados nas cinases. Um aspartato do *loop* catalítico (Asp¹⁶⁶ na PKA) interage com a hidroxila da cadeia lateral do substrato, enquanto uma asparagina (Asn¹⁷⁷ na PKA), também do *loop* catalítico, interage com outros resíduos por ligações de hidrogênio que orientam o aspartato. Em contraste com suas conformações ativas muito similares, as estruturas de cinases mostram uma diversidade de conformações inativas que refletem a variedade dos seus mecanismos regulatórios.

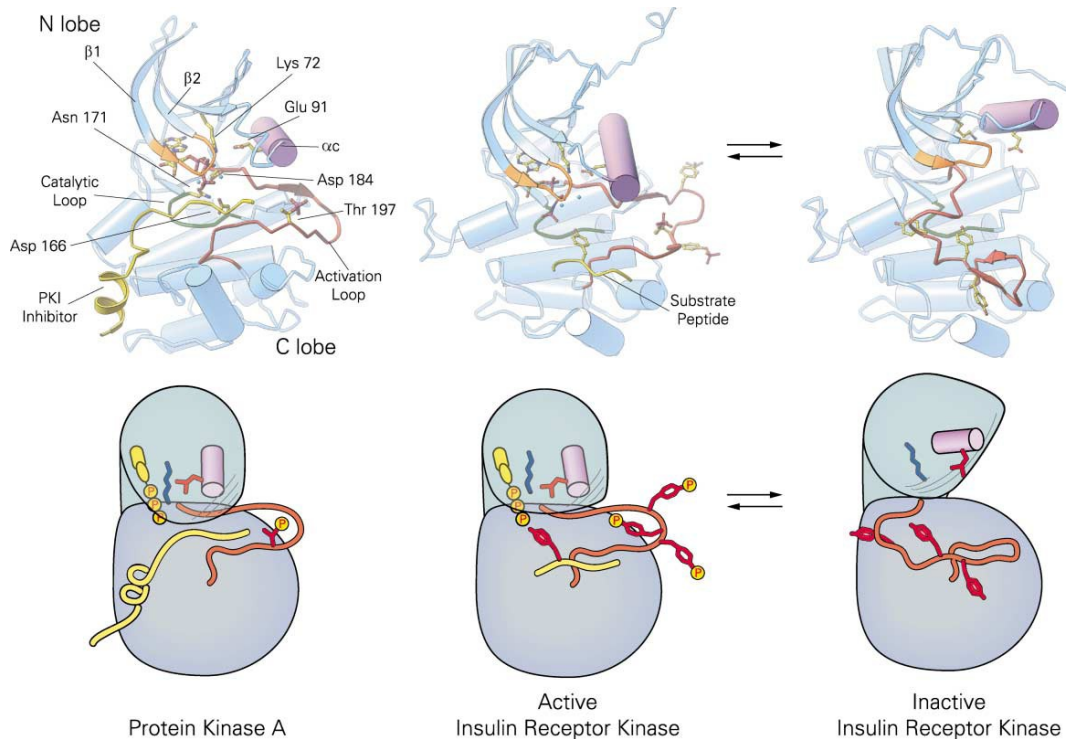


Figura 2. A conformação cataliticamente ativa do domínio de cinase. (Parte superior) As estruturas cristalográficas da proteína cinase A (PKA, uma serina/treonina cinase) (Zheng *et al.*, 1993) e do receptor de insulina (IRK, uma tirosina cinase) (Hubbard, 1997) são mostradas. Elementos estruturais chave do domínio de cinase estão coloridos como segue: *loop* de ativação, vermelho; hélice αC , roxo; *loop* de ligação ao fosfato (*P-loop*, entre as fitas $\beta 1$ e $\beta 2$), alaranjado; e *loop* catalítico, verde. O peptídeo substrato da IRK e o peptídeo inibidor PKI da PKA são mostrados em amarelo. O ATP ligado e vários resíduos conservados no sítio ativo estão indicados. É mostrada também a estrutura da IRK inativa, desfosforilada (Hubbard *et al.*, 1994), onde o *loop* de ativação adota uma conformação fechada que impede a ligação do nucleotídeo e do substrato. (Parte inferior) As três estruturas foram esquematizadas para mostrar de forma clara as transições conformacionais envolvidas na regulação da atividade de cinase, com ênfase na hélice αC e no *loop* de ativação. A lisina catalítica e o glutamato (Lys⁷² e Glu⁹¹ na PKA) são mostrados em cada esquema. Extraído de Huse & Kuriyan, 2002.

A Nek2 e a Nek7 humanas são as únicas Neks que apresentam as estruturas de seus domínios de cinase descritas, ambas por cristalografia de raios-X (Rellos *et al.*, 2007; Westwood *et al.*, 2009; Richards *et al.*, 2009). As estruturas do domínio de cinase da Nek2 apresentam a forma apo (mutante Nek2-T175A) e três diferentes complexos com ligantes (Nek2 selvagem ligada ao ADP e Nek2-T175A mutante ligada ao ATP γ S não-hidrolisável e ao inibidor SU11652) e, particularmente, ressaltam a dependência da conformação do *loop* de ativação em relação ao ligante (Figuras 3 e 4), propondo que a variabilidade conformacional do estado inativo da Nek2 seja favorável ao desenho de

inibidores mais seletivos. Esses estudos mostram que a estrutura da Nek2 forma uma plataforma rígida característica da conformação inativa, ao redor da qual as regiões variáveis, que incluem o motivo DFG, o *loop* de ativação e o motivo HRD, se organizam. O fato do motivo DFG e do *loop* de ativação poderem adotar diversas conformações estáveis seria um possível obstáculo à rápida produção de inibidores específicos para a Nek2, uma vez que pequenas modificações nos compostos poderiam induzir a estabilização de uma conformação diferente, causando confusão nas análises relacionadas à estrutura-atividade da molécula. Por outro lado, a variabilidade poderia ser considerada uma oportunidade, já que uma dessas conformações poderia fornecer o modelo certo para um inibidor seletivo. De fato, inibidores direcionados para a conformação inativa da cinase (“DFG-out”, inibidores do tipo II) são, possivelmente, os mais promissores em termos de seletividade (Noble *et al.*, 2004). A conformação da estrutura de Nek2^{ADP}, por exemplo, é a que mais se assemelha à conformação DFG-out de tirosina cinases, reconhecida por inibidores seletivos, como o Imanitib. A droga anti-câncer Gleevec também é um potente inibidor utilizado no tratamento da leucemia mielóide crônica, ligando-se seletivamente à forma inativa da cinase Abl (oncoproteína Bcr-Abl), estabilizando o *loop* de ativação em uma conformação que mimetiza o substrato ligado (Schindler *et al.*, 2000).

No caso da Nek7, sua estrutura revelou que esta cinase é mantida em uma forma cataliticamente inativa por um motivo auto-inibitório, onde um resíduo de tirosina (Tyr⁹⁷) aponta para dentro do sítio ativo, formando uma ligação de hidrogênio com o motivo DLG e bloqueando a conformação ativa (voltada para dentro) da hélice α C (Figura 5). Interessantemente, mutantes de Nek7 e Nek6 para a referida tirosina tornam-se constitutivamente ativos, e a atividade da Nek7 e da Nek6, mas não dos mutantes, é aumentada pela interação com o domínio regulatório C-terminal da Nek9 (Richards *et al.*, 2009). Esse mesmo estudo também mostrou que uma conformação similar ao equivalente resíduo de tirosina é induzida na Nek2 ligada ao inibidor CCT241950. Essa conformação “Tyr-down” encontrada na Nek7 e Nek2 é uma conformação inativa inacessível à vasta maioria das cinases, representando, assim, também um potencial ponto de partida para o desenho de inibidores seletivos.

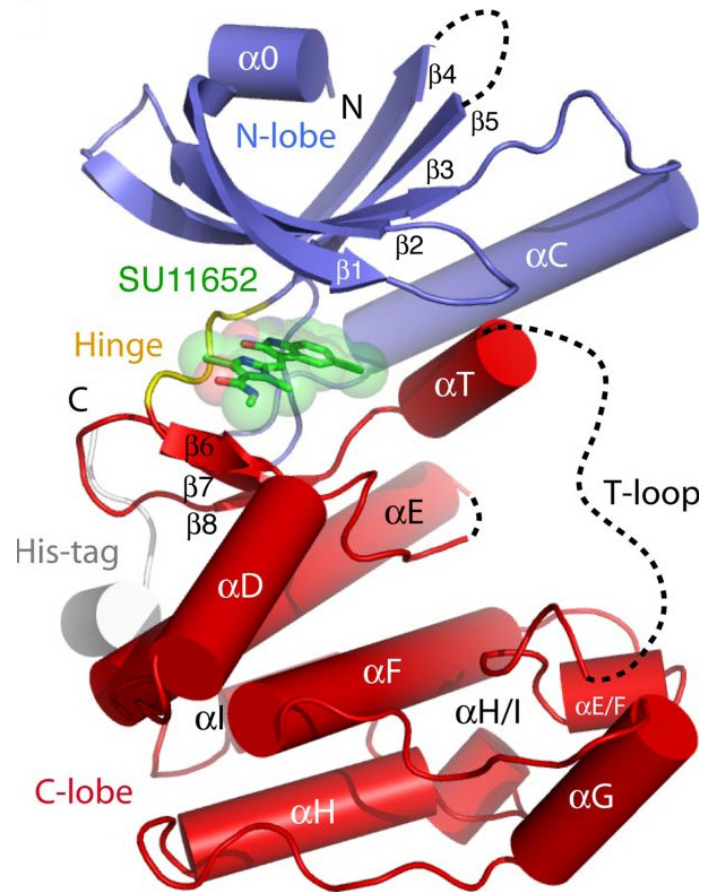


Figura 3. Estrutura do domínio de cinase da hNek2 em complexo com o inibidor SU11652. Os lobos N- e C-terminais estão mostrados em azul e vermelho, respectivamente, a região *hinge* (de dobradura), que conecta os lobos, está marcada de amarelo e o inibidor está mostrado em verde. Regiões de desordem na estrutura estão incluídas como linhas tracejadas. Extraído de Rellos *et al.*, 2007.

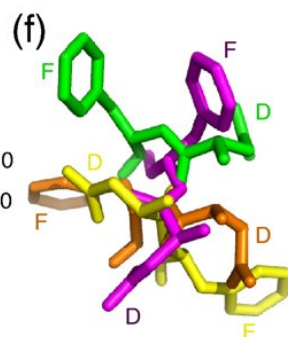
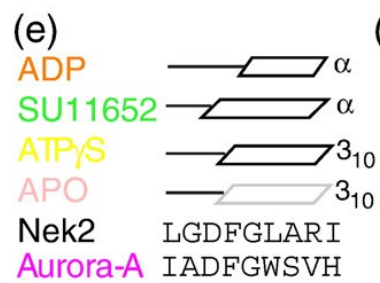
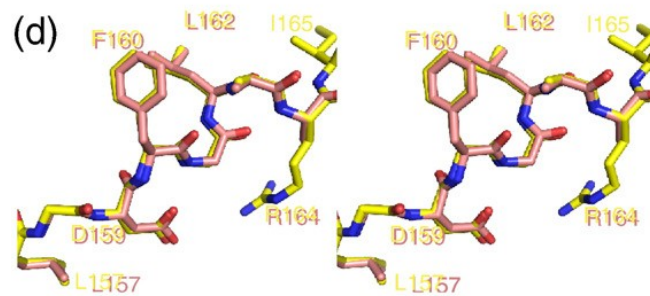
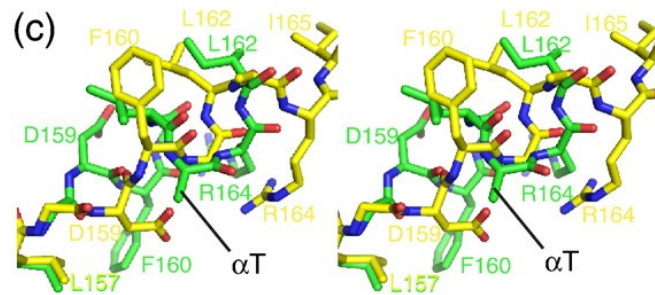
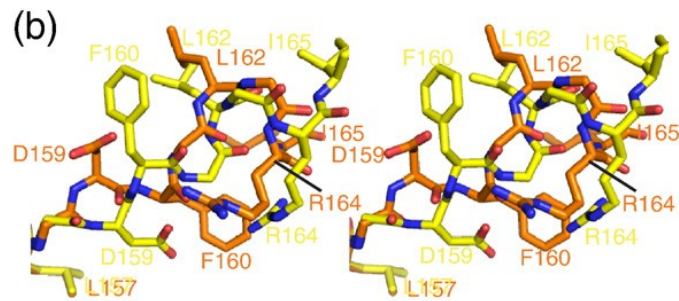
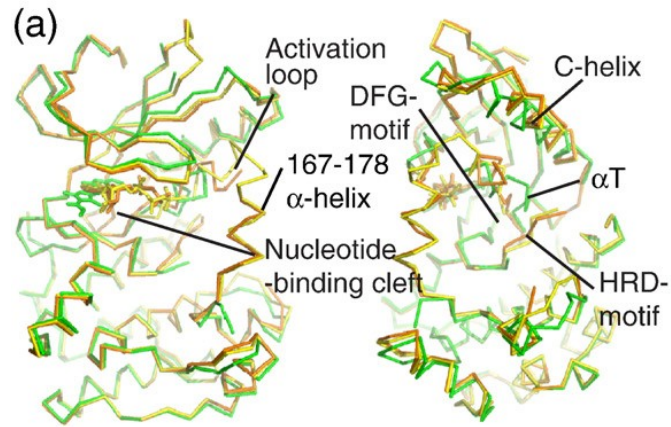


Figura 4. O motivo DFG e o loop de ativação adotam diferentes conformações dependentes do ligante. (a) Superposição das estruturas de Nek2-T175A^{ATP_γS} (amarelo), Nek2^{ADP} (alaranjado) e Nek2-T175A^{SU} (verde) mostradas em duas orientações relacionadas por uma rotação de 90° em relação ao eixo y. (b) Superposição do motivo DFG de Nek2-T175A^{ATP_γS} (átomos de carbono amarelos) e Nek2^{ADP} (átomos de carbono alaranjados). (c) Superposição do motivo DFG de Nek2-T175A^{ATP_γS} (átomos de carbono amarelos) e Nek2-T175A^{SU} (átomos de carbono verdes). (d) Superposição do motivo DFG de Nek2-T175A^{ATP_γS} (átomos de carbono amarelos) e Nek2-T175A^{Ap_o} (átomos de carbono rosa-claro). (e) Esquema das estruturas secundárias adotadas pelas quatro estruturas da Nek2 e a sequência de aminoácidos em torno do motivo DFG na Nek2 e na Aurora-A. (f) Superposição de três conformações do motivo DFG da Nek2, juntamente com a posição provavelmente adotada na conformação totalmente ativa baseada na estrutura da Aurora-A/TPX2 (magenta). A orientação é a dos painéis (b) a (d) visualizada da esquerda (abaixo) para a direita (acima). Extraído de Westwood *et al.*, 2009.

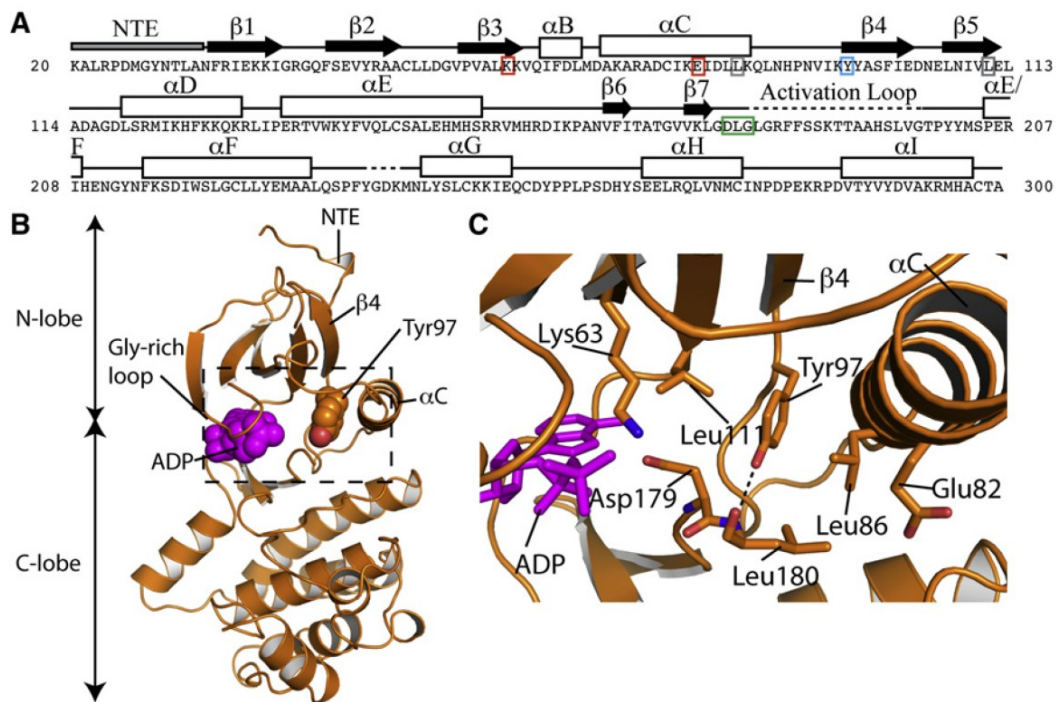


Figura 5. A estrutura cristalográfica da Nek7 mostra uma conformação auto-inibitória que sugere um mecanismo regulatório ainda não descrito para cinases. (A) Estrutura secundária e resíduos-chave estão indicados na sequência de aminoácidos da Nek7. Regiões desordenadas estão marcadas por linhas tracejadas e regiões ordenadas estão marcadas por linhas sólidas, setas pretas e retângulos brancos, correspondendo a *random coils*, fitas-β e α-hélices, respectivamente. Os resíduos de Lys⁶³ e Glu⁸² estão marcados em caixas vermelhas, Leu⁸⁶ e Leu¹¹¹ em caixas cinza, Tyr⁹⁷ em caixa azul, e o motivo DLG em caixa verde. (B) Visão geral da estrutura da Nek7 ligada ao ADP. A cadeia lateral da Tyr⁹⁷ e o ADP (magenta) são mostrados como esferas. A caixa tracejada indica a região ampliada em (C). (C) Representação da Tyr⁹⁷ e seu ambiente circundante. A ligação de hidrogênio entre a Tyr⁹⁷ e a Leu¹⁸⁰ é mostrada como uma linha tracejada.

2.3. Nek1 e Nek8: Cílios, Ciclo Celular e Rins Policísticos

A proteína Nek1, primeira da família a ser descrita, foi relacionada à etiologia da doença renal policística progressiva (PKD: *Polycystic Kidney Disease*), uma vez que camundongos mutantes em Nek1 desenvolvem esta doença (Upadhyya *et al.*, 2000). Estes autores relataram ainda o aparecimento de efeitos pleiotrópicos nos mutantes de Nek1, incluindo dimorfismo facial, nanismo, esterilidade masculina, anemia e formação de cistos no plexo coróide. Interessantemente, um ensaio de duplo-híbrido anterior do nosso grupo, utilizando a Nek1 como isca, identificou proteínas envolvidas na PKD, tais como KIF3A e tuberina (Surpili *et al.*, 2003).

Além disso, foi demonstrada a participação de Nek1 no controle do ciclo celular, particularmente no reparo do DNA (Letwin *et al.*, 1992; Polci *et al.*, 2004). Foi observado que, após indução de dano ao DNA, há um aumento na expressão da Nek1, a qual migra do citoplasma para o núcleo, para as regiões onde os danos ocorreram. Ainda, células que não expressam Nek1 apresentam hipersensibilidade a efeitos letais da radiação ionizante.

A Nek1, assim como outras Neks, apresenta também um papel na integridade do centróssomo, afetando tanto a cilogênese quanto a estabilidade do centróssomo (White & Quarmby, 2008). Essa proteína é transportada através do núcleo, sugerindo sua participação na transdução de mensagens da região do corpo basal dos cílios à regulação da expressão gênica (Hilton *et al.*, 2009).

A proteína Nek8, assim como a Nek1, apresenta funções relacionadas aos cílios e ciclo celular (Quarmby & Mahjoub, 2005), mas seu papel na célula ainda é pouco compreendido. Assim como outros membros conservados da família, a Nek8 encontra-se relacionada a patologias. Além da Nek1, mutações no gene da Nek8 também demonstraram causar a formação de cistos renais em modelo murino da doença renal policística juvenil recessiva, *jck* (*juvenile cystic kidney*). A expressão *in vitro* da Nek8 mutante resultou em células aumentadas, multinucleadas e com um anormal citoesqueleto de actina. (Liu *et al.*, 2002). Estudos recentes sugerem que a Nek8 interage com as vias de sinalização das policistinas e pode controlar o direcionamento dessas proteínas ciliares na célula. Esses estudos também sugerem que a Nek8 mutada pode levar à cistogênese, alterando a estrutura e função dos cílios na região distal do néfron (Sohara *et al.*, 2008). A Nek8 encontra-se, ainda, super-expressa em tumores de mama em humanos (Bowers & Boylan, 2004).

2.4. Nek6 e Nek7: Simplicidade Estrutural e Cascata de Sinalização na Mitose

As proteínas Nek6 e Nek7 são as menores e, estruturalmente, as mais simples Neks constituídas, praticamente, apenas por seus domínios catalíticos que se localizam na região C-terminal, ao contrário das demais Neks, apresentando uma curta extremidade N-terminal (O'Connel *et al.*, 2003). A Nek6 endógena é ativada durante a mitose, concomitante com um aumento do seu nível de expressão (Belham *et al.*, 2003), enquanto a Nek7, ao contrário, parece ser relativamente constante ao longo do ciclo celular (Kim *et al.*, 2007). Além disso, a Nek7 foi descrita por se localizar no centrossomo de células U2OS e HeLa tanto na intérfase quanto na mitose (Yissachar *et al.*, 2006; Kim *et al.*, 2007), enquanto a Nek6 apresenta uma distribuição difusa, principalmente citoplasmática. Contudo, a super-expressão de mutantes cataliticamente inativos das Neks 6 e 7 produzem fenótipos similares, como células exibindo elevados índices mitóticos, defeitos no fuso mitótico, anormalidades nucleares e apoptose (Yin *et al.*, 2003; Yissachar *et al.*, 2006). Esses fenótipos são também observados a partir da depleção das Neks 6 e 7 em células HeLa, utilizando-se RNAi, ocorrendo a retenção das células na metáfase, apresentando uma normal condensação da cromatina e alinhamento, mas uma incapacidade de completar a segregação dos cromossomos. A atividade das Neks 6 e 7, portanto, parece ser necessária para a progressão da anáfase, onde as células são retidas no ponto de controle do fuso mitótico e entram em apoptose, ou completam a mitose, mas com a aquisição de anormalidades nucleares durante o processo (Yin *et al.*, 2003; Yassachar *et al.*, 2006; Kim *et al.*, 2007).

Nek6 e Nek7 co-purificam com a Nek9 como resultado de uma interação específica e forte, ligando entre o domínio RCC1 e o motivo de *coiled-coil* da Nek9 (Roig *et al.*, 2002). É sabido que a Nek6 apresenta grande expressão e maior atividade catalítica durante a mitose, mas para isso é necessária a fosforilação no resíduo Ser²⁰⁶, que é realizada diretamente pela Nek9 *in vitro* e *in vivo*; Nek7 é também fosforilada pela Nek9 no resíduo de Ser¹⁹⁵, ambos os sítios encontrados nos *loops* de ativação das duas cinases, respectivamente (Belham *et al.*, 2003). Estes fatos levaram a um modelo em que as Neks 6, 7 e 9 atuam como parceiros de uma mesma cascata de sinalização, sendo as Neks 6 e 7 substratos da Nek9, onde esta se mantém inativa durante a intérfase e ativa na mitose, ativando as Neks 6 e 7 de forma semelhante que, por sua vez, coordenam a formação e manutenção do fuso mitótico (Roig *et al.*, 2002).

2.5. Nek9: Regulador de Nek6 e Nek7 na Mitose?

A proteína Nek9, também denominada de Nercc1, é uma das maiores Neks com 979 aminoácidos, apresentando um grande domínio regulatório C-terminal, o qual contém sete *repeats* homólogos aos da proteína RanGEF, RCC1 (*Regulator of Chromosome Condensation*), um segmento rico em Ser/Thr/Pro e, assim como em Nek2, possui um motivo *coiled-coil* de dimerização (Roig *et al.*, 2002).

A Nek9 foi primeiramente isolada apresentando atividade catalítica para β -caseína em extratos de pulmões de coelhos tratados com IL-1, revelando a co-cromatografia de uma segunda proteína homóloga à Bicaudal D de *Drosophila*, Bicd2, a qual é fosforilada *in vitro* pela Nek9 e assemelha-se a uma estrutura do citoesqueleto (Holland *et al.*, 2002). Além disso, a imunoprecipitação da Nek9 de extratos de ovo de *Xenopus laevis* apresenta γ -tubulina e outros membros do complexo do anel de γ -tubulina (γ -TuRC), essencial para a atividade de nucleação de microtúbulos dos centrossomos (Roig *et al.*, 2005). A microinjeção de anticorpos anti-Nek9 em células humanas durante a prófase, após a condensação dos cromossomos, interfere na organização dos fusos e na correta segregação dos cromossomos, resultando na parada do ciclo na prometáfase ou aneuploidia (Roig *et al.*, 2002).

A expressão da proteína Nek9 permanece constante em diferentes fases do ciclo celular (G1/S, G2, M, G1); no entanto, assim como em NIMA, há um específico aumento de sua atividade catalítica durante a mitose, e esta ativação é desencadeada *in vitro* e *in vivo* por eventos de fosforilação (Roig *et al.*, 2002). A Nek9 selvagem recombinante apresenta baixa atividade quando extraída de células em crescimento exponencial, mas sua pré-incubação com ATP e Mg^{2+} induz sua auto-fosforilação e ativação no resíduo de Thr²¹⁰ presente em seu *loop* de ativação, enquanto mutantes sem o motivo *coiled-coil* de dimerização apresentam atividade significativamente reduzida (Roig *et al.*, 2002; Roig *et al.*, 2005). Curiosamente, a deleção da região RCC1 leva a uma hiperatividade catalítica, indicando que esta região possa ser necessária para a auto-inibição da proteína (Roig *et al.*, 2002). É possível que a ativação da Nek9 na mitose envolva uma porcentagem muito pequena (<5%) do total de proteína expressa e, em contraste com a vasta maioria de polipeptídeos inativos, a Nek9 ativa (Thr210P) se torna evidente, primeiramente, durante a prófase, concentrada no centrossomo, onde pode ser fosforilada pela Cdk1/ciclina B (Jackman *et al.*, 2003), se estendendo até a metáfase. Com a transição para a anáfase, a imuno-reatividade da Nek9 (Thr210P) nos

centrossomos diminui e se torna detectável nos cromossomos, um padrão evidente até a telófase. Antes de desaparecer, a Nek9 ativa é detectada no fuso central (*midbody*), como dois pontos flanqueando o sulco de clivagem durante a citocinese (Roig *et al.*, 2005).

Devido ao seu provável papel na organização do fuso mitótico e segregação dos cromossomos, além de ser ativada durante a mitose e interagir com as Neks 6 e 7, é possível, portanto, que alguns ou todos os fenótipos observados com a microinjeção de IgG anti-Nek9 nas células humanas sejam causados pela interferência com as funções das Neks 6 e 7, sendo a Nek9 um provável regulador positivo dessas Neks (Roig *et al.*, 2002).

3. Neks: Alvos de Inibidores em Terapias Anti-Câncer

Aproximadamente 518 proteínas cinases compõem o cinoma humano e, dentre as muitas cinases descritas, aquelas que atuam na regulação do ciclo celular têm sido consideradas, atualmente, os mais promissores alvos terapêuticos anti-câncer (Capra *et al.*, 2006, Vieth *et al.*, 2003, Vieth *et al.*, 2005). A progressão da mitose e a montagem do fuso mitótico são reguladas por várias serina/treonina cinases, incluindo membros das famílias das cinases dependentes de ciclina (Cdk: *Cyclin-dependent kinases*), cinases do tipo Polo (Plk: *Polo-like kinases*), cinase Aurora, e cinases relacionadas à NIMA (Nek: *NIMA-related kinases*) (Barr *et al.*, 2004; Carmena *et al.*, 2003; Nigg *et al.*, 2001; O'Regan *et al.*, 2007). Essas cinases atuam nos principais pontos de checagem do ciclo celular: no final da fase G1 (ponto de restrição), na passagem de G2 para mitose e dentro da própria mitose (na metáfase). Perdas ou falhas nestes pontos de controle vêm sendo associadas com o desenvolvimento de células neoplásicas, uma vez que essas deixam de obedecer o ritmo de divisão celular e apresentam um acúmulo de erros no DNA (Malumbres & Barbacid, 2007).

Dentre as Neks humanas, Nek2, Nek3 e Nek8 encontram-se super-expressas em tumores de mama (Tsunoda *et al.*, 2009; McHale *et al.*, 2008; Bowers & Boylan, 2004), e o gene NEK10 foi recentemente descrito como um gene potencial causador de câncer de mama (Ahmed *et al.*, 2009), enquanto a Nek2 apresenta ainda seus níveis aumentados em tumores de Ewing, linfomas de células B, colangiocarcinomas, adenocarcinomas de pulmão e seminomas testiculares (Wai *et al.*, 2002; de Vos *et al.*, 2003; Kokuryo *et al.*, 2010; Landi *et al.*, 2008; Barbagallo *et al.*, 2009). A Nek6

humana também foi recentemente associada à carcinogênese. Ela é super-expressa em câncer gástrico e o aumento nos níveis do mRNA de Nek6 correlaciona-se com a super-expressão da peptidil-prolil isomerase Pin1 em 70% dos carcinomas de células hepáticas, enquanto a super-expressão da Nek6 inativa reduz a taxa de crescimento de células humanas de câncer de mama (Takeno *et al.*, 2008; Chen *et al.*, 2006; Yin *et al.*, 2003). Além disso, em um *screening* em larga escala por serina/treonina cinases em diferentes tipos de tumores humanos, a Nek6 encontrou-se super-expressa em linfomas não-Hodgkin, e ambas Nek6 e Nek7 mostraram-se super-expressas em tumores de mama, laringe e colorretal (Capra *et al.*, 2006). Recentemente, foi demonstrado que os níveis do transcrito, da proteína e da atividade de cinase de Nek6 mostraram-se altamente elevados em tumores malignos e linhagens de células humanas cancerosas em comparação aos tecidos normais e células de fibroblastos, indicando um importante papel para a Nek6 na tumorigênese (Nassirpour *et al.*, 2010).

Além de super-expressas em tumores, outro estudo notável baseado no ressequenciamento sistemático de genomas de câncer em busca de mutações somáticas nos éxons codificadores dos 518 genes de cinases, mostrou que as Neks 1, 4, 6, 7, 8, 10 e 11 apresentam uma probabilidade condicional de carregar pelo menos uma mutação do tipo “*driver*”, implicada no desenvolvimento de câncer (Greenman *et al.*, 2007). Por outro lado, as Neks também se encontram relacionadas a outras patologias. Nek1 e Nek8 foram implicadas na função ciliar e associadas com a doença renal policística em modelos murinos (Upadhyya *et al.*, 2000; Liu *et al.*, 2002), caracterizada pelo desenvolvimento de cistos devido a uma anormalidade na diferenciação celular, associada à proliferação celular sustentada e algum grau de apoptose aumentada, secreção transepitelial de fluidos e remodelamento da matriz extracelular. De fato, em um estudo anterior de duplo-híbrido realizado por nosso grupo, foram identificados parceiros de interação para a hNek1 envolvidos com a PKD, como as proteínas KIF3A, β -catenina, tuberina, entre outras (Surpili *et al.*, 2003). Todos esses fatos ressaltam as Neks como potenciais alvos quimioterápicos.

De modo geral, os genes que codificam as Neks humanas encontram-se super-expressos, mas também são alvos de mutações em câncer (Greenman *et al.*, 2007). Isso sugere que mutações nas Neks podem conferir vantagens seletivas para a sobrevivência e crescimento das células cancerígenas. Sendo assim, as Neks também são ótimos candidatos para varreduras de identificação de novos inibidores que possam, eventualmente, ser utilizados em novas estratégias terapêuticas anti-câncer.

II. OBJETIVOS

1. Objetivo Geral

Este trabalho teve como objetivo geral a compreensão dos papéis exercidos pelas proteínas Nek1 e Nek6 na célula através da análise de suas interações com outras proteínas e de suas estruturas.

2. Objetivos Específicos

- 2.1. Clonagem das seqüências codificadoras das proteínas humanas Neks 1 e 6 em vetores de expressão em sistemas procariotos e eucariotos.
- 2.2. Mutagênese sítio-dirigida do domínio de cinase da hNek 6, visando a obtenção de proteínas recombinantes mais estáveis e menos tóxicas às células hospedeiras.
- 2.3. Expressão e purificação das proteínas recombinantes hNeks 1 e 6 e do mutante inativo hNek6(S206A) em *E. coli* e células de mamífero.
- 2.4. Estudos funcionais: duplo-híbrido, *pull down*, imunoprecipitação, localização celular e/ou ensaios de fosforilação para identificação e caracterização de proteínas que interagem e/ou são substratos das hNeks 1 e 6.
- 2.5. Estudos estruturais/biofísicos: dicroísmo circular (CD), espalhamento dinâmico de luz (DLS), gel-filtração analítica, cromatografia de exclusão molecular acoplada a espalhamento de luz em múltiplos ângulos (SEC-MALS), espalhamento de raios-X a baixos ângulos (SAXS), e cristalografia de raios-X das hNeks 1 e 6.

III. RESULTADOS

1. Artigo I:

CHARACTERIZATION OF hNEK6 INTERACTOME REVEALS AN IMPORTANT ROLE FOR ITS SHORT N-TERMINAL DOMAIN AND COLOCALIZATION WITH PROTEINS AT THE CENTROSOME

GABRIELA VAZ MEIRELLES, DANIEL CARLOS FERREIRA LANZA, JÚLIO
CÉSAR DA SILVA, JÉSSICA SANTANA BERNACHI, ADRIANA FRANCO PAES
LEME, AND JÖRG KOBARG

JOURNAL OF PROTEOME RESEARCH, v. 9(12), p. 6298-316, 2010.

(doi: 10.1021/pr100562w)

Characterization of hNek6 Interactome Reveals an Important Role for Its Short N-Terminal Domain and Colocalization with Proteins at the Centrosome

Gabriela Vaz Meirelles,^{†,‡} Daniel Carlos Ferreira Lanza,^{†,‡} Júlio César da Silva,^{§,||}
 Jéssica Santana Bernachi,[†] Adriana Franco Paes Leme,[†] and Jörg Kobarg^{*,†,‡}

Laboratório Nacional de Biociências, Campinas SP, Brazil, Departamento de Bioquímica-Programa de Pós-graduação em Biologia Funcional e Molecular, Instituto de Biologia, Universidade Estadual de Campinas, Campinas, SP, Brazil, Laboratório Nacional de Luz Síncrotron, Campinas SP, Brazil, and Instituto de Física “Gleb Wataghin”, Universidade Estadual de Campinas, Campinas, SP, Brazil

Received June 5, 2010

Physical protein–protein interactions are fundamental to all biological processes and are organized in complex networks. One branch of the kinome network is the evolutionarily conserved NIMA-related serine/threonine kinases (Neks). Most of the 11 mammalian Neks studied so far are related to cell cycle regulation, and due to association with diverse human pathologies, Neks are promising chemotherapeutic targets. Human Nek6 was associated to carcinogenesis, but its interacting partners and signaling pathways remain elusive. Here we introduce hNek6 as a highly connected member in the human kinase interactome. In a more global context, we performed a broad data bank comparison based on degree distribution analysis and found that the human kinome is enriched in hubs. Our networks include a broad set of novel hNek6 interactors as identified by our yeast two-hybrid screens classified into 18 functional categories. All of the tested interactions were confirmed, and the majority of tested substrates were phosphorylated *in vitro* by hNek6. Notably, we found that hNek6 N-terminal is important to mediate the interactions with its partners. Some novel interactors also colocalized with hNek6 and γ -tubulin in human cells, pointing to a possible centrosomal interaction. The interacting proteins link hNek6 to novel pathways, for example, Notch signaling and actin cytoskeleton regulation, or give new insights on how hNek6 may regulate previously proposed pathways such as cell cycle regulation, DNA repair response, and NF- κ B signaling. Our findings open new perspectives in the study of hNek6 role in cancer by analyzing its novel interactions in specific pathways in tumor cells, which may provide important implications for drug design and cancer therapy.

Keywords: Nek6 • N-terminal domain • kinome network • hubs • centrosome • signal transduction • carcinogenesis

Introduction

Physical protein–protein interactions (PPIs) are fundamental to all biological processes, which are integrated by large, complex networks. Analysis of PPI networks provides novel insights into protein function as it indicates a possible biological role for a protein regarding the physical interactions in which this protein participates. Moreover, interaction networks are the focus in the systems biology field, as they help to unravel how cellular networks are organized in time and space.¹

Until recently, classical random network theory^{2,3} was used to model complex networks. It assumes that any two nodes (proteins) in a homogeneous network are connected with random probability p and the degrees of the nodes follow a Poisson distribution, which has a strong peak at the average degree, K . To explain the heterogeneous nature of complex networks, a “scale-free” model was recently proposed in which the degree distribution in many large networks follows a power-law [$P(k) \approx k^{-\gamma}$].^{4,5} A remarkable characteristic of this distribution is that most of the nodes within these networks have very few links (k ; interactions), with only a few of them being highly connected (hubs). The existence of hubs and their minor frequency provides two important features to large complex networks: increased robustness with regard to random defects and shorter path length (distances) between any two nodes, that is, a signal can travel from any node to another by traversing a small number of intervening nodes.^{6,7}

* To whom correspondence should be addressed. Jörg Kobarg, Centro Nacional de Pesquisa em Energia e Materiais, Laboratório Nacional de Biociências, Rua Giuseppe Máximo Scolfaro 10.000, C.P. 6192, 13084-971 Campinas - SP, Brazil. Tel.: (+55)19-3512-1125. Fax: (+55)19-3512-1006. E-mail: jorg.kobarg@lnbio.org.br.

[†] Laboratório Nacional de Biociências.

[‡] Instituto de Biologia, Universidade Estadual de Campinas.

[§] Laboratório Nacional de Luz Síncrotron.

^{||} Instituto de Física “Gleb Wataghin”, Universidade Estadual de Campinas.

Within this context, the human kinome and all the interactions made by protein kinases comprise an important network of vital regulators of cellular functions, since kinase directed phosphorylation is one of the most common forms of post-translational modification in the cell environment.^{8,9} Furthermore, the protein kinase gene family is the domain most commonly found among known cancer genes¹⁰ and thus deserves in-depth scrutiny.

The NIMA-related kinases (Neks) are widespread among eukaryotes. In mammalian, they represent an evolutionarily conserved family of 11 serine/threonine kinases, containing 40–45% identity to the *Aspergillus nidulans* mitotic regulator NIMA (never in mitosis gene A) within their catalytic domain. NIMA kinase is involved in multiple aspects of mitotic progression including mitotic entry, chromatin condensation, spindle organization, and cytokinesis.¹¹ Among the mammalian Nek proteins, those that have been studied appear to have cell cycle-related functions^{12–20} and are described as related to pathologies.^{21–27}

Human Nek6 (hNek6) was recently found to be linked to carcinogenesis. It is overexpressed in gastric cancer and up-regulation of Nek6 mRNA correlates with the peptidyl-prolyl isomerase Pin1 upregulation in 70% of hepatic cell carcinomas, while the overexpression of a catalytically inactive Nek6 reduces the growth rate of human breast cancer cells.^{28,29,14} Moreover, in a large-scale screening of serine/threonine kinases on different types of human tumors, Nek6 was shown to be upregulated in non-Hodgkin's lymphomas and breast, colorectal, and lung tumors.³⁰ Recently, it was demonstrated that transcript, protein, and kinase activity levels of Nek6 were highly elevated in the malignant tumors and human cancer cell lines compared with normal tissue and fibroblast cells, indicating an important role for Nek6 in tumorigenesis.³¹ These facts highlight Nek6 as a potential chemotherapeutic target, but as for the majority of the Nek kinases, its interacting partners and signaling pathways are still unknown.

Here we describe the identification of a broad set of 66 novel hNek6 protein partners by yeast two-hybrid screens, which were classified into 18 Gene Ontology (GO) biological processes. All of the tested interactions were confirmed, and the majority of tested substrates were phosphorylated *in vitro* by hNek6. Notably, hNek6 unfolded N-terminal is important to mediate the interactions with its partners. These novel interactors also colocalized with hNek6 and γ -tubulin in human cells, indicating that hNek6 may interact with them in the centrosomes, where hNek6 was described previously to exert spindle formation and cell cycle related functions.²⁰ Our newly identified hNek6 protein partners show common functional and structural properties and provide new insights in how hNek6 may be involved in these novel signaling pathways as well as how it may regulate previously proposed ones. In a broader context, our analysis also showed that the human kinome is enriched in network hubs and that hNek6 could be classified as a high confidence hub kinase within a set of likely essential kinase genes.

Experimental Procedures

Plasmid Constructions. The full-length hNEK6 gene sequence was amplified from a human fetal brain cDNA library (Clontech). The PCR product was cloned into pGEM-T easy vector (Promega) and subcloned into *EcoRI* restriction site of the modified vector pBTM116KQ³² in fusion with the LexA DNA binding domain (Clontech). To express full-length hNek6 fused to a 6xHis tag, the full-length nucleotide sequence was PCR-

amplified using a specific primer set, 5'-CGGAATCCATATG-CAGGACAGCCCGCCAC-3' and 5'-GGGGAAGCTTTCAGGT-GCTGGACATCCAGATG-3', and then inserted into *NdeI* and *HindIII* restriction sites of the modified bacterial expression vector pET28a-TEV (Novagen/EMD Biosciences). To express truncated hNek6 corresponding to its kinase domain only (the N-terminal region was deleted) fused to a 6xHis tag, another specific primer set was used 5'-CGAATCCATATGTTCCA-GATCGAAAAGAAGATAGG-3' and 5'-GGGGAAGCTTTCAGGT-GCTGGACATCCAGATG-3', and the PCR-product was also inserted into pET28a-TEV using the same restriction sites. Selected nucleotide sequences encoding the full-length or truncated proteins identified to interact with the full-length hNek6 were subcloned from the vector pACT2 (Clontech) into various types of the bacterial expression vector pGEX (GE Healthcare), which allows the expression of the proteins in the form of a Glutathione S-transferase (GST) fusion. The orientation, frame, and correctness of sequence of each DNA insert were confirmed by restriction endonuclease analysis and automated DNA sequencing.

Site-Directed Mutagenesis. The hNek6 activation loop mutation S206A was introduced by PCR-based mutagenesis of the pET28a-TEV-hNEK6 construct using the Quick-Change Site-Directed Mutagenesis kit (Stratagene). Mutation was confirmed by DNA sequencing.

Yeast Two-Hybrid Screens and DNA Sequence Analysis. The yeast two-hybrid screens³³ of three human cDNA libraries (Clontech) - fetal brain, bone marrow and leucocyte - were performed by using *S. cerevisiae* strain L40 (trp1–901, his3 Δ 200, leu2–3, ade2 LYS2::(*lexAop*)4-HIS3 URA3::(*lexAop*)8-lac GAL4) and hNEK6 gene as a bait fused to the yeast LexA DNA binding domain sequence in the modified vector pBTM116KQ.³² The autonomous activation test for HIS3 was performed for yeast cells transformed with both the bait construct (pBTM116KQ-hNEK6) and the empty prey vector (pACT2) in minimal medium plates without tryptophan, leucine and histidine but containing 0, 5, 10, 20, 30, 50, 70, and 100 mM of 3-Amino-1,2,4-triazole (3-AT), the inhibitor of His3p. Furthermore, the autonomous activation of LacZ was measured by the β -galactosidase filter assay described before.^{23,34} Yeast cells were transformed according to the protocols supplied by Clontech. As long as the bait construction autoactivates the yeast reporter genes, but the cell growth is disrupted in the presence of 30 mM of 3-AT, the screenings were performed in minimal medium plates without tryptophan, leucine and histidine but containing 3-AT. Half of the transformed cells were plated on selective medium containing 30 mM 3-AT, and the other half was plated on selective medium containing 50 mM 3-AT. All grown colonies were plated in resuspended drops of 4.0 μ L on selective medium containing 0, 30, 50, 70, and 100 mM 3-AT to confirm and compare their growth levels, and only the ones showing the best growth in all conditions were selected for further analysis. Recombinant pACT2 plasmids of positive clones were isolated and their DNA inserts sequenced with a 3130xl Genetic Analyzer (Applied Biosystems). The obtained DNA sequence data were compared with sequences in the NCBI data bank using the BLASTX 2.2.12 program (<http://www.ncbi.nlm.nih.gov/BLAST/>). Sequences that corresponded to the noncoding region were eliminated. As frameshift mutations can lead to expression of the correct reading frame in yeast,³⁵ these sequences were retained for further analysis.

PPI Confirmation in Yeast Cells. Each prey plasmid DNA was cotransformed in the yeast strain L40 with the bait

construct pBTM116KQ-hNEK6 or the empty bait vector (pBTM116KQ). The presence of both types of plasmids (prey and bait vectors) was controlled by growth on minimal medium plates without tryptophan and leucine.³⁶ Yeast clones were then streaked in triplicate drops of 4.0 μ L on minimal medium plates without tryptophan, leucine, and histidine but containing 0, 30, 50, and 100 mM of 3-AT for testing their growth capacity under interaction-selective conditions. Clones containing the prey plasmid and the bait construct showing a higher level of growth compared to the ones containing the prey plasmid and the empty bait vector were selected positive for interaction.

Protein Expression and Purification. The GST fusions of the proteins identified in the yeast two-hybrid screens were expressed in *E. coli* BL21 (DE3) cells at 37 °C using 0.5 mM isopropyl 1-thio- β -D-galactopyranoside (IPTG) or in BL21 (DE3/pRARE) cells at 18 °C using 1.0 mM IPTG for 4 h.

Soluble full-length hNek6 wild-type, 6xHis-hNek6wt, and mutant, 6xHis-hNek6(S206A), or truncated hNek6 wild-type kinase domain, 6xHis-hNek6(Δ 1–44), fused to a 6xHis tag were purified for *in vitro* analysis from *E. coli* BL21 (DE3/pRARE) cells that were induced for 4 h at 18 °C (wild-type proteins) and 37 °C (mutant), using 1.0 and 0.5 mM IPTG, respectively. Cells were harvested and lysed in lysis buffer (50 mM HEPES, pH 7.5, 5 mM sodium phosphate, 300 mM NaCl, 5% glycerol, 20 mM imidazole) by sonication. Soluble and insoluble fractions were separated by centrifugation at 28 500 \times g for 40 min at 4 °C. The cleared supernatant was then loaded onto a HiTrap chelating column (GE Healthcare). Bound hNek6 was eluted in lysis buffer plus 300 mM imidazole.

Phosphorylation Sites Determination. For identification of phosphorylation sites by mass spectrometry, gel bands corresponding to 6xHis-hNek6wt (upper and lower bands) and 6xHis-hNek6(S206A) (single band) were excised and in-gel trypsin digestion was performed according to Hanna et al.³⁷ An aliquot (4.5 μ L) of the peptide mixture was separated by C18 (100 μ m \times 100 mm) RP-UPLC (nanoAcquity UPLC, Waters) coupled with nanoelectrospray tandem mass spectrometry on a Q-ToF Ultima API mass spectrometer (MicroMass/Waters) at a flow rate of 600 nL/min. The gradient was 0–80% acetonitrile in 0.1% formic acid over 45 min. The instrument was operated in the “top three” mode, in which one MS spectrum is acquired followed by MS/MS of the top three most-intense peaks detected. The resulting spectra were processed using Mascot Distiller 2.2.1.0, 2008, Matrix Science (MassLynx V4.1) and searched against human nonredundant protein database (NCBI) using Mascot, with carbamidomethylation as fixed modification, oxidation of methionine and phosphorylation of Ser, Thr, and Tyr as variable modifications, one trypsin missed cleavage and a tolerance of 0.1 Da for both precursor and fragment ions. The phosphorylation sites were manually validated.

In Vitro Binding Assays. One milliliter of soluble bacterial extracts of GST or GST fusion proteins was allowed to bind to 30 μ L of glutathione-Uniflow resin (Clontech) in PBS for 1 h at 4 °C. After incubation, the beads containing bound recombinant proteins were washed three times with PBS at 4 °C. 12.5 μ g of purified full-length 6xHis-hNek6wt or truncated 6xHis-hNek6(Δ 1–44) fusion proteins were added to the resins containing GST or GST fusion proteins and incubated for 2 h at 4 °C to allow protein–protein interactions to occur. The beads were then washed three times with 0.5 mL of PBS, followed by three washes with 0.5 mL of PBS containing 0.1% Triton X-100, then three washes with 0.5 mL of PBS only. Resin-

bound proteins were analyzed by SDS-PAGE and immunoblotting as previously described.^{23,34}

In Vitro Kinase Assays. Reaction mixtures in kinase buffer (50 mM MOPS, pH 7.4, 300 mM NaCl, 10 mM MgCl₂, 0.1 mM PMSF) containing 100 μ M ATP, 185 kBq [γ -³²P]ATP (222 TBq/mmol; NEN) and 0.1 μ g/ μ L of purified full-length 6xHis-hNek6wt or 6xHis-hNek6(S206A) recombinant proteins were incubated at 30 °C; 20 μ L aliquots were removed at the times indicated and the reactions were terminated by the addition of an SDS electrophoresis buffer. In parallel, 1 mL of soluble bacterial extracts containing GST or the indicated GST fusion proteins, and a whole lysate of empty pET28a vector (Novagen/EMD Biosciences) transformed BL21 cells also induced with IPTG, were allowed to bind to 30 μ L of glutathione-Uniflow resin (Clontech) in PBS for 1 h at 4 °C and then washed three times with kinase buffer. Twenty microliters of reaction mixtures equally prepared were added to the resins containing GST or unspecific bound proteins from the whole lysate as controls, or GST fusion proteins as substrates, and incubated at 30 °C for 30 min. The reaction products were separated on SDS-PAGE and phosphorylated proteins were detected by autoradiography.

Cell Culture. Human monocytic leukemic cells (THP1) were kindly provided from the Department of Clinical Medicine, Universidade Estadual de Campinas, by Dr. Kleber G. Franchini. Cell suspension was grown in a humidified 5% CO₂ atmosphere at 37 °C in RPMI culture medium supplemented with 10% FBS and penicillin/streptomycin (100 units/mL). Adherent HEK293 cells were cultivated in DMEM medium supplemented with 10% FBS and penicillin/streptomycin (100 units/mL) in the same conditions.

Immunofluorescence, Commercial Antibodies and Confocal Microscopy. THP1 nonadherent cells (7.5×10^4) were plated on coverslips by centrifugation with a cytospin, while adherent HEK293 cells were cultivated on coverslips at a concentration of 2.5×10^4 cells/plate (24 well). Cells were fixed in a solution containing 2% (w/v) paraformaldehyde, 50 μ M Taxol and 50 mM EGTA at room temperature for 20 min and then permeabilized and blocked in a mixture of 0.3% (v/v) Triton X-100, and 3% (w/v) glycine solution in PBS at room temperature for 30 min. After blocking in 0.1% (w/v) sterile BSA in PBS for 1 h, coverslips were incubated for 2 h with goat or rabbit polyclonal anti-NEK6, goat polyclonal anti-RAD26L, goat polyclonal anti-TRIP4, rabbit polyclonal anti-P2P-R(RBBP6), rabbit polyclonal anti-ATF4, rabbit polyclonal anti-CIR, mouse monoclonal anti-CDC42, mouse monoclonal anti-RPS7, mouse monoclonal anti-NEK9, mouse monoclonal anti-RELB, or mouse monoclonal anti-PHF1 primary antibodies (Santa Cruz Biotechnology) diluted 1:100, or with mouse monoclonal anti- γ -tubulin (Sigma) diluted 1:5000, in PBS containing 0.1% BSA (w/v). Subsequently, the cells were incubated at room temperature for 1 h with FITC or rhodamine-conjugated secondary antibodies (1:200, Santa Cruz Biotechnology). DAPI dye was used to stain the nuclei. Cell cultures prepared for immunofluorescence were examined with Nikon fluorescence microscope. Confocal microscopy analyses were performed on a Zeiss LSM 510 confocal laser scanning microscope (Zeiss LSM 510; Carl Zeiss, Jena, Germany). Individual random fields were collected using a Plan-Apochromat 63x/1.4 Oil DIC immersion objective lens. Images were processed using LSM 5 Image Examiner or ZEN 2009 Light Edition (Carl Zeiss) softwares.

In Vivo Binding Assays. THP1 cells were harvested (approximately 1×10^7 cells) and washed in PBS, resuspended in 200 μ L of immunoprecipitation buffer (IP buffer) containing

50 mM Tris-HCl (pH 7.2), 100 mM NaCl, 1 mM EDTA, 0.1% NP-40, 10 mM β -glycerophosphate, 1 mM sodium orthovanadate, 1 mM PMSF plus 0.5% protease inhibitor cocktail, and sonicated on ice. After centrifugation ($10\,000\times g$ at 4°C) for 10 min the supernatant was incubated with a goat anti-NEK6 polyclonal antibody (Santa Cruz Biotechnology) in G-Sepharose 4 fast flow beads (GE Healthcare) for 8 h. As a negative control we used the goat polyclonal antibody anti-GM-CSF (Santa Cruz Biotechnology), since Granulocyte macrophage colony-stimulating factor (GM-CSF) is not described to interact with Nek6 or RelB. Next, beads were thoroughly washed with the IP buffer and then subjected to Western blotting with goat polyclonal anti-NEK6 or mouse monoclonal anti-RELB primary antibodies (Santa Cruz Biotechnology) and HRP-conjugated rabbit anti-goat (Sigma) or goat anti-mouse (Santa Cruz Biotechnology) secondary antibodies.

In Silico PPI Analysis and Network Parameters. The biological processes and cellular localization of hNek6 novel interacting proteins were based on the Gene Ontology (GO; <http://www.geneontology.org/>) and Uniprot (<http://www.uniprot.org/>) databases, and the gene coexpression analysis was accessed by Gemma database and software system (<http://www.chibi.ubc.ca/Gemma/>); the prediction of disordered amino acid residues in the retrieved protein sequences was calculated by PONDR VL-XT predictor (<http://www.pondr.com/>), the domain composition of these sequences was obtained by Pfam (<http://pfam.sanger.ac.uk/>), PROSITE (<http://www.expasy.ch/prosite/>) or InterPro (<http://www.ebi.ac.uk/interpro/>) databases, and putative phosphorylation sites by hNek6 or NIMA were determined by searching for similar consensus sequences as described by Lizcano et al.³⁸ or Lu et al.,³⁹ respectively. The lethality phenotypes of human protein kinases were accessed by the Knockout Mouse Project (KOMP) Repository (<http://www.komp.org/>).

The May 1, 2009 release of interaction data (BIOGRID-ORGANISM-Homo_sapiens-2.0.52.tab.txt) was downloaded from the BioGRID (<http://www.thebiogrid.org/>) to be analyzed and visualized by Osprey 1.2.0. software (<http://biodata.mshri.on.ca/osprey/>). For analysis of physical interactions, six networks were constructed from the BioGRID: (1) NIN (hNek6 Interaction Network; 92 nodes, 114 links), including the hNek6 interactions identified by our yeast two-hybrid screens and the ones described in the human BioGRID; (2) PIN (Protein Interaction Network; 7,718 nodes and 49,368 links), including every physical interaction from the hand-curated literature citation interaction database and the hNek6 interactions identified by our yeast two-hybrid screens; (3) KIN (Kinase Interaction Network; 1,998 nodes and 4,327 links), including 366 kinases annotated in the human genome⁸ and their direct interacting proteins (including the novel hNek6 protein partners); (4) RPIN1 (Random Protein Interaction Network 1; 1,898 nodes and 2,248 links), including 366 randomly selected nodes from PIN and their links; (5) RPIN2 (Random Protein Interaction Network 2; 1,971 nodes and 2,497 links), including 366 randomly selected nodes from PIN and their links; and (6) RPIN3 (Random Protein Interaction Network 3; 1,871 nodes and 2,120 links), including 366 randomly selected nodes from PIN and their links. To statistically compare the connectivity among the proteins in the networks, the degree distribution $P(k)$ and the average degree (K) of each network was calculated as described by Stelzl et al.⁴⁰ For the degree distribution $P(k)$, the probability that a given protein interacts with exactly k other proteins was plotted against the number of links (k) in a

log–log plot; the degree exponents (γ) and R-squares were determined by linear fitting where $P(k)$ approximates a power-law: $P(k) \approx k^{-\gamma}$.

Results

Identification of Novel Human Nek6 Interacting Partners. To inhibit the observed autoactivation of hNek6 bait, the screens were performed in minimal medium plates without tryptophan, leucine and histidine but containing 30 or 50 mM 3-AT, since cell growth was disrupted in the presence of 30 mM of 3-AT. We employed the yeast two-hybrid system³³ for three human cDNA libraries—fetal brain, bone marrow, and leukocyte—using hNek6 as bait, and a total of about 1.5×10^6 transformants for each screen was plated. Streaked colonies showing the best growth in all conditions (from 30 to 100 mM 3-AT) had their prey plasmid DNAs extracted and sequenced. A total of 371 plasmid DNAs from positive clones were sequenced. One-hundred twenty-eight different prey proteins were identified, but only 66 were confirmed in yeast cells under interaction-selective conditions (Table S1, Supporting Information). These were classified into 18 functional categories based on the GO (<http://www.geneontology.org/>) biological processes (proteins may be found into more than one category) (Figure 1, Table S3, Supporting Information).

Experimental Confirmation of Interactions. To reduce false-positives and check if hNek6 may really interact with the proteins codified by the plasmids isolated in the yeast two-hybrid screens, two experiments were employed. First, we tested all 128 retrieved interacting proteins for their *in vivo* association with Nek6 in yeast cells based on their growth capacity under stringent interaction-selective conditions (see Experimental Procedures for details), yielding 66 confirmed interactions (Table S1, Supporting Information). Second, we selected 20 biologically relevant interacting proteins among the 66 confirmed, to test their *in vitro* association with hNek6 in pull-down assays. However, only 12 of the 20 subcloned cDNAs resulted in the expression of soluble proteins. The interaction of these proteins—Ankyrin repeat family A protein 2 (ANKRA2), Activating transcription factor 4 (ATF4), Cell division cycle 42 (Cdc42; CDC42), CBF1 interacting corepressor (CIR), Promyelocytic leukemia-retinoic acid receptor alpha (PML-RAR α) regulated adaptor molecule 1 (PRAM-1; PRAM1), Peroxiredoxin 3 (Prx-III; PRDX3), Pleiotrophin (PTN), Putative DNA repair and recombination protein RAD26-like (RAD26L), Retinoblastoma-binding protein 6 (RBQ-1; RBBP6), Ribosomal protein S7 (RPS7), Sorting nexin 26 (SNX26) and Thyroid hormone receptor interactor 4 (TRIP-4; TRIP4)—in fusion with GST, with full-length wild-type hNek6 in fusion with a 6xHis tag (6xHis-hNek6wt) was then tested by *in vitro* pull-down assays, and all 12 interactions were confirmed (Figure 2). The high number of washes suggests that the interactions were strong. The specificity of the observed interactions was demonstrated because no interaction of hNek6 with free GST was observed under the same conditions. The smaller bands seen in the anti-GST Western blotting are degradation products probably due to expression and purification procedures (Figure 2). Table 1 summarizes the screenings characteristics and principal biological processes of the proteins confirmed to interact with hNek6.

Human Nek6 N-Terminal is Important for the Interactions with its Partners. Human Nek6 and Nek7 are the smallest mammalian Neks and the only ones in the family consisting of a C-terminal catalytic domain and a short N-terminal

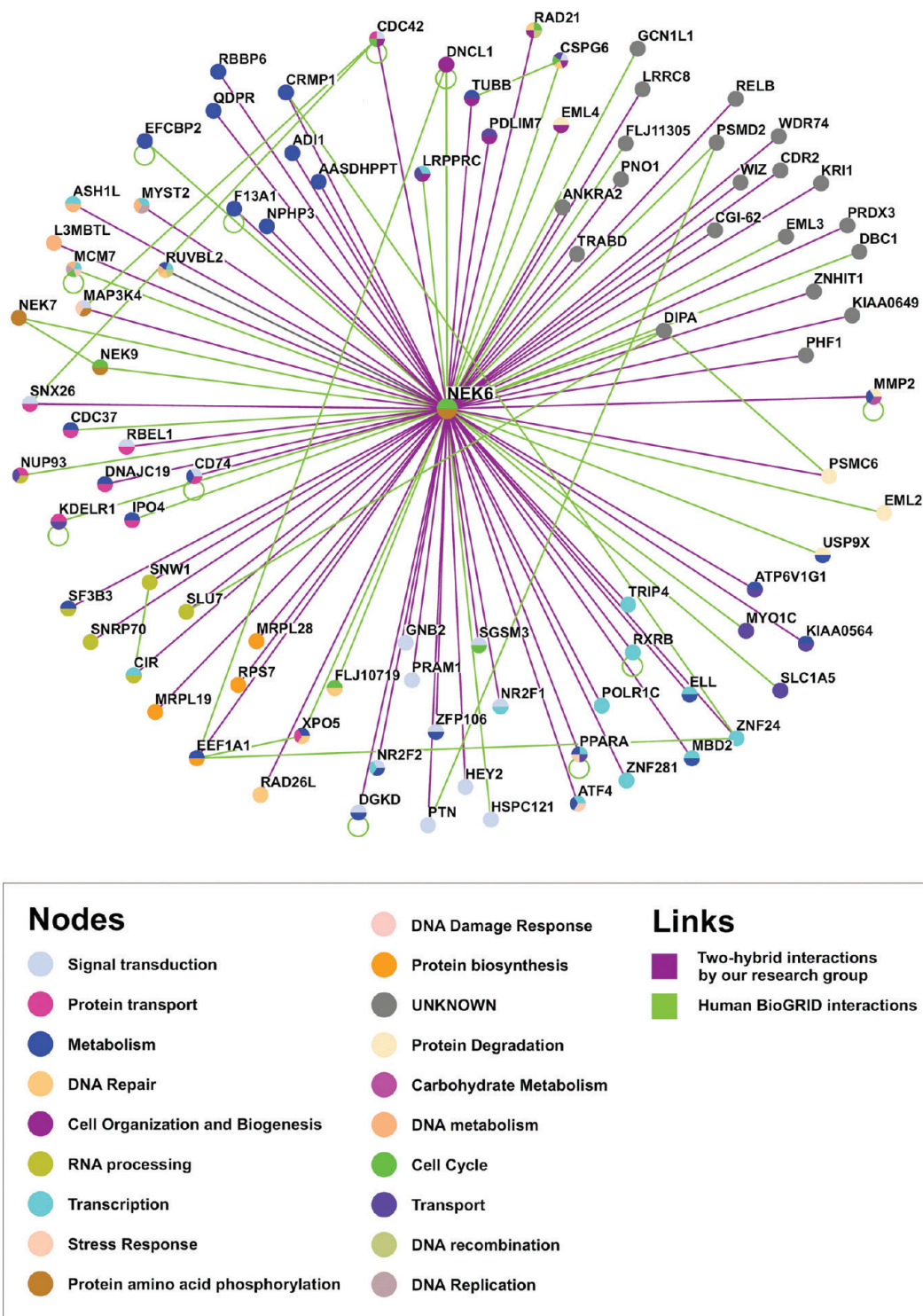


Figure 1. Human Nek6 interaction network (NIN). The network has 92 proteins (colored nodes, including the bait hNek6 and its partners identified by our yeast two-hybrid screens and the ones described in the human BioGRID database) and 114 interactions involving them (purple and green links), including the known interactions within all the proteins. The nodes are colored based on the GO biological processes. The purple links represent the new interactions connecting the bait hNek6 and the prey proteins identified by our screens; the green links refer to the human BioGRID interactions. The network was generated using Osprey 1.2.0. software.

extension, while the other Neks presents a conserved N-terminal catalytic domain and usually long C-terminal regulatory domains.²⁰ This fact associated to modeling and disorder prediction analysis that indicate an unfolded structure for hNek6 N-terminal (data not shown), lead us to confirm if this short region of approximately 40 amino acid residues is important for hNek6 interactions. We then retested eight

confirmed interaction partners—Prx-III, CDC42, Sorting nexin 26, Ankyrin repeat family A protein 2, RBQ-1, Rad26-like, TRIP4 and Ribosomal protein S7 (data not shown)—fused to GST by *in vitro* pull-down assays with 6xHis-hNek6wt and 6xHis-hNek6(Δ 1–44) to see if hNek6 kinase domain (without its N-terminal extension) was sufficient to allow coprecipitation by the interaction partners. Figure 3 shows that the kinase domain

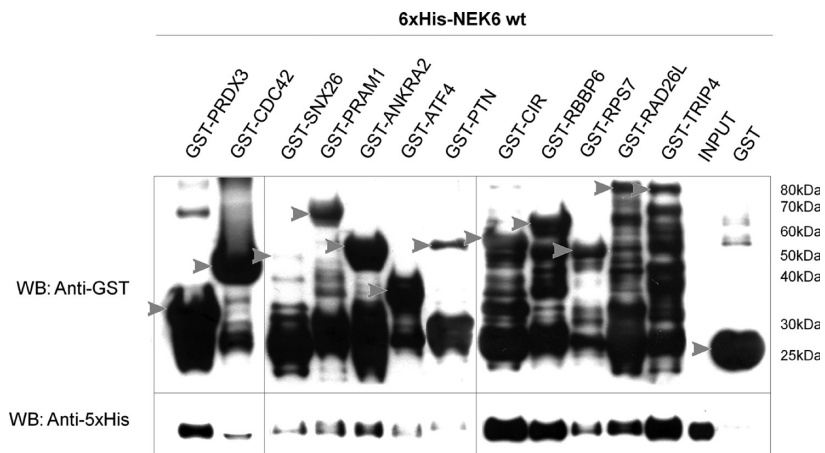


Figure 2. *In vitro* confirmation of the interaction between human Nek6 and the selected proteins retrieved in the yeast two-hybrid screens. *In vitro* pull-down assays between full-length 6xHis-hNek6wt and the indicated protein fragments fused to GST (see Table 1 for details). Free GST control protein or the indicated GST fusion proteins were loaded on glutathione-Sepharose beads, and after washing the beads, they were incubated with the purified full-length 6xHis-Nek6wt fusion protein. After high stringency washes using PBS/Triton X-100, the samples were loaded in replicate SDS-PAGE gels for blot transfer. Monoclonal mouse anti-GST antibody 5.3.3 and a mouse anti-5xHis antibody were used for detection of GST- or His-tagged fusion proteins, respectively. The gray arrows indicate the GST-fusion proteins in anti-GST Western blotting.

alone was not efficiently coprecipitated with any of the interacting proteins, indicating a possible role for hNek6 N-terminal as a regulatory domain, mediating hNek6 interactions.

Human Nek6 is Purified From Bacteria as a Phosphorylated Protein. 6xHis-hNek6wt recombinant protein purified from *E. coli* migrates as a doublet on SDS-PAGE as previously described for the protein expressed in human cells,¹⁵ whereas the activation loop mutant 6xHis-hNek6(S206A) migrates as a single band more rapid in mobility to the more rapidly migrating band of wild-type Nek6 (Figure 4C) or as a doublet with an additional lower band. As only the slower moving band of wild-type hNek6 exhibits autophosphorylation and only this upper band catalyzes substrate phosphorylation, indicating that the activity of hNek6 is dependent on hNek6 polypeptide phosphorylation,¹⁵ we aimed to identify by mass spectrometry possible phosphorylation sites in 6xHis-hNek6wt and 6xHis-hNek6(S206A) to compare their phosphorylation and activation status and check how similar they are to the one expressed in human cells.

6xHis-hNek6wt and 6xHis-hNek6(S206A) were subjected to SDS-PAGE in replicate gels for Pro-Q Diamond (Figure 4A), Sypro Ruby (Figure 4B), and Coomassie Blue (Figure 4C) staining. Pro-Q Diamond staining was used for in-gel detection of phosphate groups attached to serine, threonine, or tyrosine residues, showing specific staining for the wild-type doublet and the mutant single band as the molecular weight standard proteins were not detected. Sypro Ruby was used after Pro-Q Diamond staining in the same gel for detection of the total amount of proteins. As both wild-type and mutant hNek6 showed phosphoprotein staining, the corresponding bands were analyzed by liquid chromatography coupled with mass spectrometry in tandem (LC-MS/MS) to confirm and identify the sites of phosphorylation. 6xHis-hNek6wt showed the same pattern of phosphopeptides as described for the recombinant protein expressed in human cells,¹⁵ being probably very similar to each other. The phosphorylated Ser²⁰⁶ was confirmed and some evidence suggest that Thr²⁰¹ or Thr²⁰² is also phosphorylated in the same identified phosphopeptide F¹⁹⁶FSSETTAA-HpSLVGTPYYMSPER²¹⁸, whereas 6xHis-hNek6(S206A), as expected, yielded this peptide with spectra confirming the

mutation S206A, with an additional oxidized Met²¹⁴ and a phosphorylated Thr residue (Thr²⁰¹ or Thr²⁰²). Another phosphopeptide H³²PNTLpSFR³⁹ was also identified for 6xHis-hNek6wt, and evidence suggest that Ser³⁷ is phosphorylated (Figure 4D). Therefore, we propose that the more rapid electrophoretic migration of the mutated hNek6 compared to the wild-type protein is due to the lack of phosphorylation at Ser²⁰⁶ which is necessary for its increased activation status¹⁵ that may be responsible for autophosphorylation at other sites, as observed for the wild-type protein.

Human Nek6 Interacting Partners are also Putative Substrates. To confirm whether hNek6 identified protein partners could also behave as substrates and if the full-length 6xHis-hNek6wt and 6xHis-hNek6(S206A) have the ability to autophosphorylate, *in vitro* kinase assays were performed. As expected, in the presence of radiolabeled ATP, wild-type hNek6 autophosphorylates within a short period of time (15 min) while the mutant hNek6(S206A) showed autophosphorylation only when incubated for a much longer time (Figure 5A). In a longer autoradiography film exposition, the mutant was visualized to autophosphorylate from 30 min to 12 h, although in a considerable lesser degree when compared to the wild-type (data not shown). Furthermore, 6xHis-hNek6wt could strongly phosphorylate six proteins in fusion with GST (Activating transcription factor 4, CBF1 interacting corepressor, Pleiotrophin, RAD26-like, RBQ-1 and TRIP-4) of seven tested in total (Figure 5B). Interestingly, all proteins phosphorylated have putative consensus phosphorylation sites for hNek6 (Tables 2 and S2, Supporting Information). Ribosomal protein S7 seems not to be phosphorylated by hNek6, although also showing a putative phosphorylation site, which might not be the preferable one. For the six proteins, some smaller degradation products were also phosphorylated. On the other hand, 6xHis-hNek6(S206A) could not phosphorylate any of the proteins (except maybe for a little fraction of CBF1 interacting corepressor and RBQ-1) (Figure 5B), which confirms the specificity of 6xHis-hNek6wt phosphorylation against these six putative substrates and suggests that they could be *in vivo* substrates as well. As expected, the negative control proteins in the whole lysate (LYSATE lanes) and the GST protein alone (GST lanes) were

Table 1. Human Nek6 Interacting Proteins Identified by the Yeast Two-Hybrid System Screens (only interactions that were confirmed by pull-down are shown here)

protein interacting with hNek6 (aliases) ^a	gene	accession no.	coded protein residues (retrieved/complete sequence) ^b	expressed protein length (kDa) ^c	frame	redundancy in library ^d			growth score ^e	biological process (GO) ^f
						FB	BM	L		
cell division cycle 42 (GTP binding protein, 25 kDa)	CDC42	AAH03682.1	1–191/191	48	+2	1			2/1	Cell organization and biogenesis
Putative DNA repair and recombination protein RAD26-like	RAD26L	A4D997.3	1–531/531	87	+1	2			3/1	DNA repair
retinoblastoma-binding protein 6 (p53-associated cellular protein Testis-derived, P2P-R, RBQ-1)	RBBP6	BAC77636.1	1–259/1792	57	+1			1	4/1	Metabolism
NIMA-related kinase 9 (Nek9)	NEK9	AAH93881.1	806–979/979	–	+2	1		1	4/1	Protein amino acid phosphorylation
ribosomal protein S7	RPS7	AAH02866.1	1–194/194	49	+1	11	58	58	4/1	Protein biosynthesis
sorting nexin 26 (TC10/CDC42 GTPase-activating protein)	SNX26	O14559.2	1115–1287/1287	45	+1	1			4/1	Protein transport
CBF1 interacting corepressor	CIR	AAH46098.1	1–240/450	55	+1	3			4/1	RNA processing
PML-RARA regulated adaptor molecule 1	PRAM1	AAH28012.1	360–670/670	61	+1		2	2	4/1	Signal transduction
pleiotrophin (heparin binding growth factor 8, neurite growth-promoting factor 1), isoform CRA_c	PTN	AAH05916.1	1–168/168	49	+1	31	1		4/1	Signal transduction
activating transcription factor 4 (cAMP-responsive element-binding protein 2, CREB-2)	ATF4	AAH16855.1	252–351/351	38	+1	1	6	3	2/0	Stress response
thyroid hormone receptor interactor 4 (TRIP-4, ASC-1, activating signal cointegrator 1)	TRIP4	AAH12448.1	46–581/581	87	+1	2		1	2/1	Transcription
ankyrin repeat family A protein 2	ANKRA2	AAH12917.1	78–313/313	52	+1	2			4/1	UNKNOWN
peroxiredoxin 3 (Prx-III, AOP-1, HBC189)	PRDX3	AAH08435.1	183–256/256	35	+1		1		4/1	UNKNOWN

^a Results obtained from BLASTX (GenBank). ^b It is depicted the minimum length of the retrieved sequences which could be visualized by forward DNA sequencing only. ^c Approximated length of the proteins expressed as a GST fusion in *E. coli*. ^d Absolute number of sequences retrieved from each human library (FB: fetal brain, BM: bone marrow, L: leukocyte). ^e The numbers (scores 0–4) refer to the relative growth levels of the yeast clones after co-transformation of each retrieved sequence in pACT2 vector and the bait construction pBTM116KQ-hNEK6 (x/–) or the empty pBTM116KQ vector (–/Y) when streaked in triplicate drops on minimal medium plates containing 3-AT e.g. 2/1 indicates twice the growth for CDC42 in the presence of hNEK6 relative to the empty vector. ^f Biological process based on the GO database (other functions may be known; see also Table 3).

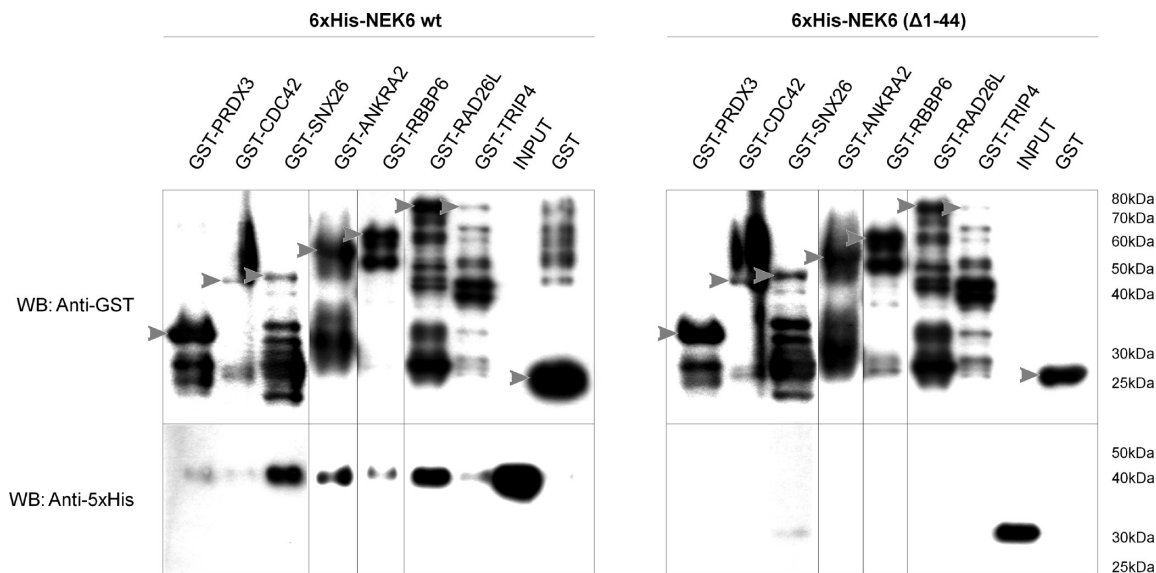


Figure 3. Interaction of hNek6 with seven selected proteins shows that its N-terminal domain is essential to mediate the interactions. *In vitro* pull-down assays between the truncated 6xHis-hNek6(Δ 1–44) and the indicated protein fragments fused to GST. The gray arrows indicate the GST-fusion proteins in anti-GST Western blotting.

not phosphorylated by wild-type or mutant hNek6, the phosphorylation being thus specific for the proteins tested. Moreover, wild-type hNek6 was shown to autophosphorylate in all conditions (Figure 4B, 32 P Autorad.), while mutant hNek6 autophosphorylation was detected only at high protein quantities (Figure 4B, 32 P Autorad., INPUT lane).

Human Nek6 Colocalizes with its Interacting Partners to the Centrosome in Human Cells and Interacts *in vivo* with the Transcription Factor RelB. Endogenous hNek6 interacts and colocalizes with γ -tubulin in HeLa cells.²⁰ Here, we observed by confocal and fluorescence microscope that hNek6 colocalizes with Activating transcription factor 4, CBF1 interacting corepressor, Cdc42, Ribosomal protein S7, Nek9, transcription factor RelB (RELB), PHD finger protein 1 (PHF1), Rad26-like, TRIP-4 and RBQ-1 in HEK293 cells (Figure 6A–J, Figure S1, Supporting Information). The same colocalization pattern was observed for these proteins in THP1 cells (data not shown). These *in vivo* subcellular colocalization studies also showed that Activating transcription factor 4 and CBF1 interacting corepressor, besides hNek6, colocalize with γ -tubulin in HEK293 cells (Figure 7A–C), indicating that both novel protein partners may interact with hNek6 in the centrosomes. As the same pattern of colocalization with hNek6 was observed for Cdc42, Ribosomal protein S7, Nek9, RelB, PHF1, Rad26-like, TRIP-4 and RBQ-1 (both proteins localized in a punctate perinuclear region), it strongly suggests that these interactions may also occur in the centrosomes. In the case of RelB, regarding its important function in the nuclear factor κ B (NF- κ B) signaling, and considering the difficulties in expressing it in bacteria as a soluble protein for *in vitro* pull-down assays, we developed immunoprecipitation assays using THP1 cells, which enabled us to confirm its interaction with hNek6 (Figure 6K).

Human Nek6 Interacting Partners Show Common Functional and Structural Properties. Biological Processes Enrichment. To visualize and compare the functional and structural properties within hNek6 interacting proteins identified by our yeast two-hybrid screens, computational analyses were carried out. As in the literature hNek6 was described to have other

protein partners discovered by large-scale experiments,^{41,42} we used the hand-curated literature citation interaction database, BioGRID, to construct a network composed of all hNek6 protein partners, including the novel ones identified by our screens: NIN (hNek6 Interaction Network) (Figure 1). The resultant NIN was analyzed using Osprey 1.2.0. software (<http://biodata.mshri.on.ca/osprey/>) to access the GO biological processes and cellular components for each protein in NIN. It is interesting to note that the proteins retrieved in our screenings and all others from the BioGRID are distributed in essentially the same GO biological process categories, in a way validating the putative signaling pathways that hNek6 is involved. Considering only the novel interactors identified by our screenings, it is notable that the analysis showed enrichment in processes such as Signal Transduction (21%) and Transcription (21%), since the connectivity of a protein is related to its function⁴³ and high connectivity is often associated with proteins involved in signaling and transcription.⁴⁴

Cross-Referencing Gene Coexpression Data. Increased similarity of gene expression profiles for genes encoding interacting proteins has been demonstrated in yeast,⁴⁵ while preliminary evidence in higher eukaryotes has been reported for *Caenorhabditis elegans*⁴⁶ and humans.^{47,42} Moreover, studies of expression profiles in *Sacharomyces cerevisiae* protein–protein interaction network led to the identification of two types of hub proteins: static hubs (party hubs) and dynamic hubs (date hubs), where party hubs have multiple simultaneous interactions and high levels of coexpression with their partners, while date hubs have multiple sequential interactions separated in time or in space.⁴⁸ Here we used a compendium of coexpression measurements generated from hundreds of public microarray data sets,⁴⁹ to search for coexpression data within the prey proteins identified to interact with hNek6. Using each prey protein/gene as a search query at Gemma database (<http://www.chibi.ubc.ca/Gemma/>), many were found as coexpressed genes (Table S3, Supporting Information), although none was found to coexpress with hNek6. In most cases of coexpression where both genes were involved in the same biological processes, these corresponded to Transcription, that is, His-

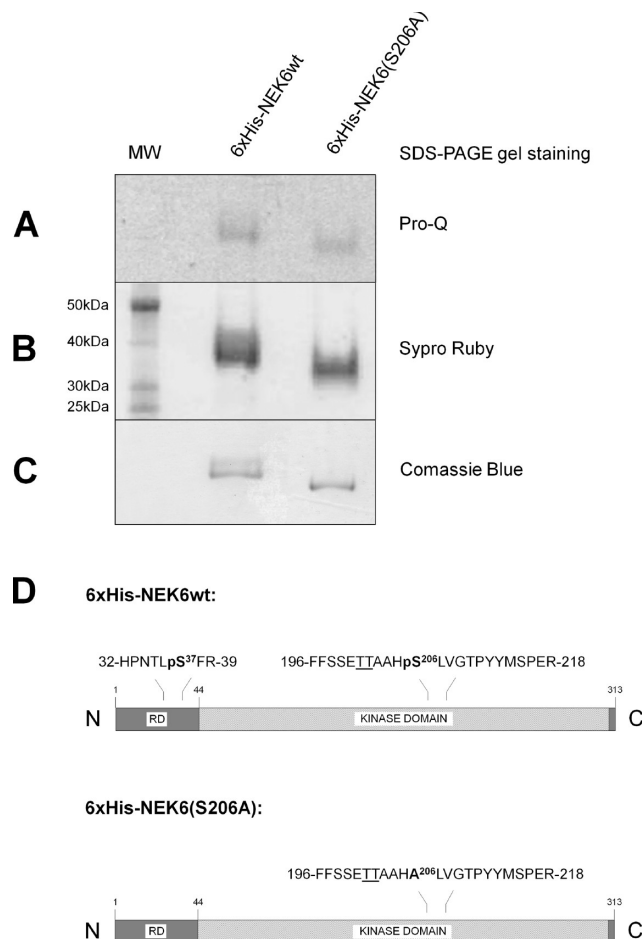


Figure 4. Human Nek6 autophosphorylates when expressed in *E. coli*. Purified recombinant 6xHis-hNek6wt is resolved as a doublet in SDS-PAGE and 6xHis-hNek6(S206A) predominantly as a single band. Bands corresponding to 6xHis-hNek6wt and 6xHis-hNek6(S206A) were excised, digested *in situ* with trypsin, and analyzed by liquid chromatography/MS/MS. (A) Pro-Q Diamond-stained gel shows the phosphorylated proteins. (B) Sypro Ruby-stained gel shows the total amount of proteins. (C) Coomassie Blue-stained gel shows the difference in electrophoretic mobility for both proteins. (D) Schematic representation of the wild-type and mutant hNek6 proteins. 6xHis-hNek6wt shows specific Ser²⁰⁶ autophosphorylation as identified by MS/MS (RD, regulatory domain; MW, BenchMark molecular weight standard; it is not present in Coomassie Blue-stained gel).

tone-lysine N-methyltransferase ash1 (ASHL1), Methyl-CpG binding domain protein 2 (MBD2), Nuclear receptor subfamily 2 group F member 2 (NR2F2) and Retinoic acid receptor RXR-beta (RXRB); TRIP-4 and MYST histone acetyltransferase 2 (MYST2). Apparently, hNek6 interacting proteins form groups of coexpressed proteins related in function, which are separated into different biological processes, or modules,⁵⁰ while hNek6 may interact with them in a nonsimultaneous way at different times and/or locations in the cell.

Consensus Phosphorylation Site Analysis. Next, we sought to evaluate if the proteins retrieved in our yeast two-hybrid screens could be targets of hNek6 phosphorylation. The substrate specificities for NIMA³⁹ and hNek6³⁸ have been determined and revealed novel and unique nature of substrate recognition sites by this group of kinases. The recognition sites include a preferable phenylalanine (for NIMA) or leucine (for hNek6) or other hydrophobic residues at position -3 relative

to the phosphorylated Ser/Thr residue. We found that 53 proteins have the preferable -3 Leu, 18 proteins have the preferable -3 Leu and a $+1$ aromatic residue, 50 proteins have a -3 hydrophobic residue and a $+1$ Phe/Trp/Tyr/Leu/Met/Ile/Val/Arg/Lys residue (as described in a substitution chip by Lizzcano et al.³⁸), and three proteins have the -3 Phe (Table S2, Supporting Information). These results are in agreement with our *in vitro* kinase assays (Figure 5B), demonstrating that at least six proteins are likely to be hNek6 substrates *in vivo*.

Domain Composition and Disorder Prediction. The retrieved protein sequences were also analyzed for their structural properties concerning their domain composition and percentage of disordered amino acid residues. hNek6 protein partners showed to be organized in a wide variety of domain families (Table S3, Supporting Information), some of them being shared by the neighboring proteins, i.e. zing finger (134 proteins), Ras (2 proteins) and AAA domains (2 proteins). Short linear regions (proline-rich, arginine-rich and leucine-rich regions) and repeats (hemopexin, tetratricopeptide, G-beta and ankyrin) were also found to be recurrent. Another predominant characteristic among hNek6 interacting proteins is the presence of disordered regions, that is, regions that lack a clear structure. Table S3 shows the percentage of disordered residues among the proteins. The range of structural types fell into three broad classes (as indicated in the 'Percent disordered residues' column): mostly disordered (85–100% disordered; 3 proteins), partially disordered (15–85%; 64 proteins) and mostly ordered (0–15%; 1 protein). These regions have been suggested to be important for flexible or rapidly reversible binding^{51,52} and, interestingly, an investigation of the functions performed by intrinsically disordered regions reveals that they are often involved in molecular recognition and protein modifications, such as phosphorylation.⁵¹

Table 2 summarizes the putative phosphorylation sites by hNek6 and NIMA and Table 3 summarizes the domain composition, percentage of disordered residues, cellular localization, biological processes and gene coexpression *in silico* analysis for the proteins confirmed to interact with hNek6.

Human Nek6 is a Putative High Confidence Hub Kinase in a Kinome Enriched in Network Hubs. For analysis of the protein interaction data, we constructed two other major networks, aiming at a better comprehension concerning the connectivity among the proteins in each case: PIN (Protein Interaction Network) and KIN (Kinase Interaction Network) (Figure 8A and B). PIN represents the largest data set, composed of every physical interactions from the BioGRID and the novel ones identified by our screenings with hNek6. KIN was assembled from the concatenation of all kinases present in the BioGRID and all their partners (including the novel hNek6 interacting proteins), consisting of kinase–kinase and kinase–nonkinase interactions only.

We calculated the degree distribution $P(k)$ of the human proteins, for PIN and KIN, measuring the probability that a given protein interacts with exactly k other proteins. As KIN was constructed with the purpose to facilitate the connectivity analysis of the kinase group among all other groups of proteins in PIN, only the degree distribution for kinases are considered in KIN, since potential interactions between nonkinases were filtered. As shown in Figure 8, the degree distributions of the three networks approximate a power-law and hence are scale-free in topology,⁵³ which is in agreement with interaction studies for model organisms.⁴⁰ On average, proteins in PIN have 6.40 interaction partners. However, 5,329 proteins with k

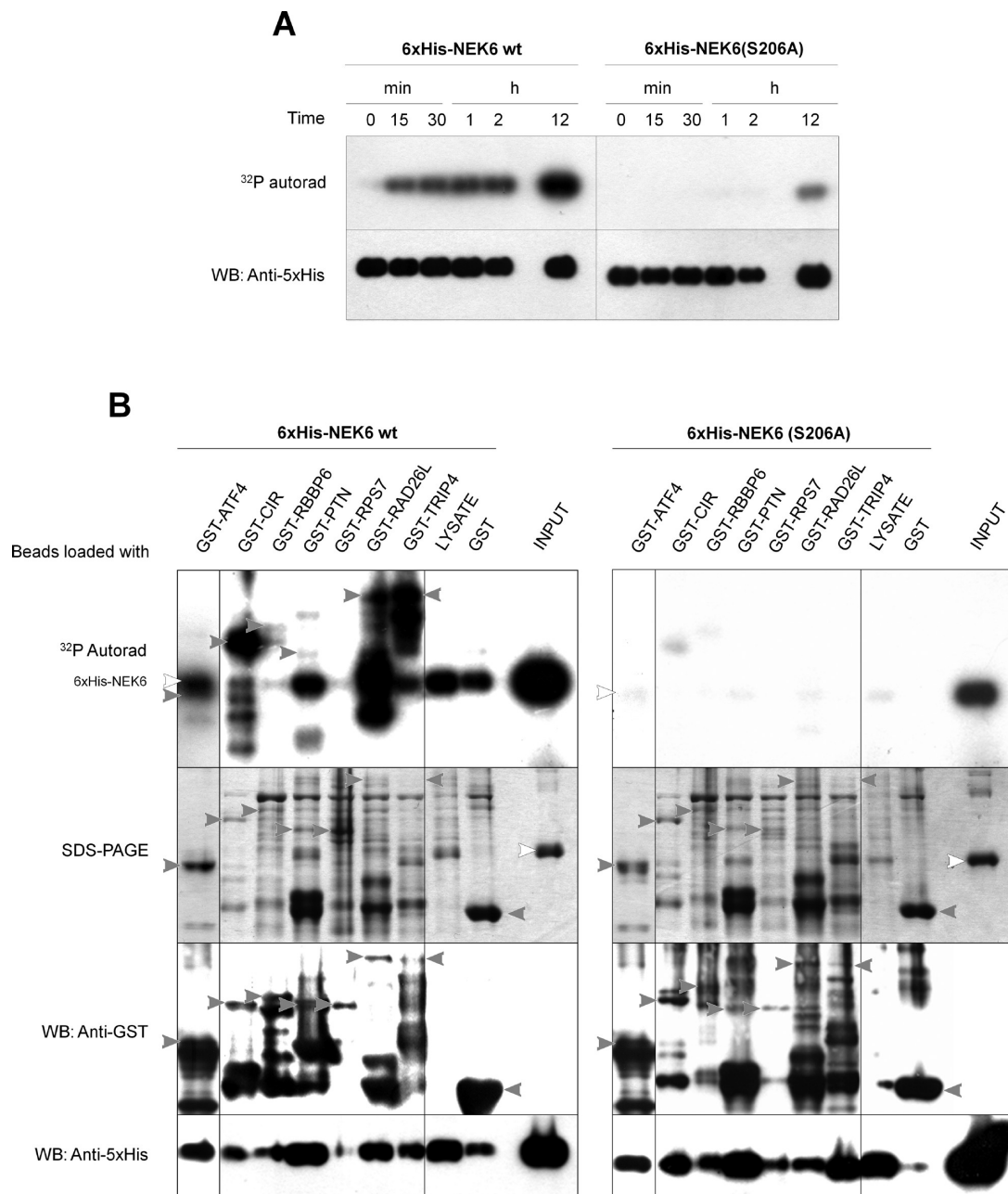


Figure 5. Human Nek6 *in vitro* autophosphorylation and phosphorylation of proteins retrieved in the yeast two-hybrid screens. (A) Time course of autophosphorylation of wild-type and mutant hNek6. Purified proteins were incubated at 30 °C in kinase buffer for the indicated times with 100 μ M ATP, and 185 kBq radiolabeled ATP. Resulting ³²P incorporation was monitored by SDS-PAGE coupled with autoradiography and blot transfer. (B) Qualitative phosphorylation by wild-type and mutant hNek6 of selected proteins identified in the yeast two-hybrid screens. Soluble extracts of these protein fragments in fusion with GST bound to glutathione-Uniflow resin (Clontech, CA) were incubated at 30 °C in kinase buffer for 30 min with 100 μ M ATP, 185 kBq radiolabeled ATP, and 0.1 μ g/ μ L of purified full-length 6xHis-hNek6wt or 6xHis-hNek6(S206A) recombinant proteins. The gray arrows indicate the positions of the GST fusion proteins in the ³²P autoradiography, SDS-PAGE and anti-GST Western blot, while the white arrows indicate the positions of the 6xHis-tagged proteins in the ³²P autoradiography and SDS-PAGE. INPUT lanes refer to the 6xHis-tagged proteins autophosphorylation without being added to the resin. Neither the lysate nor GST negative controls showed unspecific substrate phosphorylation, and all conditions showed wild-type hNek6 autophosphorylation, while mutant hNek6 autophosphorylation was detected only at high protein quantities (INPUT lane).

≤ 5 (nonhubs), 1,581 intermediately connected proteins with $5 < k < 15$, 808 hubs with $k \geq 15$, as well as 161 high confidence hubs⁵⁴ (defined here as hubs with more than 35 partners) were detected. On the other hand, kinases in KIN have a mean of 11.82 interactions. Notably, approximately 10% of the proteins in PIN are hubs ($k \geq 15$), whereas 25% are hubs in KIN, reflecting an enrichment of hub proteins among the kinase

group. In order to confirm this finding, 3 other major networks were constructed: RPIN1–3 (Random Protein Interaction Network 1–3) (Figure 8C–E). They were designed to group a random set of 366 proteins and their links, extracted from PIN, in order to compare their degree distribution analysis to the one obtained for the 366 kinases from KIN. As expected, KIN showed nearly twice the average degree compared to the

Table 2. Putative Phosphorylation Sites Present in Human Nek6 Interacting Proteins (only interactions that were confirmed by pull-down are shown here)

gene	coded protein residues (retrieved/complete sequence) ^a	putative phosphorylation sites by Nek6 ^b		
		general (L-X-X-S/T-X)	preferable (L-X-X-S/T-F/W/Y)	other acceptable (L/F/W/Y-X-X-S/T-F/W/Y/M/L/I/V/R/K)
CDC42	1–191/191	GLFDTAGQE LLVGTQIDL	CLLISYTTN	EYVPTVFDN NYAVTVMIG
RAD26L	1–531/531	TLPHTKKGQ RLENTMKDQ SLSVSHFSF PLYISNPVN		HFSFSKQSH FEVDSVSQF
RBBP6	1–259/1792	GLHISLCDL PLLTTEESL DLQITNAQT QLTKTANLA MLTNTGKYA		TYVISRTEP
NEK9	806–979/979	CLLGTDSR		
RPS7	1–194/194	KLDGSRLIK ELNITAAKE		
SNX26	1115–1287/1287	MLGQSPPLH PLHRSPDFL HLGYSAPQH	LNASYGML	DFLLSYPPA
CIR	1–240/450			EFLKSLTTK
PRAM1	360–670/670	DLRRTRSAA PLPSSASES GLVHSGGAR GLRPSHPPR		
PTN	1–168/168			EWQWSVCVP
ATF4	252–351/351	LCGSARPK		
TRIP4	46–581/581 3–581/581	RLDETIQAI TLVCTHEEQ GLDVSEEI	QLRKTFGLD ELQATYRLL	GWCLSVHQP LFCGTLVCT QYVLSIESA LYLATRIEQ
ANKRA2	78–313/313	LLANSLSVH SLACSKGYT MLESAGDP		
PRDX3	183–256/256			

^a Only minimum lengths of the retrieved sequences that could be visualized by forward DNA sequencing are depicted. ^b Phosphorylated residue (Ser/Thr) is in bold and the preferable –3 Leu or another acceptable hydrophobic residue, at position –3,³⁸ are underlined.

random networks (Figure 8F), reinforcing that human kinases should behave as general network hubs.

Moreover, the putative hubs identified by our analysis were compiled into a list including all high confidence hub kinases ranked by average degree (Table 4). This ranking showed that hNek6, with 91 protein partners, is a putative high confidence hub kinase found within the four highest connected kinases. Previous studies in yeast have demonstrated that proteins acting as hubs are three times more likely to be essential for cells than proteins with only a small number of links.⁵⁵ Therefore, the 25 high confidence hub kinases from KIN were used as query genes on the Knockout Mouse Project (KOMP) Repository (<http://www.komp.org/>) to identify the kinases with lethal phenotypes. Most of them (17 kinases) were found as essential genes (hNEK6 was considered a putative essential gene because its knockdown in HeLa cells resulted in increased apoptosis¹⁴) while only three kinase genes did not show knockout phenotype in mouse ('unknown' refers to nontested genes in KOMP) (Table 4). These remarkably results in a 68% probability of lethality attributed to random deletion of one of the 25 high confidence hubs and indicates a likely tendency for hub kinases to be preserved in an evolutionary perspective. Another previous study in yeast revealed a 32% chance of lethality among 19 high confidence kinase hubs.⁵⁴

Discussion

The many interactors identified and confirmed show for the first time that hNek6 is a hub kinase possibly involved in several known or novel cellular pathways, such as cell cycle, DNA repair, actin cytoskeleton regulation, NF- κ B and Notch signalings, through interactions with and phosphorylation of proteins composed of disordered regions and diverse domains and repeats.

Cell Cycle Signaling. In the Cell Cycle category, it is important to point out that hNek9 was retrieved twice (2 clones) in our screenings, helping to validate our study, as hNek6 was

described to copurify with hNek9 in a specific interaction between the RCC1 domain and the coiled-coil motif of hNek9 (amino acids 732–891).¹⁷ Interestingly, among the 2 retrieved cDNA clones that suggested this interaction, both had substantially overlapping sequences (amino acids 635–860 and 806–979) with that described binding region (Table S3, Supporting Information). It is proposed that Nek9 acts upstream of Nek6 and Nek7 phosphorylating and activating these kinases specifically in mitosis.¹⁵ However, it is, to our knowledge, the first time that hNek9 and hNek6 are shown together in human cells colocalized in punctate perinuclear regions that strongly resemble the centrosomes (Figure 6E). Furthermore, Nek6, Nek7, Nek9 and also Nek1 localize to centrosomes, supporting the model that this is a major site of action for this family of kinases in spindle formation and other cell cycle related functions.^{18,20,12} In this context, Cdc42 was also retrieved in our screenings and was confirmed to interact with hNek6 *in vitro* (Figure 2) and to colocalize with it in human cells (Figure 6C). Notably, Cdc42 was described to be a regulator of centrosome organization and function during the cell cycle.⁵⁶

Another protein that deserves attention in our screenings and which interaction is still not well understood is the Ribosomal protein S7, representing 42.2% of the total cDNAs (127 clones). It also colocalized with hNek6 in punctate regions in human cells (Figure 6D), although it is a structural constituent of the 40S ribosome subunit related to Protein Biosynthesis. However, recent studies have shown that it interacts with the E3 ubiquitin-protein ligase Mdm2, modulating the p53-Mdm2 binding through the formation of a stable ternary complex that prevents p53 ubiquitination mediated by Mdm2, inhibiting cell proliferation and activating the apoptosis.⁵⁷

Cytoskeleton Organization Signaling. The Rho family of small GTPases plays important roles in cytoskeletal remodeling as well as membrane trafficking, transcriptional regulation, and cell growth, for example, Cdc42 triggers outgrowth of peripheral spike-like protrusions called filopodia.⁵⁸ In this context, besides

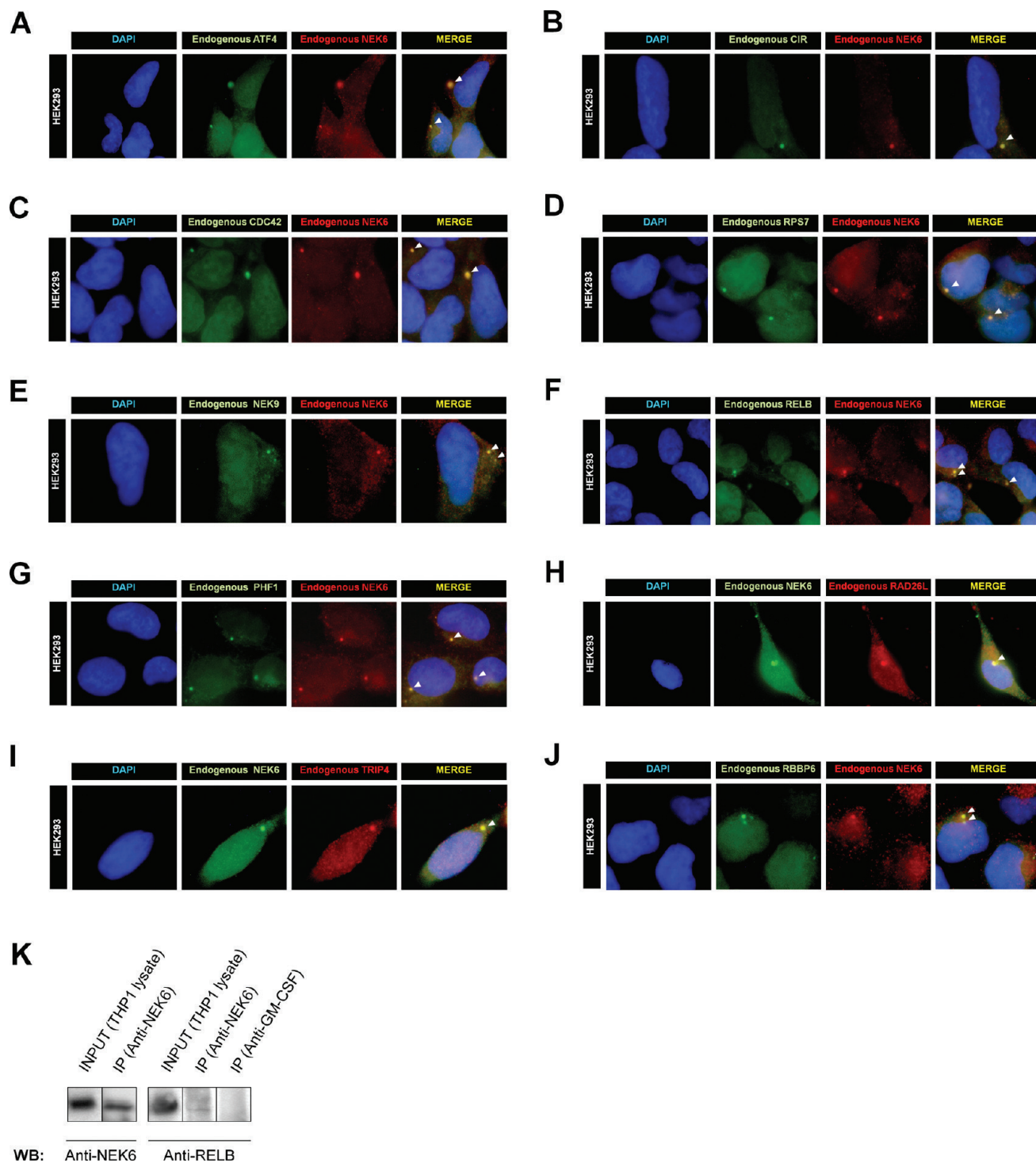


Figure 6. Human Nek6 colocalizes with all tested interacting proteins in human cells, and interacts *in vivo* with RelB. Endogenous hNek6 colocalizes with endogenous (A) activating transcription factor 4, (B) CBF1 interacting corepressor, (C) Cdc42, (D) ribosomal protein S7, (E) Nek9, (F) RelB, (G) PHF1, (H) Rad26-like, (I) TRIP-4, and (J) RBO-1 in HEK293 cells (white arrowheads), as visualized by fluorescence microscopy. Nuclei were stained by DAPI. (K) Endogenous RelB is detected in anti-NEK6 immunoprecipitate (IP) from THP1 cells, but not in the control anti-GM-CSF immunoprecipitate (IP).

Cdc42, the brain-enriched TC10/CDC42 GTPase-activating protein, also called Sorting nexin 26, was also identified in our screenings and confirmed to interact with hNek6 (Figure 2). It was recently identified as a RhoGAP that specifically interacts via its GAP domain with Cdc42.⁵⁹

DNA Repair Signaling. The DNA Repair functional category identified in our screenings reiterates the importance of this

context among the functions mediated by Neks in general. In a previous yeast two-hybrid screen performed by our group using hNek1 as bait,²³ proteins that take part in the dsDNA repair during the G2/M transition phase of the cell cycle were identified, and three recent studies suggest that Nek1, Nek6 and Nek11 are important regulators of this biological process.^{60–62} Besides the double-strand-break repair protein Rad21

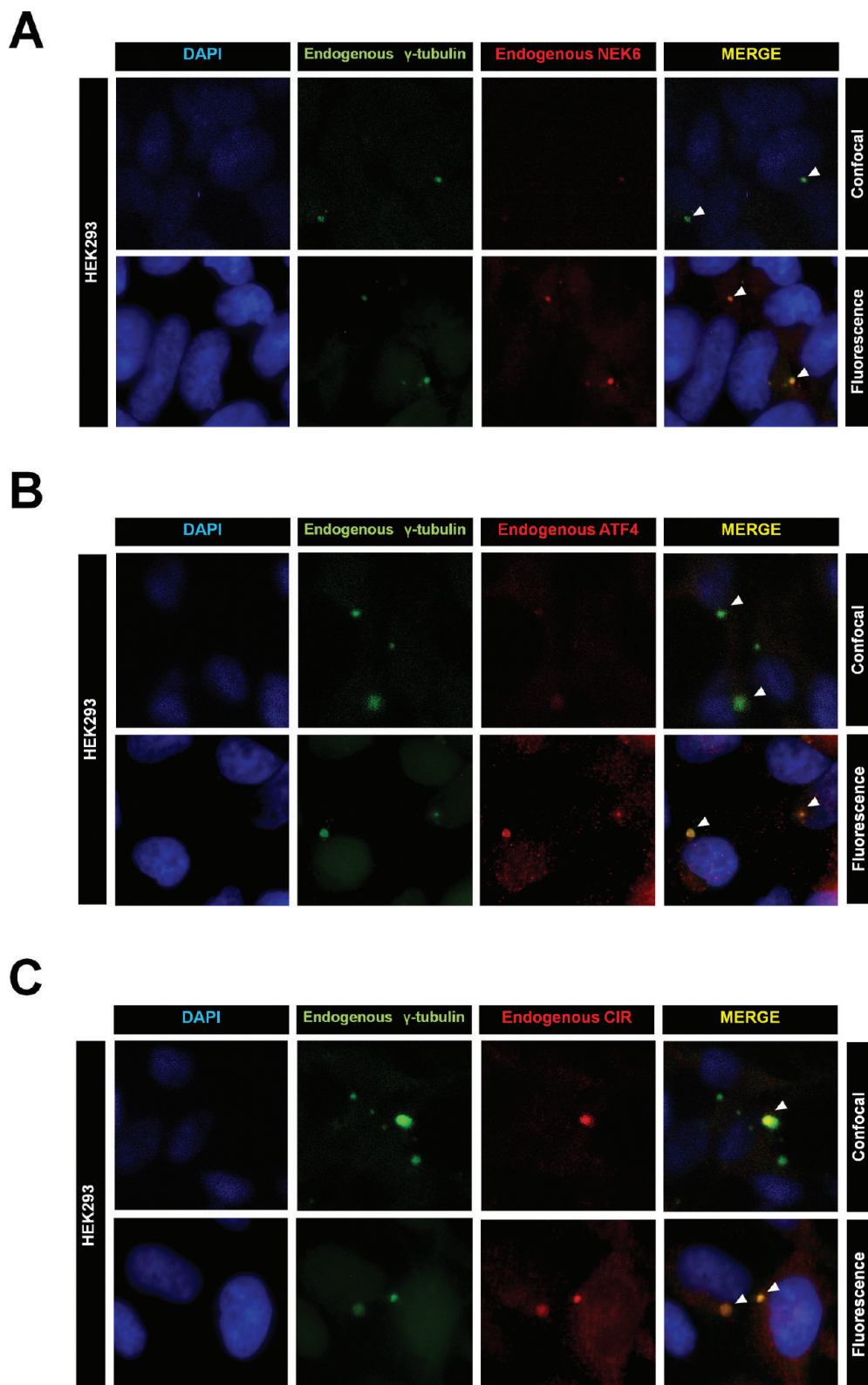


Figure 7. Human Nek6 colocalizes with Activating transcription factor 4 and CBF1 interacting corepressor to the centrosomes of human cells. Endogenous (A) hNek6, (B) activating transcription factor 4, and (C) CBF1 interacting corepressor colocalize with endogenous γ -tubulin in HEK293 cells (white arrowheads). Nuclei were stained by DAPI. Images were visualized by confocal and fluorescence microscopy.

homologue (hHR21; RAD21), which is involved in double-strand-break repair during the cell cycle,⁶³ we also identified RAD26-like in our screenings. Although there is no study to date characterizing the mammalian protein, Rad26 is described

in yeast to be required for two processes dependent on microtubules: chromosome segregation and cell polarity.⁶⁴ Therefore, associated to the fact that RAD26-like colocalizes with hNek6 in human cells (Figure 6H) and is also a substrate

Table 3. *In Silico* Analysis of Human Nek6 Interacting Proteins Structural and Functional Properties (only interactions that were confirmed by pull-down are shown here)

gene	coded protein residues (retrieved/complete sequence) ^a	domain composition (Pfam, PROSITE or InterPro) ^b	percent disordered residues (PONDR) ^c	cellular component (GO) ^d	biological processes (GO) ^e	coexpressed genes (GEMMA) ^f
CDC42	1–191/191	Ras family domain	18.32	Cytoplasm (filopodium), plasma membrane	Cell cycle, Cell organization and biogenesis, Protein transport, Signal transduction	
RAD26L	1–531/531	UNDESCRIBED	36.35	Nucleus	DNA repair	
RBBP6	1–259/1792	DWNN domain, Zinc knuckle domain	35.14	Nucleus	Metabolism	
NEK9	806–979/979	Proline-rich region, Coiled-coil domain ^g	52.87	Nucleus, cytoplasm	Cell cycle, Protein amino acid phosphorylation	
RPS7	1–194/194	Ribosomal protein S7e family domain	53.61	Nucleus (nucleolus) and cytoplasm (ribosome)	Protein biosynthesis	
SNX26	1115–1287/1287	CDC42 GTPase-activating protein family domain, Proline-rich region	88.44	Cytoplasm, plasma membrane	Protein transport, Signal transduction	CRMP1, PSMC6
CIR	1–240/450	N-terminal domain of CBF1 interacting corepressor CIR	32.64	Nucleus (nuclear speck and HDAC)	RNA processing, Transcription	F13A1
PRAM1	360–670/670	SH2 containing adaptor PRAM-1 related family domain, SH3 domain, Proline-rich region	69.45	UNDESCRIBED	Signal transduction	
PTN	1–168/168	PTN/MK heparin-binding protein family N-terminal domain	35.71	Cytoplasm (ER), ECM	Signal transduction	
ATF4	252–351/351	bZIP transcription factor family domain	72.00	Nucleus, cytoplasm, plasma membrane	Metabolism, Stress response, Transcription	
TRIP4	46–581/581	Putative zinc finger motif (C2HC5-type), ASCH domain	38.25	Nucleus, cytoplasm	Transcription	CRMP1, PSMC6, MYST2
ANKRA2	78–313/313	Ankyrin repeat	23.31	Cytoplasm (cytoskeleton)	UNKNOWN	RAD21, RBBP6, SLU7
PRDX3	183–256/256	C-terminal domain of 1-Cys peroxiredoxin, AhpC/TSA family domain	33.78	Cytoplasm (mitochondrion)	UNKNOWN	PSMC6

^a Only the minimum lengths of the retrieved sequences that could be visualized by forward DNA sequencing are depicted. ^b Domain composition of the retrieved sequences obtained by Pfam, PROSITE or InterPro databases (other domains may be present). ^c Percentage of disordered amino acid residues in the retrieved sequences obtained by PONDR. ^d Cellular components based on the GO and Uniprot databases.

^e Biological processes based on the GO database. ^f Coexpressed genes obtained by GEMMA database, including only the ones whose products were identified to interact with hNek6 by our two-hybrid screens.

^g Domain composition described by Roig et al.¹⁷

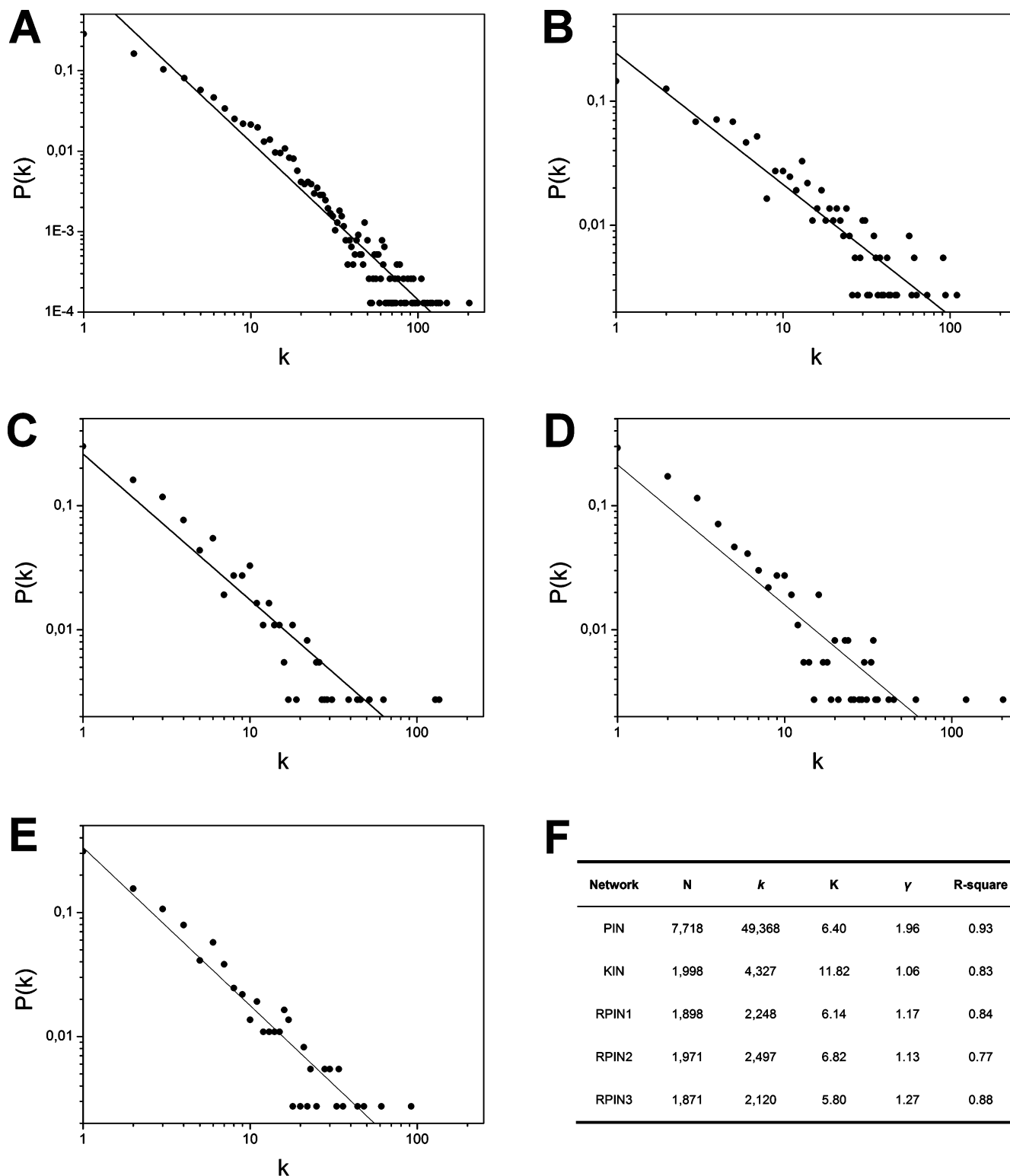


Figure 8. Degree distribution of the network proteins. (A) PIN (Protein Interaction Network). (B) KIN (Kinase Interaction Network). (C) RPIN1 (Random Protein Interaction Network 1). (D) RPIN2 (Random Protein Interaction Network 2). (E) RPIN3 (Random Protein Interaction Network 3). (F) Degree statistics of the networks. The five networks approximate a power-law [$P(k) \approx k^{-\gamma}$] and are scale-free in topology (N, total number of nodes; k , total number of links; K, average degree; γ , slope of the distribution on the log–log plot; R-square, square of the correlation coefficient).

in vitro (Figure 5B), it is an interesting interacting target to be studied, as it might link hNek6 to the DNA repair function and/or cell cycle in processes dependent on microtubules. Another protein identified related to DNA repair is PHF1, a polycomb group (PcG) chromatin modifier which was recently involved

in the response to DNA double-strand breaks (DSBs),⁶⁵ and was found to colocalize with hNek6 in human cells (Figure 6G).

NF- κ B Signaling. Among the proteins retrieved in our screenings, there are three described to be related to the NF- κ B signaling: RelB, Prx-III and TRIP-4. NF- κ B plays an impor-

Table 4. High Confidence Hub Kinases Ranked by Degree from KIN Network

gene	BioGRID node ID	lethality ^a	degree
SRC	EG6714	yes	110
EGFR	EG1956	yes	94
NEK6	RP11-101K10.6	yes ^b	91
FYN	RP1-66H14.1	yes	91
RAF1	EG5894	yes	73
ABL1	RP11-83J21.1	yes	63
CDK2	EG1017	yes	61
LYN	EG4067	no	61
MAPK1	EG5594	yes	59
AKT1	EG207	yes	57
JAK2	EG3717	yes	57
PTK2	EG5747	yes	57
PTK2B	EG2185	no	48
MAPK8	EG5599	yes	47
LCK	EG3932	no	44
SYK	EG6850	yes	43
MAPK14	RP1-179N16.5	unknown	42
MAPK3	EG5595	yes	42
JAK1	EG3716	unknown	40
GSK3B	EG2932	yes	39
PRKDC	EG5591	unknown	38
STK24	RP11-111L24.5	unknown	38
ILK	EG3611	yes	37
ATM	EG472	yes	36
PRKCA	EG5578	no	36

^a Observed lethality phenotypes from the Knockout Mouse Project (KOMP) Repository. ^b Knockdown of endogenous Nek6 expression results in mitotic arrest and increased apoptosis.¹⁴

tant role in inflammation, autoimmune response, cell proliferation, and apoptosis by regulating the expression of genes involved in these processes. Interestingly, NEK6 gene was described among others to activate the NF- κ B signaling pathway, in a large-scale screening.⁶⁶ However to our knowledge, there is no explanation of how hNek6 activates NF- κ B and the first possible links to that question are addressed here. hNek6 may regulate the NF- κ B signaling pathway directly by phosphorylating/activating RelB, which functions as a transcriptional activator when associated to p50 or p52, or as a repressor when associated to p65 (RelA). Notably, RelB colocalized and interacted with hNek6 in human cells (Figure 6F and K). On the other hand, hNek6 could regulate this pathway indirectly by interacting with Prx-III or phosphorylating/activating TRIP-4. Prx-III is an antioxidant protein that acts synergistically with leucine zipper-bearing kinase (LZK) protein in the activation of NF- κ B in the cytosol.⁶⁷ In the case of TRIP-4, it is a transcription coactivator molecule that stimulates transactivation by Serum response factor (SRF), Activating protein 1 (AP-1), and NF- κ B through direct binding to SRF, c-Jun, p50, and p65.⁶⁸ Moreover, TRIP-4 has many putative phosphorylation sites for hNek6 (Table S2) and was found to be strongly phosphorylated by it *in vitro* (Figure 5B), in addition to have colocalized with hNek6 in human cells (Figure 6I).

Notch Signaling. In our screenings, we identified the Recombining binding protein suppressor of hairless (CBF1) interacting corepressor (CIR), which was confirmed to interact with hNek6 (Table 1, Figure 2). The mechanism of CBF1-mediated repression implicates the presence of CBF1 interacting corepressor in this activity, which participates in the recruitment of histone deacetylase (HDAC) to DNA-bound CBF1.⁶⁹ Furthermore, it is interesting to note that SNW domain containing 1 (SNW1) is a component of the CBF1 corepressor

complex and interacts with CBF1 interacting corepressor,⁷⁰ since it was also retrieved in our screenings using hNek6 as bait (Table S1, Supporting Information). These facts suggest a putative role for hNek6 in Notch signaling through interactions with CBF1 interacting corepressor and SNW domain containing 1, which might behave as hNek6 substrates, since both have putative phosphorylation sites (Table S2, Supporting Information) and CIR was found to colocalize with hNek6 in human cells (Figure 6B) and to be phosphorylated by it *in vitro* (Figure 5B).

Cancer-Related Interactions. hNek6 also retrieved proteins described to be related to carcinogenesis. One confirmed to interact, colocalize *in vivo* and to be phosphorylated *in vitro* by hNek6 (Figures 2, 6J, and 5B) is RBQ-1, which is a 250 kDa splicing-associated protein that has been identified as an E3 ligase due to the presence of a RING finger domain. Structural studies also showed that the N-terminal 81 amino acids of RBQ-1 constitute a novel ubiquitin-like domain called DWNN (Table 3).⁷¹ RBQ-1 was described to suppress the binding of p53 to DNA,⁷² and has been shown to be highly upregulated in esophageal cancer.⁷³

hNek6 also retrieved Activating transcription factor 4, which is upregulated in primary human tumors and facilitates tumor growth in xenograft models.^{74,75} It is induced by stress signals and regulates the expression of genes involved in oxidative stress, amino acid synthesis, differentiation, metastasis and angiogenesis.⁷⁶ As Activating transcription factor 4 colocalized with hNek6 in human cells (Figure 6A) and was confirmed to interact and be phosphorylated *in vitro* by hNek6 (Figures 2, 5B), it might be regulated by hNek6 in pathways related to metabolism, transcription and/or stress response (Figure 1).

Conclusions

Hub proteins are generally expected to have multidomains, repeats, and to be at least partially disordered, as an increase in binding regions and flexibility may result in a higher connectivity.^{44,77} We showed here that hNek6 is a putative high confidence hub protein kinase within an enriched set of essential kinase genes (Table 4), although being a mostly ordered and globular protein, revealed by studies on circular dichroism, small-angle X-ray scattering and by disorder prediction analysis (data not shown). On the other hand, we showed by *in silico* analysis that the structure of its putative interacting partners have repeats and disordered regions (Table S3) and, most notably, we demonstrated by *in vitro* binding assays that hNek6 unfolded short N-terminal extension is necessary for hNek6 to bind to its partners (Figure 3).

In summary, confirmative assays with a total of 15 Nek6 interacting proteins showed that all eight of the tested interactions in pull-down assays were confirmed in a N-terminal dependent fashion and that all of the ten interactions tested in cellular assays demonstrate colocalization with Nek6 at the centrosome (Table 5). Interestingly, three proteins (RAD26-like, TRIP-4 and RBQ-1) that colocalized with hNek6 at the centrosome also depended on hNek6 N-terminus to bind to it and were furthermore phosphorylated *in vitro* by hNek6. It seems therefore that binding to the N-terminus and colocalization to the centrosome may be a general phenomenon of our hNek6 identified interactions. However, further experiments are needed to clarify if phosphorylation is important for the interactors to bind or colocalize with hNek6. It will also be interesting to uncover the sequence of steps by which hNek6 binds to each

Table 5. Summary of Results from Assays Developed to Confirm the Interactions with Human Nek6

genes ^a	pull-down with Nek6wt ^b	lack of pull-down with Nek6(Δ 1–44) ^b	kinase assays with Nek6wt and Nek6(S206A) ^b	colocalization with Nek6 ^b
CDC42	+	+	n.t.	+
RAD26L	+	+	+	+
RBBP6	+	+	+	+
NEK9	+ ^c	n.t.	n.t.	+
RPS7	+	+	–	+
SNX26	+	+	n.t.	n.t.
CIR	+	n.t.	+	+
PRAM1	+	n.t.	n.t.	n.t.
PTN	+	n.t.	+	n.t.
ATF4	+	n.t.	+	+
TRIP4	+	+	+	+
ANKRA2	+	+	n.t.	n.t.
PRDX3	+	+	n.t.	n.t.
RELB	n.t.	n.t.	n.t.	+
PHF1	n.t.	n.t.	n.t.	+

^a Genes used in the different assays. ^b +, confirmative result; –, no confirmation; n.t., not tested. ^c The interaction of Nek6 and Nek9 has been previously shown.¹⁷

of its partners (e.g., the partner binds to hNek6 N-terminus at the centrosome, then it is phosphorylated and so on).

Furthermore, our hNek6 interactome, combined with functional *in vitro* and *in vivo* assays and its analysis in a broader network context, has defined hNek6 participation in numerous biological processes and, importantly, has brought up the tendency for human kinases to be enriched in hubs. Thus, given the importance of hNek6 in regulating a variety of cellular functions through the interaction with several putative relevant partners described here, it would be desirable to determine if these interactions are stimulated or abrogated in cancer cells. Further studies may provide useful information and possible implications for drug design and cancer therapy.

Acknowledgment. We thank Maria Eugênia Camargo, Thaís C. D. Dombroski, Bianca A. Pauletti, Carla C. Judice, Jackeline de Lima, and Janine S. Sabino for technical assistance. We are also grateful to Dr. Kleber G. Franchini for help in providing the THP1 cells, and to Dr. Sara T. O. Saad for the use of the confocal microscope. This work was supported by Fundação de Amparo à Pesquisa do Estado São Paulo (FAPESP), Conselho Nacional de Pesquisa e Desenvolvimento (CNPq), and the Associação Brasileira de Tecnologia de Luz Síncrotron (ABTLuS).

Supporting Information Available: Supplementary Figure S1. Colocalization of human Nek6 with Activating transcription factor 4, CBF1 interacting corepressor, Cdc42, Ribosomal protein S7, Nek9 and RelB in human cells. Endogenous hNek6 colocalizes with endogenous (A) Activating transcription factor 4, (B) CBF1 interacting corepressor, (C) Cdc42, (D) Ribosomal protein S7, (E) Nek9, and (F) RelB in HEK293 cells (white arrowheads), as visualized by confocal microscopy. Nuclei were stained by DAPI. Supplementary Table S1. Human Nek6 interacting proteins identified by the yeast two-hybrid system screens. Supplementary Table S2. Putative phosphorylation sites present in human Nek6 interacting proteins. Supplementary Table S3. *In silico* analysis of human Nek6 interacting proteins functional and structural properties. This material is available free of charge via the Internet at <http://pubs.acs.org>.

Note Added after ASAP Publication. This paper was published on the Web on Oct 22, 2010, with errors in the first paragraph of the Conclusions and the Supporting Information. The corrected version was reposted on Oct 28, 2010.

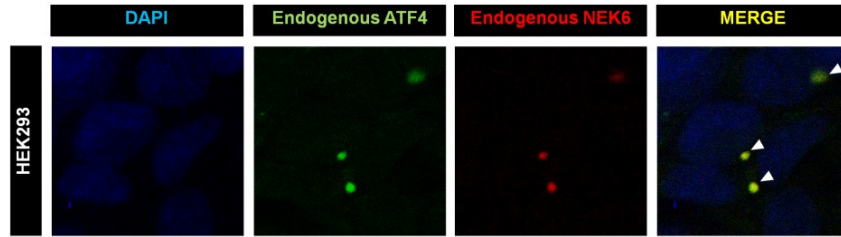
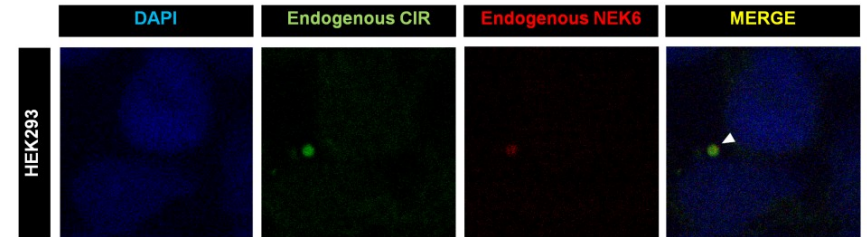
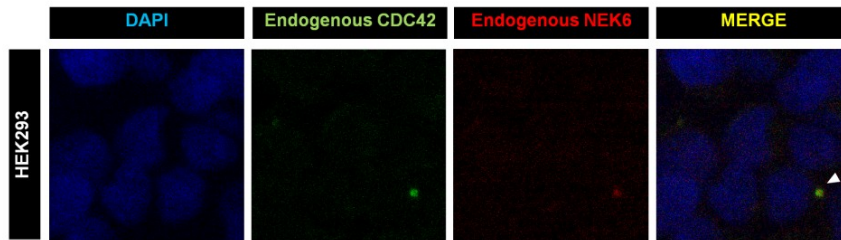
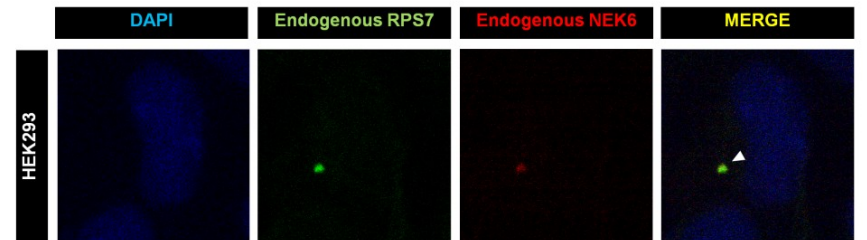
References

- (1) Ge, H.; Walhout, A. J.; Vidal, M. Integrating 'omic' information: a bridge between genomics and systems biology. *Trends Genet.* **2003**, *19*, 551–560.
- (2) Albert, R.; Barabasi, A. L. Statistical mechanics of complex networks. *Rev. Mod. Phys.* **2002**, *74*, 47–97.
- (3) Erdos, P.; Renyi, A. On random graphs I. *Publ. Math.* **1959**, *6*, 290–297.
- (4) Barabasi, A. L.; Albert, R. Emergence of scaling in random networks. *Science* **1999**, *286*, 509–512.
- (5) Albert, R.; Jeong, H.; Barabasi, A. L. Error and attack tolerance of complex networks. *Nature* **2000**, *406*, 378–382.
- (6) Barabasi, A. L.; Bonabeau, E. Scale-free networks. *Sci. Am.* **2003**, *288*, 60–69.
- (7) Watts, D. J.; Strogatz, S. H. Collective dynamics of 'small-world' networks. *Nature* **1998**, *393*, 440–442.
- (8) Manning, G.; Whyte, D. B.; Martinez, R.; Hunter, T.; Sudarsanam, S. The protein kinase complement of the human genome. *Science* **2002**, *298*, 1912–1934.
- (9) Hunter, T. Signaling--2000 and beyond. *Cell* **2000**, *100* (1), 113–127.
- (10) Futreal, P. A.; Coin, L.; Marshall, M.; Down, T.; Hubbard, T.; et al. A census of human cancer genes. *Nature Rev. Cancer* **2004**, *4*, 177–183.
- (11) O'Regan, L.; Blot, J.; Fry, A. M. Mitotic regulation by NIMA-related kinases. *Cell Div.* **2007**, *2*, 25.
- (12) Mahjoub, M. R.; Trapp, M. L.; Quarmby, L. M. NIMA-related kinases defective in murine models of polycystic kidney diseases localize to primary cilia and centrosomes. *J. Am. Soc. Nephrol.* **2005**, *16* (12), 3485–3489.
- (13) Fletcher, L.; Cerniglia, G. J.; Yen, T. J.; Muschel, R. J. Live cell imaging reveals distinct roles in cell cycle regulation for Nek2A and Nek2B. *Biochim. Biophys. Acta* **2005**, *1744* (2), 89–92.
- (14) Yin, M. J.; Shao, L.; Voehringer, D.; Smeal, T.; Jallal, B. The serine/threonine kinase Nek6 is required for cell cycle progression through mitosis. *J. Biol. Chem.* **2003**, *278* (52), 52454–52460.
- (15) Belham, C.; Roig, J.; Caldwell, J. A.; Aoyama, Y.; Kemp, B. E.; Comb, M.; Avruch, J. A. Mitotic cascade of NIMA family kinases. Nercc1/Nek9 activates the Nek6 and Nek7 kinases. *J. Biol. Chem.* **2003**, *278* (37), 34897–34909.
- (16) Yissachar, N.; Salem, H.; Tennenbaum, T.; Motro, B. Nek7 kinase is enriched at the centrosome, and is required for proper spindle assembly and mitotic progression. *FEBS Lett.* **2006**, *580* (27), 6489–6495.
- (17) Roig, J.; Mikhailov, A.; Belham, C.; Avruch, J. Nercc1, a mammalian NIMA-family kinase, binds the Ran GTPase and regulates mitotic progression. *Genes Dev.* **2002**, *16* (13), 1640–1658.
- (18) Roig, J.; Groen, A.; Caldwell, J.; Avruch, J. Active Nercc1 protein kinase concentrates at centrosomes early in mitosis and is necessary for proper spindle assembly. *Mol. Biol. Cell* **2005**, *16* (10), 4827–4840.
- (19) Noguchi, K.; Fukazawa, H.; Murakami, Y.; Uehara, Y. Nucleolar Nek11 is a novel target of Nek2A in G1/S-arrested cells. *J. Biol. Chem.* **2004**, *279* (31), 32716–32727.
- (20) O'Regan, L.; Fry, A. M. The Nek6 and Nek7 protein kinases are required for robust mitotic spindle formation and cytokinesis. *Mol. Cell Biol.* **2009**, *29* (14), 3975–3990.
- (21) Upadhya, P.; Birkenmeier, E. H.; Birkenmeier, C. S.; Barker, J. E. Mutations in a NIMA-related kinase gene, Nek1, cause pleiotropic effects including a progressive polycystic kidney disease in mice. *Proc. Natl. Acad. Sci. U.S.A.* **2000**, *97* (1), 217–221.
- (22) Liu, S.; Lu, W.; Obara, T.; Kuida, S.; Lehoczky, J.; et al. A defect in a novel Nek-family kinase causes cystic kidney disease in the mouse and in zebrafish. *Development* **2002**, *129* (24), 5839–5846.
- (23) Surpili, M. J.; Delben, T. M.; Kobarg, J. Identification of proteins that interact with the central coiled-coil region of the human protein kinase NEK1. *Biochemistry* **2003**, *42*, 15369–15376.
- (24) Tsunoda, N.; Kokuryo, T.; Oda, K.; Senga, T.; Yokoyama, Y.; et al. Nek2 as a novel molecular target for the treatment of breast carcinoma. *Cancer Sci.* **2009**, *100* (1), 111–116.
- (25) McHale, K.; Tomaszewski, J. E.; Puthiyaveetil, R.; Livolsi, V. A.; Clevenger, C. V. Altered expression of prolactin receptor-associated signaling proteins in human breast carcinoma. *Mod. Pathol.* **2008**, *21* (5), 565–571.

- (26) Bowers, A. J.; Boylan, J. F. Nek8, a NIMA family kinase member, is overexpressed in primary human breast tumors. *Gene* **2004**, *328*, 135–142.
- (27) Ahmed, S.; Thomas, G.; Ghousaini, M.; Healey, C. S.; Humphreys, M. K.; et al. Newly discovered breast cancer susceptibility loci on 3p24 and 17q23.2. *Nat. Genet.* **2009**, *41* (5), 585–590.
- (28) Takeno, A.; Takemasa, I.; Doki, Y.; Yamasaki, M.; Miyata, H.; et al. Integrative approach for differentially overexpressed genes in gastric cancer by combining large-scale gene expression profiling and network analysis. *Br. J. Cancer* **2008**, *99* (8), 1307–1315.
- (29) Chen, J.; Li, L.; Zhang, Y.; Yang, H.; Wei, Y.; et al. Interaction of Pin1 with Nek6 and characterization of their expression correlation in Chinese hepatocellular carcinoma patients. *Biochem. Biophys. Res. Commun.* **2006**, *341* (4), 1059–1065.
- (30) Capra, M.; Nuciforo, P. G.; Confalonieri, S.; Quarto, M.; Bianchi, M.; et al. Frequent alterations in the expression of serine/threonine kinases in human cancers. *Cancer Res.* **2006**, *66* (16), 8147–8154.
- (31) Nassirpour, R.; Shao, L.; Flanagan, P.; Abrams, T.; Jallal, B.; Smeal, T.; Yin, M. J. Nek6 Mediates Human Cancer Cell Transformation and Is a Potential Cancer Therapeutic Target. *Mol. Cancer Res.* **2010**, *8* (5), 717–728.
- (32) Bartel, P. L.; Fields, S. Analyzing protein-protein interactions using two-hybrid system. *Methods Enzymol.* **1995**, *254*, 241.
- (33) Chien, C. T.; Bartel, P. L.; Sternglanz, R.; Fields, S. The two-hybrid system: a method to identify and clone genes for proteins that interact with a protein of interest. *Proc. Natl. Acad. Sci. U.S.A.* **1991**, *88*, 9578.
- (34) Assmann, E. M.; Alborghetti, M. R.; Camargo, M. E.; Kobarg, J. FEZ1 dimerization and interaction with transcription regulatory proteins involves its coiled-coil region. *J. Biol. Chem.* **2006**, *281*, 9869–9881.
- (35) Albers, M.; Kranz, H.; Kober, I.; Kaiser, C.; Klink, M.; et al. Automated yeast two-hybrid screening for nuclear receptor-interacting proteins. *Mol. Cell. Proteomics* **2005**, *4* (2), 205–213.
- (36) Vojtek, A. B.; Hollenberg, S. M. Ras-Raf interaction: two-hybrid analysis. *Methods Enzymol.* **1995**, *255*, 331–342.
- (37) Hanna, S. L.; Sherman, N. E.; Kinter, M. T.; Goldberg, J. B. Comparison of proteins expressed by *Pseudomonas aeruginosa* strains representing initial and chronic isolates from a cystic fibrosis patient: an analysis by 2-D gel electrophoresis and capillary column liquid chromatography-tandem mass spectrometry. *Microbiology* **2000**, *146*, 2495–2508.
- (38) Lizcano, J. M.; Deak, M.; Morrice, N.; Kieloch, A.; Hastie, C. J.; et al. Molecular basis for the substrate specificity of NIMA-related kinase-6 (NEK6). Evidence that NEK6 does not phosphorylate the hydrophobic motif of ribosomal S6 protein kinase and serum- and glucocorticoid-induced protein kinase in vivo. *J. Biol. Chem.* **2002**, *277* (31), 27839–27849.
- (39) Lu, K. P.; Kemp, B. E.; Means, A. R. Identification of substrate specificity determinants for the cell cycle-regulated NIMA protein kinase. *J. Biol. Chem.* **1994**, *269* (9), 6603–6607.
- (40) Stelzl, U.; Worm, U.; Lalowski, M.; Haenig, C.; Brembeck, F. H.; et al. A human protein-protein interaction network: a resource for annotating the proteome. *Cell* **2005**, *122* (6), 957–968.
- (41) Ewing, R. M.; Chu, P.; Elisma, F.; Li, H.; Taylor, P.; et al. Large-scale mapping of human protein-protein interactions by mass spectrometry. *Mol. Syst. Biol.* **2007**, *3*, 89.
- (42) Rual, J. F.; Venkatesan, K.; Hao, T.; Hirozane-Kishikawa, T.; Dricot, A.; et al. Towards a proteome scale map of the human protein-protein interaction network. *Nature* **2005**, *437*, 1173–1178.
- (43) Kunin, V.; Pereira-Leal, J. B.; Ouzounis, C. A. Functional evolution of the yeast protein interaction network. *Mol. Biol. Evol.* **2004**, *21*, 1171–1176.
- (44) Ekman, D.; Light, S.; Björklund, A. K.; Elofsson, A. What properties characterize the hub proteins of the protein-protein interaction network of *Saccharomyces cerevisiae*. *Genome Biol.* **2006**, *7* (6), R45.
- (45) Ge, H.; Liu, Z.; Church, G. M.; Vidal, M. Correlation between transcriptome and interactome mapping data from *Saccharomyces cerevisiae*. *Nat. Genet.* **2001**, *29*, 482–486.
- (46) Li, S.; Armstrong, C. M.; Bertin, N.; Ge, H.; Milstein, S.; et al. A map of the interactome network of the metazoan *C. elegans*. *Science* **2004**, *303*, 540–543.
- (47) Hahn, A.; Rahnenfuhrer, J.; Talwar, P.; Lengauer, T. Confirmation of human protein interaction data by human expression data. *BMC Bioinformatics* **2005**, *6*, 112.
- (48) Han, J. D.; Bertin, N.; Hao, T.; Goldberg, D. S.; Berriz, G. F.; et al. Evidence for dynamically organized modularity in the yeast protein-protein interaction network. *Nature* **2004**, *430*, 88–93.
- (49) Lee, H. K.; Hsu, A. K.; Sajdak, J.; Qin, J.; Pavlidis, P. Coexpression analysis of human genes across many microarray data sets. *Genome Res.* **2004**, *14* (6), 1085–1094.
- (50) Hartwell, L. H.; Hopfield, J. J.; Leibler, S.; Murray, A. W. From molecular to modular cell biology. *Nature* **1999**, *402*, C47–C52.
- (51) Dunker, A. K.; Brown, C. J.; Lawson, J. D.; Iakoucheva, L. M.; Obradovic, Z. Intrinsic disorder and protein function. *Biochemistry* **2002**, *41*, 6573–6582.
- (52) Ward, J. J.; Sodhi, J. S.; McGuffin, L. J.; Buxton, B. F.; Jones, D. T. Prediction and functional analysis of native disorder in proteins from the three kingdoms of life. *J. Mol. Biol.* **2004**, *337*, 635–645.
- (53) Barabasi, A. L.; Oltvai, Z. N. Network biology: understanding the cell's functional organization. *Nat. Rev. Genet.* **2004**, *5*, 101–113.
- (54) Lee, R. E.; Megeney, L. A. The yeast kinome displays scale free topology with functional hub clusters. *BMC Bioinform.* **2005**, *6*, 271.
- (55) Jeong, H.; Mason, S. P.; Barabasi, A. L.; Oltvai, Z. N. Lethality and centrality in protein networks. *Nature* **2001**, *411*, 41–42.
- (56) Kodani, A.; Kristensen, I.; Huang, L.; Sütterlin, C. GM130-dependent control of Cdc42 activity at the Golgi regulates centrosome organization. *Mol. Biol. Cell* **2009**, *20* (4), 1192–2000.
- (57) Chen, D.; Zhang, Z.; Li, M.; Wang, W.; Li, Y.; et al. Ribosomal protein S7 as a novel modulator of p53-MDM2 interaction: binding to MDM2, stabilization of p53 protein, and activation of p53 function. *Oncogene* **2007**, *26* (35), 5029–5037.
- (58) Hall, A. Rho GTPases and the actin cytoskeleton. *Science* **1998**, *279*, 509–514.
- (59) Chiang, S. H.; Hwang, J.; Legendre, M.; Zhang, M.; Kimura, A.; Saltiel, A. R. TC GAP, a multidomain Rho GTPase-activating protein involved in insulin-stimulated glucose transport. *EMBO J.* **2003**, *22* (11), 2679–2691.
- (60) Chen, Y.; Chen, P. L.; Chen, C. F.; Jiang, X.; Riley, D. J. Never-in-mitosis related kinase 1 functions in DNA damage response and checkpoint control. *Cell Cycle* **2008**, *7* (20), 3194–3201.
- (61) Lee, M. Y.; Kim, H. J.; Kim, M. A.; Jee, H. J.; Kim, A. J.; et al. Nek6 is involved in G2/M phase cell cycle arrest through DNA damage-induced phosphorylation. *Cell Cycle* **2008**, *7* (17), 2705–2709.
- (62) Melixetian, M.; Klein, D. K.; Sørensen, C. S.; Helin, K. NEK11 regulates CDC25A degradation and the IR-induced G2/M checkpoint. *Nat. Cell Biol.* **2009**, *11* (10), 1247–1253.
- (63) Sonoda, E.; Matsusaka, T.; Morrison, C.; Vagnarelli, P.; Hoshi, O.; et al. Sec1/Rad21/Mcd1 is required for sister chromatid cohesion and kinetochore function in vertebrate cells. *Dev. Cell* **2001**, *1* (6), 759–770.
- (64) Baschal, E. E.; Chen, K. J.; Elliott, L. G.; Herring, M. J.; Verde, S. C.; et al. The fission yeast DNA structure checkpoint protein Rad26/ATRP/LCD1/UVSD accumulates in the cytoplasm following microtubule destabilization. *BMC Cell Biol.* **2006**, *7*, 32.
- (65) Hong, Z.; Jiang, J.; Lan, L.; Nakajima, S.; Kanno, S.; et al. A polycomb group protein, PHF1, is involved in the response to DNA double-strand breaks in human cell. *Nucleic Acids Res.* **2008**, *36* (9), 2939–2947.
- (66) Matsuda, A.; Suzuki, Y.; Honda, G.; Muramatsu, S.; Matsuzaki, O.; et al. Large-scale identification and characterization of human genes that activate NF-kappaB and MAPK signaling pathways. *Oncogene* **2003**, *22* (21), 3307–3318.
- (67) Masaki, M.; Ikeda, A.; Shiraki, E.; Oka, S.; Kawasaki, T. Mixed lineage kinase LZK and antioxidant protein-1 activate NF-kappaB synergistically. *Eur. J. Biochem.* **2003**, *270* (1), 76–83.
- (68) Kim, H. J.; Yi, J. Y.; Sung, H. S.; Moore, D. D.; Jhun, B. H.; et al. Activating signal cointegrator 1, a novel transcription coactivator of nuclear receptors, and its cytosolic localization under conditions of serum deprivation. *Mol. Cell. Biol.* **1999**, *19*, 6323–6332.
- (69) Hsieh, J. J.; Zhou, S.; Chen, L.; Young, D. B.; Hayward, S. D. CIR a corepressor linking the DNA binding factor CBF1 to the histone deacetylase complex. *Proc. Natl. Acad. Sci. U.S.A.* **1999**, *96* (1), 23–28.
- (70) Zhou, S.; Fujimuro, M.; Hsieh, J. J.; Chen, L.; Miyamoto, A.; et al. SKIP, a CBF1-associated protein, interacts with the ankyrin repeat domain of Notch1C to facilitate Notch1C function. *Mol. Cell. Biol.* **2000**, *20* (7), 2400–2410.
- (71) Pugh, D. J.; Ab, E.; Faro, A.; Luty, P. T.; Hoffmann, E.; et al. DWNN, a novel ubiquitin-like domain, implicates RBBP6 in mRNA processing and ubiquitin-like pathways. *BMC Struct. Biol.* **2006**, *6*, 1.
- (72) Simons, A.; Melamed-Bessudo, C.; Wolkowicz, R.; Sperling, J.; Sperling, R.; et al. PACT: cloning and characterization of a cellular p53 binding protein that interacts with Rb. *Oncogene* **1997**, *14*, 145–155.
- (73) Yoshitake, Y.; Nakatsura, T.; Monji, M.; Senju, S.; Matsuyoshi, H.; et al. Proliferation potential-related protein, an ideal esophageal cancer antigen for immunotherapy, identified using complementary DNA microarray analysis. *Clin. Cancer Res.* **2004**, *10*, 6437–6448.

- (74) Ameri, K.; Lewis, C. E.; Raida, M.; Sowter, H.; Hai, T.; et al. Anoxic induction of ATF-4 through HIF-1-independent pathways of protein stabilization in human cancer cells. *Blood* **2004**, *103*, 1876–1882.
- (75) Bi, M.; Naczki, C.; Koritzinsky, M.; Fels, D.; Blais, J.; et al. ER stress-regulated translation increases tolerance to extreme hypoxia and promotes tumor growth. *EMBO J.* **2005**, *24*, 3470–3481.
- (76) Ameri, K.; Harris, A. L. Activating transcription factor 4. *Int. J. Biochem. Cell Biol.* **2008**, *40* (1), 14–21.
- (77) Dunker, A. K.; Cortese, M. S.; Romero, P.; Iakoucheva, L. M.; Uversky, V. N. Flexible nets. The roles of intrinsic disorder in protein interaction networks. *FEBS J.* **2005**, *272* (20), 5129–5148.

PR100562W

A**B****C****D**

88

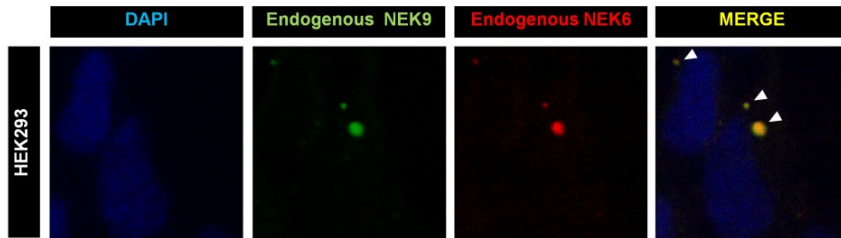
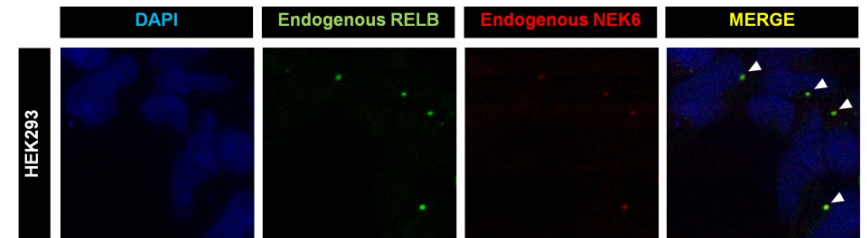
E**F**

Figure S1. Colocalization of human Nek6 with Activating transcription factor 4, CBF1 interacting corepressor, Cdc42, Ribosomal protein S7, Nek9 and RelB in human cells. Endogenous hNek6 colocalizes with endogenous (A) Activating transcription factor 4, (B) CBF1 interacting corepressor, (C) Cdc42, (D) Ribosomal protein S7, (E) Nek9, and (F) RelB in HEK293 cells (white arrowheads), as visualized by confocal microscopy. Nuclei were stained by DAPI.

Table S1. Human Nek6 interacting proteins identified by the yeast two-hybrid system screens.

Protein interacting with hNek6 (aliases) ¹	Gene	Accession no.	Coded protein residues (retrieved/ complete sequence) ²	Frame	Redundancy in library ³			Growth score ⁴	Biological process (GO) ⁵
					FB	BM	L		
matrix metalloproteinase-2 (72 kDa type IV collagenase precursor, Gelatinase A, TBE- 1)	MMP2	AAH02576.1	385-614/ 660	+1		3		2/1	Carbohydrate metabolism
PDZ and LIM domain 7 (enigma)	PDLIM7	AAH01093.1	243-457/ 457	+1			2	4/0	Cell organization and biogenesis
cell division cycle 42 (GTP binding protein, 25kDa)	CDC42	AAH03682.1	1-191/ 191	+2	1			2/1	Cell organization and biogenesis
double-strand-break repair protein RAD21 homolog (hHR21, nuclear matrix protein 1, NXP-1, SCC1 homolog)	RAD21	AAH50381.1	549-631/ 631	+1		1		2/1	Cell organization and biogenesis
tubulin beta chain (M40)	TUBB	CAG46756.1	372-430/ 445	+2	2			2/1	Cell organization and biogenesis
I(3)mbt-like isoform II (human homolog of Drosophila lethal(3)malignant brain tumor)	L3MBTL	EAW75959.1	539-738/ 738	+1	2			4/2	DNA metabolism
MYST histone acetyltransferase 2 (MOZ, YBF2/SAS3, SAS2 and TIP60 protein 2)	MYST2	AAL56649.1	54-321/ 611	+1			1	4/1	DNA metabolism
histone-lysine N-methyltransferase ash1 (absent small and homeotic disks protein 1 homolog)	ASH1L	AAF68983.1	620-819/ 2969	+1			1	3/2	DNA metabolism
Putative DNA repair and recombination protein RAD26-like	RAD26L	A4D997.3	1-531/ 531	+1	2			3/1	DNA repair
retinoblastoma-binding protein 6 (p53-associated cellular protein Testis-derived, P2P-R, RBQ-1)	RBBP6	BAC77636.1	1-259/ 1792	+1			1	4/1	Metabolism
aminoadipate-semialdehyde dehydrogenase-phosphopantetheinyl transferase (HAH-P, CGI-80)	AASDHPTT	AAF86879.1	13-283/ 333	+1	5			4/1	Metabolism
collapsin response mediator protein 1 (dihydropyrimidinase-related protein 1, DRP-1)	CRMP1	AAH00252.1	1-168/ 572	+1	1			3/1	Metabolism
quinoid dihydropteridine reductase (HDHPR)	QDPR	AAH00576.1	1-244/ 244	+1	2			3/1	Metabolism
acireductone dioxygenase 1 (1,2-dihydroxy-3-keto-5-methylthiopentene dioxygenase, ARD, MTCBP-1)	ADI1	AAH01467.1	1-179/ 179	+1		1	1	4/1	Metabolism
coagulation factor XIII A chain (transglutaminase A chain)	F13A1	AAL12161.1	1-291/ 732 480-730/ 732	+1 +2		1	1	4/1 4/1	Metabolism
nephrocystin 3 (nephronophthisis 3)	NPHP3	AAP83423.1	1038-1314/ 1330	+1			1	2/1	Metabolism
NIMA-related kinase 9 (Nek9)	NEK9	AAH93881.1	806-979/ 979 635-860/ 979	+2 +1	1		1	4/1 4/1	Protein amino acid phosphorylation
mitogen-activated protein kinase kinase kinase 4 (MAPK/ERK kinase kinase 4, MEKK4)	MAP3K4	AAB68804.1	1214-1555/ 1607	+1		1		4/1	Protein amino acid phosphorylation
mitochondrial ribosomal protein L19	MRPL19	AAH30144.2	2-267/ 292	+1	1	5	1	2/1	Protein biosynthesis

ribosomal protein S7	RPS7	AAH02866.1	1-194/ 194	+1	11	58	58	4/1	Protein biosynthesis	
mitochondrial ribosomal protein L28	MRPL28	AAH00507.2	4-191/ 256	+1		1	2	1/0	Protein biosynthesis	
eukaryotic translation elongation factor 1 alpha 1	EEF1A1	AAH71841.1	1-301/ 462	+3			1	3/1	Protein biosynthesis	
proteasome 26S ATPase subunit 6 (26S protease regulatory subunit S10B, proteasome subunit p42)	PSMC6	AAB61616.1	8-201/ 389	+1	1			3/1	Protein degradation	
sorting nexin 26 (TC10/CDC42 GTPase-activating protein)	SNX26	O14559.2	1115-1287/ 1287	+1	1			4/1	Protein transport	
Rab-like GTP-binding protein 1 (partner of ARF)	RBEL1	ABO84837.1	1-258/ 729	+1			1	4/3	Protein transport	
CD74 antigen (invariant polypeptide of major histocompatibility complex, p33)	CD74	AAH18726.1	9-232/ 232	+1			2	2/1	Protein transport	
DnaJ (Hsp40) homolog, subfamily C, member 19	DNAJC19	AAH09702.1	1-37/ 116	+3			1	2/1	Protein transport	
U1 small nuclear ribonucleoprotein 70 kDa	SNRP70	AAH01315.1	1-437/ 437	+1			3	2/1	RNA processing	
splicing factor 3b, subunit 3, 130kDa (Spliceosome-associated protein 130, STAF130)	SF3B3	AAH68974.1	763-1046/ 1217	+1	4			2/1	RNA processing	
step II splicing factor SLU7	SLU7	AAD13774.1	1-236/ 586	+1			1	4/1	RNA processing	
CBF1 interacting corepressor	CIR	AAH46098.1	1-240/ 450	+1	3			4/1	RNA processing	
SNW domain containing 1 (Ski-interacting protein, nuclear protein SkiP, NCoA-62)	SNW1	AAI08904.1	184-417/ 536	+1			1	4/1	RNA processing	
nuclear receptor subfamily 2, group F, member 1 (COUP transcription factor 1, V-ERBA-related protein EAR-3)	NR2F1	AAH04154.1	1-253/ 423	+1	1			2/1	Signal transduction	
small G protein signaling modulator 3 (RUN and TBC1 domain-containing protein 3, RabGAPLP)	SGSM3	AAH08078.1	435-741/ 749	+1	5			4/1	Signal transduction	
nuclear receptor subfamily 2, group F, member 2 (ARP-1, COUP-TF2)	NR2F2	AAH14664.1	83-375/ 414	+1	1			2/1	Signal transduction	
PML-RARA regulated adaptor molecule 1	PRAM1	AAH28012.1	360-670/ 670	+1			2	2	4/1	Signal transduction
hairy/enhancer-of-split related with YRPW motif 2 (hCHF1, HESR-2, hHRT2, protein gridlock homolog)	HEY2	AAH07707.1	1-228/ 337	+1			2		4/2	Signal transduction
pleiotrophin (heparin binding growth factor 8, neurite growth-promoting factor 1), isoform CRA_c	PTN	AAH05916.1	1-168/ 168	+1	31		1		4/1	Signal transduction
diacylglycerol kinase, delta 130kDa isoform 2	DGKD	BAC11809.1	665-871/ 1214	+1				1	4/2	Signal transduction
zinc finger protein 106 homolog (zinc finger protein 474)	ZFP106	AAG35666.1	118-335/ 1883	+1				1	4/1	Signal transduction
guanine nucleotide binding protein (G protein), beta polypeptide 2-like 1	GNB2	AAH00214.1	55-299/ 317	+1				1	4/2	Signal transduction

activating transcription factor 4 (cAMP-responsive element-binding protein 2, CREB-2)	ATF4	AAH16855.1	252-351/ 351	+1	1	6	3	2/0	Stress response
peroxisome proliferator-activated receptor alpha (nuclear receptor subfamily 1 group C member 1)	PPARA	AAO13489.1	29-327/ 468	+1			1	2/0	Stress response
thyroid hormone receptor interactor 4 (TRIP-4, ASC-1, activating signal cointegrator 1)	TRIP4	AAH12448.1	46-581/ 581 3-581/ 581	+1	2		1	2/1 4/1	Transcription
DNA-directed RNA polymerases I and III subunit RPAC1 (RPC40)	POLR1C	AAH08863.1	1-290/ 346	+1	6			2/1	Transcription
methyl-CpG binding domain protein 2 isoform 1	MBD2	AAH32638.1	110-404/ 411	+1		1	5	4/1	Transcription
RNA polymerase II elongation factor ELL (Eleven-nineteen lysine-rich leukemia protein)	ELL	AAA57120.1	37-621/ 621	+1			1	4/1	Transcription
retinoic acid receptor RXR-beta (retinoid X receptor beta, nuclear receptor subfamily 2 group B member 2)	RXRB	AAA60293.1	162-293/ 533	+1			1	4/1	Transcription
zinc finger protein 24 (KOX17, ZFP191, RSG-A, zinc finger and SCAN domain-containing protein 3)	ZNF24	AAB70216.1	45-315/ 368	+1		1		4/1	Transcription
zinc finger protein 281 (transcription factor ZBP-99, GC-box-binding zinc finger protein 1)	ZNF281	AAD21084.1	42-324/ 895	+1			1	2/1	Transcription
vacuolar H+ ATPase G1 (ATPase, H+ transporting, lysosomal 13kDa, V1 subunit G1)	ATP6V1G1	AAC39868.1	1-118/ 118	+3			1	2/1	Transport
KIAA0564 protein (FLJ21779)	KIAA0564	AAH53674.2	638-820/ 1039	+1			4	4/1	Transport
leucine-rich repeat-containing 8, member A	LRRC8A	AAH51322.1	612-810/ 810	+1	5			4/1	UNKNOWN
ankyrin repeat family A protein 2	ANKRA2	AAH12917.1	78-313/ 313	+1	2			4/1	UNKNOWN
KIAA0649 (1A6/DRIM-interacting protein)	KIAA0649	AAH47935.1	572-846/ 1209	+1	1			2/1	UNKNOWN
UPF0418 protein FAM164A	CGI-62	AAH09074.1	160-325/ 325	+1	2			2/1	UNKNOWN
WD repeat-containing protein 74 (NOP seven-associated protein 1)	WDR74	AAS48499.1	217-385/ 385	+1		2		4/2	UNKNOWN
TraB domain containing, isoform CRA_b (FLJ00037)	TRABD	AAH93029.1	224-292/ 292	+1			3	1/0	UNKNOWN
partner of NOB1 homolog (putative 28 kDa protein)	PNO1	AAH08304.1	1-252/ 252	+1			2	3/1	UNKNOWN
cerebellar degeneration-related protein 2 (paraneoplastic cerebellar degeneration-associated antigen)	CDR2	AAH17503.2	237-454/ 454	+1			1	3/1	UNKNOWN
KRI1 homolog	KRI1	Q8N9T8.2	40-708/ 709	+1		1		3/1	UNKNOWN
widely-interspaced zinc finger-containing protein (zinc finger protein 803)	WIZ	BAG53783.1	420-614/ 835	+1		1		4/2	UNKNOWN
zinc finger, HIT domain containing 1 (cyclin-G1-binding protein 1, ZNFN4A1, p18 Hamlet)	ZNHIT1	AAH17333.1	1-154/ 154	+1	1			2/1	UNKNOWN

peroxiredoxin 3 (Prx-III, AOP-1, HBC189)	PRDX3	AAH08435.1	183-256/ 256	+1		1		4/1	UNKNOWN
PHD finger protein 1 (T-complex testis-expressed 3, Polycomb-like protein 1)	PHF1	AAH08834.1	36-317/ 567	+1	5	1	1	4/2	UNKNOWN
v-rel reticuloendotheliosis viral oncogene homolog B	RELB	AAH28013.1	167-367/ 579	+3				2/1	UNKNOWN

¹ Results obtained from BLASTX (GenBank).

² It is depicted the minimum length of the retrieved sequences which could be visualized by forward DNA sequencing only.

³ Absolut number of sequences retrieved from each human library (FB: fetal brain, BM: bone marrow, L: leukocyte).

⁴ The numbers (scores 0-4) refer to the relative growth levels of the yeast clones after cotransformation of each retrieved sequence in pACT2 vector and the bait construction pBTM116KQ-hNEK6 (X/-) or the empty pBTM116KQ vector (-/Y) when plated in triplicate drops on minimal medium plates containing 3-AT, e.g. 2/1 indicates twice the growth in the presence of hNEK6 relative to the empty vector.

⁵ Biological process based on the GO database (other functions may be known; see also Table S3).

Table S2. Putative phosphorylation sites present in human Nek6 interacting proteins.

Gene	Coded protein residues (retrieved/ complete sequence) ¹	Putative phosphorylation sites by Nek6 ²			Putative phosphorylation sites by NIMA ²
		General (L-X-X-S/T-X)	Preferable (L-X-X-S/T-F/W/Y)	Other acceptable (L/F/W/Y-X-X-S/T-F/W/Y/M/L/I/V/R/K)	(F-R-X-S/T-X)
MMP2	385-614/ 660	GL <u>E</u> HSQDPG	LL <u>V</u> ATFWPE	A <u>E</u> NWSKNKK I <u>Y</u> TYTKNFR	N <u>F</u> RLSQDDI
PDLIM7	243-457/ 457	PL <u>C</u> CKSHAFS	AL <u>G</u> FSWHDT AL <u>K</u> MKTWHVH		
CDC42	1-191/ 191	GL <u>F</u> DTAGQE LL <u>V</u> GTQIDL	CL <u>L</u> ISYTTN	E <u>Y</u> VPTVFDN N <u>Y</u> AVTMVIG	
RAD21	549-631/ 631	AL <u>A</u> KTGAES			
TUBB	372-430/ 445				
L3MBTL	539-738/ 738	L <u>P</u> HTRTSK EL <u>S</u> DSSEASA SL <u>F</u> MSALSA		GE <u>V</u> QTLTGC	
MYST2	54-321/ 611	PL <u>R</u> QTRSSG SL <u>K</u> DSGSDL		RE <u>H</u> ESYNFN T <u>Y</u> GNTREPL	
ASH1L	620-819/ 2969	SL <u>S</u> TSLSQSK KL <u>S</u> SSMCVS EL <u>E</u> RSSELFK SL <u>S</u> NSNSEP KL <u>S</u> SKSTAPS LL <u>A</u> DSEKPS			
RAD26L	1-531/ 531	TL <u>P</u> HTKKGQ RL <u>E</u> NTMKDQ SL <u>S</u> VSHFSF PL <u>Y</u> ISNPVN		HE <u>S</u> FSKQSH FE <u>V</u> DVSVSQF	
RBBP6	1-259/ 1792	GL <u>H</u> ISLCDL PL <u>L</u> TTTEESL DL <u>Q</u> ITNAQT QL <u>T</u> KTANLA ML <u>T</u> TNTGKYA		T <u>Y</u> VISRTEP	
AASDHPPT	13-283/ 333	CL <u>V</u> PSMEGV RL <u>Q</u> RTAKGK	AL <u>K</u> ESFIKA	TW <u>L</u> PSRAEW AF <u>E</u> ESKIDE V <u>Y</u> KETRLFL	
CRMP1	1-168/ 572		SL <u>L</u> TSFEKW	FE <u>Q</u> GTRAAL	
QDPR	1-244/ 244	QL <u>C</u> QSLAGK VL <u>P</u> VTLDTP AL <u>D</u> GTGPMI	FL <u>V</u> ETFHDW	WWW <u>A</u> SVDVV MW <u>K</u> QSIWTS I <u>W</u> TSTISSH	
ADI1	1-179/ 179	IL <u>D</u> GSgyFD FL <u>A</u> QTA			
F13A1	1-291/ 732 480-730/ 732	PL <u>K</u> ETLRNV KL <u>I</u> ASMSSD VL <u>R</u> TSRNPE FL <u>N</u> VTSVHL	KL <u>S</u> ITFRNN	DF <u>K</u> LSITFR TF <u>D</u> VTLLEPL	
NPHP3	1038-1314/ 1330	FL <u>K</u> RSLEMR SL <u>A</u> YTVKHL	LL <u>M</u> FSFSKD	I <u>Y</u> EDSLGRM ME <u>S</u> FSKDKG	
NEK9	806-979/ 979 635-860/ 979	CL <u>L</u> GTDSCR RL <u>A</u> MTPTER			GE <u>R</u> GTM ² EAD
MAP3K4	1214-1555/ 1607	FL <u>T</u> SSGLIK		DE <u>G</u> C ² SVKLK E <u>Y</u> EHTFQLL	
MRPL19	2-267/ 292	RL <u>D</u> DSLLYL IL <u>R</u> VTTADP DL <u>C</u> LTEQQM	GL <u>G</u> RSFQAA GL <u>G</u> ATFILR		
RPS7	1-194/ 194	KL <u>D</u> GSRLIK EL <u>N</u> ITAAKE			
MRPL28	4-191/ 256			HY <u>L</u> RSLEEE KE <u>T</u> VTVTMR	

EEF1A1	1-301/ 462	LLAYTLGVK ILPPTTRPTD MLEPSANMP		KEFETSKYYV KYVYVTIIDA GWKVTRKDG
PSMC6	8-201/ 389	QLDKSKLKP ALDMTTLTI ELPLTNPEL		
SNX26	1115-1287/ 1287	MLGQSPPLH PLHRSPDFL HLGYSAPQH	LNASYGML	DELLSYPPA
RBEL1	1-258/ 729	KLVGSDQAP		
CD74	9-232/ 232	HLKNTMETI GLGVTKQDL KLTVTTSQNL	PLKGSFPEN	LEEMSRHSL
DNAJC19	1-116/ 116	SLPKSAFSG ILGVSP TAN		
SNRP70	1-437/ 437			
SF3B3	763-1046/ 1217	NLPESIFGA PLQYTPRKF FLHKTPVEE		GEVYTYKLV
SLU7	1-236/ 586	PLSGSKEMS		QYISSVPWY
CIR	1-240/ 450			EELKSLTTK
SNW1	184-417/ 536			LENQSKGYG
NR2F1	1-253/ 423	NLTYTCRAN DLQITDQVS		FEKRSVRRN
SGSM3	435-741/ 749	VLCSLPTV	VLCKTFRLD	CEAFSLSQD
NR2F2	83-375/ 414	RLLFSAVEW RLTWSELFV GLHASPMSA VLFTSDACG NLTYTCRAN DLQITDQVS	LLRLTWSEL	FEKRSVRRN PYPTSRYGS
PRAM1	360-670/ 670	DLRRTSAA PLPSSASES GLVHSGGAR GLRPSHPPR		
HEY2	1-228/ 337	ILQMTVDHL GLDSSDPLR GLHASESTP RLVPTAFEK MLQATGGKG RLSTTSEVP		RYLSSVEGL
PTN	1-168/ 168			EWQWSVCVP
DGKD	665-871/ 1214	SLGSSASLP	LLHRTYKNL	
ZFP106	118-335/ 1883	WLSNSGAVD		SEPHSLRNG GENNTRKNS
GNB2	55-299/ 317	SLCASGGKD ALCFSPNRY SLAWSADGQ	ALSGSWDGT KLWNTLGVC	SWDGTLRLLW GYLNTVTVS
ATF4	252-351/ 351	LCGSARPK		
PPARA	29-327/ 468			FFERTIRLK
TRIP4	46-581/ 581 3-581/ 581	RLEDTIQAI TLVCTHEEQ GLDVSEEI	QLRKTFLGD ELQATYRLL	GWCLSVHQP LECGTLVCT QYVLSIESA
POLR1C	1-290/ 346			

MBD2	110-404/ 411	D_LNTTLPIR Y_LGNTVDLS G_LASADVTE A_LHTSSAPI W_LNTSQPLC		
ELL	37-621/ 621	S_LRPSIRFQ T_LSSSTHLP D_LGHSGRDC	E_YLHSKLAH	
RXRB	162-293/ 533	D_LTYSCRDN	F_EKRTIRKD	
ZNF24	45-315/ 368	G_LPSSSEDA		
ZNF281	42-324/ 895	V_LSSSTSAA V_LSSSSRT L_LSSSSRTD I_LSPSQKPH V_LIHTGERP	G_FLQSLVSI	A_FRSSYHLR
ATP6V1G1	1-118/ 118			
KIAA0564	638-820/ 1039	S_LAASLSTR L_LRISRRLS S_LARSALEK K_LRETQDPT	R_FLPSLARS	
LRRC8A	612-810/ 810	D_LFNTLPPE Y_DLSHNNL L_LKRSGLVV N_LAITANRI		
ANKRA2	78-313/ 313	L_LANSLSVH S_LACSKGYT M_LLESGADP	L_YLATRIEQ	
KIAA0649	572-846/ 1209	D_LLRSKRKL C_LSKSKRDS P_LSKTPDPL		
CGI-62	160-325/ 325	A_LKKSNSPG T_LSPSHKGI	T_YTESYIAR	
WDR74	217-385/ 385	E_LWASLEAA G_LAGSVRGL P_LLASCGLD C_LLLSGRDN P_LEDTEDE	V_LETTYGEY	
TRABD	224-292/ 292	D_LHRTIVSE		
PNO1	1-252/ 252		L_FLESFEIT	
CDR2	237-454/ 454	P_LKRSSSET S_LAGSDIVK L_GATGAYR		
KRI1	40-708/ 709	A_LDGSLMGP L_LGPTVMLG R_LQETSSQS S_LKKTCMYR	Q_LKESFRAF	T_YPRSIASS D_EYKTLSSL
WIZ	420-614/ 835	P_LPLSPLAG E_LSLTPITG	G_YLGSVAAK	
ZNHIT1	1-154/ 154	C_LKWTV		
PRDX3	183-256/ 256			
PHF1	36-317/ 567	I_LPFTSENW E_LSDTPKGE	L_YHLSVCCK L_YLGTIKKV	
RELB	167-367/ 579		C_FQASYRDQ	

¹ It is depicted the minimum length of the retrieved sequences which could be visualized by forward DNA sequencing only.

² The phosphorylated residue (Ser/Thr) is in bold and the residues Leu (for Nek6³⁸), Phe (for NIMA³⁹), or another hydrophobic residue, at position -3, are underlined.

Table S3. *In silico* analysis of human Nek6 interacting proteins functional and structural properties.

Gene	Coded protein residues (retrieved/ complete sequence) ¹	Putative domain composition (Pfam, PROSITE or InterPro) ²	Putative percent disordered residues (PONDR) ³	Cellular component (GO) ⁴	Biological processes (GO) ⁵	Coexpressed genes (GEMMA) ⁶
MMP2	385-614/ 660	Matrixin domain, Hemopexin repeat	19.57	Plasma membrane, ECM	Carbohydrate metabolism, Metabolism, Protein degradation	PDLIM7, F13A1
PDLIM7	243-457/ 457	LIM domain	17.21	Cytoplasm (stress fiber)	Cell organization and biogenesis, Transport	
CDC42	1-191/ 191	Ras family domain	18.32	Cytoplasm (filopodium), plasma membrane	Cell cycle, Cell organization and biogenesis, Protein transport, Signal transduction	
RAD21	549-631/ 631	Conserved region of Rad21/ Rec8-like protein	31.33	Nucleus (chromosome)	Cell cycle, Cell organization and biogenesis, DNA recombination, DNA repair	PSMC6
TUBB	372-430/ 445	Tubulin beta chain subfamily domain	18.64	Cytoplasm (microtubule)	Cell organization and biogenesis, Metabolism	
L3MBTL	539-738/ 738	Zinc finger (C2HC type) domain	36.00	Nucleus	DNA metabolism	
MYST2	54-321/ 611	Zinc finger (C2HC type) domain	70.15	Nucleus	DNA metabolism, DNA replication, Transcription	RPS7, RAD21
ASH1L	620-819/ 2969	SET-binding protein (SETBP) subfamily domain	40.00	Nucleus, tight junction	DNA metabolism, Transcription	MBD2, RBBP6, NR2F2, RXRB, SLU7
RAD26L	1-531/ 531	UNDESCRIBED	36.35	Nucleus	DNA repair	
RBBP6	1-259/ 1792	DWNN domain, Zinc knuckle domain	35.14	Nucleus	Metabolism	
AASDHPPT	13-283/ 333	4'-phosphopantetheinyl transferase superfamily domain	25.46	Cytoplasm	Metabolism	PSMC6, RAD21
CRMP1	1-168/ 572	Amidohydrolase family domain	23.81	Cytoplasm	Metabolism	MBD2
QDPR	1-244/ 244	Short chain dehydrogenase domain	38.52	Cytoplasm	Metabolism	
ADI1	1-179/ 179	ARD/ ARD' family domain	22.91	Nucleus, cytoplasm, plasma membrane	Metabolism	QDPR, RHOA
F13A1	1-291/ 732 480-730/ 732	Transglutaminase family domain	26.01 19.92	Cytoplasm, ECM	Metabolism	MMP2, CIR
NPHP3	1038-1314/ 1330	Tetratricopeptide repeat	28.88	Cytoplasm (microtubule)	Metabolism	
NEK9	806-979/ 979 635-860/ 979	Proline-rich region, Coiled-coil domain, RCC1, PEST region*	52.87 46.90	Nucleus, cytoplasm	Cell cycle, Protein amino acid phosphorylation	
MAP3K4	1214-1555/ 1607	Protein kinase domain	38.30	UNDESCRIBED	Protein amino acid phosphorylation, Signal transduction, Stress response	
MRPL19	2-267/ 292	Ribosomal protein L19 family domain	36.47	Nucleus, cytoplasm (ribosome and mitochondrion)	Protein biosynthesis	PSMC6, PRDX3, PNO1
RPS7	1-194/ 194	Ribosomal protein S7e family domain	53.61	Nucleus (nucleolus) and cytoplasm (ribosome)	Protein biosynthesis	

MRPL28	4-191/ 256	p53-like transcription factor (DNA binding) superfamily domain	36.70	Nucleus, cytoplasm (mitochondrial ribosome)	Protein biosynthesis	TUBB
EEF1A1	1-301/ 462	Elongation factor Tu GTP binding domain	15.28	Cytoplasm	Metabolism, Protein biosynthesis	
PSMC6	8-201/ 389	ATPase family associated with various cellular activities (AAA)	47.42	Nucleus, cytoplasm (proteasome)	Protein degradation	RAD21, MRPL19, PRDX3
SNX26	1115-1287/ 1287	CDC42 GTPase-activating protein family domain, Proline-rich region	88.44	Cytoplasm, plasma membrane	Protein transport, Signal transduction	CRMP1, PSMC6
RBEL1	1-258/ 729	Small GTPase Rab1 family domain	27.41	Nucleus, cytoplasm	Protein transport, Signal transduction	L3MBTL
CD74	9-232/ 232	CLIP (MHC2 interacting) domain	47.77	Cytoplasm (ER, lysosome and Golgi), plasma membrane	Metabolism, Protein transport, Signal transduction	
DNAJC19	1-116/ 116	DnaJ domain	25.86	Mitochondrial membrane	Metabolism, Protein transport	
SNRP70	1-437/ 437	RNA recognition motif (a.k.a. RRM, RBD or RNP domain)	49.06	Nucleus (spliceosome)	RNA processing	DGKD
SF3B3	763-1046/ 1217	CPSF A subunit region	24.30	Nucleus (spliceosome)	Metabolism, RNA processing	
SLU7	1-236/ 586	Zinc finger (CCHC-type) domain	52.97	Nucleus (nuclear speck and spliceosome), cytoplasm	RNA processing	ASH1L
CIR	1-240/ 450	N-terminal domain of CBF1 interacting corepressor CIR	32.64	Nucleus (nuclear speck and HDAC)	RNA processing, Transcription	F13A1
SNW1	184-417/ 536	SKIP/ SNW domain	68.38	Nucleus (spliceosome)	RNA processing	PSMC6
NR2F1	1-253/ 423	Zinc finger (C4 type) domain, Ligand-binding domain of nuclear hormone receptor	53.36	Nucleus	Signal transduction, Transcription	L3MBTL, NR2F2
SGSM3	435-741/ 749	SH3 domain, RUN domain	20.85	Cytoplasm	Cell cycle, Signal transduction	
NR2F2	83-375/ 414	Zinc finger (C4 type) domain, Ligand-binding domain of nuclear hormone receptor	34.47	Nucleus	Metabolism, Signal transduction, Transcription	
PRAM1	360-670/ 670	SH2 containing adaptor PRAM-1 related family domain, SH3 domain, Proline-rich region	69.45	UNDESCRIBED	Signal transduction	
HEY2	1-228/ 337	Helix-loop-helix DNA-binding domain, Hairy orange domain	49.12	Nucleus	Signal transduction	
PTN	1-168/ 168	PTN/ MK heparin-binding protein family N-terminal domain	35.71	Cytoplasm (ER), ECM	Signal transduction	
DGKD	665-871/ 1214	Diacylglycerol kinase accessory domain	58.45	Cytoplasm, plasma membrane	Metabolism, Signal transduction	SNRP70, PRDX3, TRABD
ZFP106	118-335/ 1883	UNDESCRIBED	31.65	Nucleus, cytoplasm	Metabolism, Signal transduction	
GNB2	55-299/ 317	WD domain (G-beta repeat)	6.53	Plasma membrane	Signal transduction	AASDHPPT, ZNHIT1
ATF4	252-351/ 351	bZIP transcription factor family domain	72.00	Nucleus, cytoplasm, plasma membrane	Metabolism, Stress response, Transcription	

PPARA	29-327/ 468	Zinc finger (C4 type) domain, Ligand-binding domain of nuclear hormone receptor	29.77	Nucleus	Metabolism, Stress response, Transcription, Transport	
TRIP4	46-581/ 581 3-581/ 581	Putative zinc finger motif (C2HC5-type), ASCH domain	38.25 38.69	Nucleus, cytoplasm	Transcription	CRMP1, PSMC6, MYST2
POLR1C	1-290/ 346	RNA polymerase Rpb3/ Rpb11 dimerization domain	25.86	Nucleus	Transcription	
MBD2	110-404/ 411	Methyl-CpG binding domain	59.66	Nucleus (HDAC)	Metabolism, Transcription	ASH1L, CRMP1
ELL	37-621/ 621	RNA polymerase II elongation factor ELL family domain, Occludin homology domain	50.60	Nucleus (nuclear speck)	Metabolism, Transcription	SNRP70
RXRB	162-293/ 533	Zinc finger (C4 type) domain, MYM-type zinc finger with FCS sequence motif	72.73	Nucleus	Transcription	SNRP70, ASH1L
ZNF24	45-315/ 368	SCAN domain, Zinc finger (C2H2 type) domain	40.59	Nucleus	Transcription	
ZNF281	42-324/ 895	Zinc finger (C2H2 type) domain	44.17	Nucleus	Transcription	
ATP6V1G1	1-118/ 118	Vacuolar (H ⁺)-ATPase G subunit family domain	70.34	Lysosomal membrane	Metabolism, Transport	PSMC6
KIAA0564	638-820/ 1039	ATPase family associated with various cellular activities (AAA)	20.22	Nucleus, cytoplasm (mitochondrion)	Metabolism, Transport	
LRRC8A	612-810/ 810	Leucine-rich repeat	32.66	Membrane	UNKNOWN	
ANKRA2	78-313/ 313	Ankyrin repeat	23.31	Cytoplasm (cytoskeleton)	UNKNOWN	RAD21, RBBP6, SLU7
KIAA0649	572-846/ 1209	UNDESCRIBED	85.09	Nucleus	UNKNOWN	SNW1
CGI-62	160-325/ 325	C2H2 zinc finger CGI-62-related family domain	70.48	UNDESCRIBED	UNKNOWN	
WDR74	217-385/ 385	WD domain (G-beta repeat)	48.52	Nucleus	UNKNOWN	PNO1, POLR1C
TRABD	224-292/ 292	TraB family domain	63.77	UNDESCRIBED	UNKNOWN	L3MBTL, SNRP70
PNO1	1-252/ 252	KH domain	48.02	Nucleus (nucleolus)	UNKNOWN	MRPL19, POLR1C
CDR2	237-454/ 454	UNDESCRIBED	60.09	Nucleus, cytoplasm	UNKNOWN	
KRI1	40-708/ 709	KRI1-like family domain	61.73	UNDESCRIBED	UNKNOWN	SNRP70
WIZ	420-614/ 835	Zinc finger (C2H2 type) domain	55.90	Nucleus	UNKNOWN	MYST2
ZNHIT1	1-154/ 154	HIT zinc finger domain	43.51	UNDESCRIBED	UNKNOWN	MRPL28
PRDX3	183-256/ 256	C-terminal domain of 1-Cys peroxiredoxin, AhpC/ TSA family domain	33.78	Cytoplasm (mitochondrion)	UNKNOWN	PSMC6

PHF1	36-317/ 567	PHD-finger domain	17.38	Nucleus	UNKNOWN	RXRB
RELB	167-367/ 579	Rel homology domain (RHD)	24.62	Nucleus	UNKNOWN	CD74, PDLIM7

¹ It is depicted the minimum length of the retrieved sequences which could be visualized by forward DNA sequencing only.

² Domain composition of the retrieved sequences obtained by Pfam, PROSITE or InterPro databases (other domains may be present).

³ Percentage of disordered amino acid residues in the retrieved sequences obtained by PONDR.

⁴ Cellular components based on the GO and Uniprot databases.

⁵ Biological processes based on the GO database.

⁶ Coexpressed genes obtained by GEMMA database, including only the ones whose products were identified to interact with hNek6 by our two-hybrid screens.

* Domain composition described by Roig et al.¹⁷.

2. Artigo II:

**HUMAN NEK6 IS A MONOMERIC MOSTLY GLOBULAR KINASE WITH AN
UNFOLDED SHORT N-TERMINAL DOMAIN**

GABRIELA V. MEIRELLES, JÚLIO C. SILVA, YURI DE A. MENDONÇA,
CARLOS H. I. RAMOS, IRIS L. TORRIANI, AND JÖRG KOBARG

BMC STRUCTURAL BIOLOGY, v. 11(1), p. 12, 2011.

(doi: 10.1186/1472-6807-11-12)

RESEARCH ARTICLE

Open Access

Human Nek6 is a monomeric mostly globular kinase with an unfolded short N-terminal domain

Gabriela V Meirelles^{1,2}, Júlio C Silva¹, Yuri de A Mendonça^{1,2,3}, Carlos HI Ramos^{2,3}, Iris L Torriani^{4,5}, Jörg Kobarg^{1,2*}

Abstract

Background: The NIMA-related kinases (Neks) are widespread among eukaryotes. In mammals they represent an evolutionarily conserved family of 11 serine/threonine kinases, with 40–45% amino acid sequence identity to the *Aspergillus nidulans* mitotic regulator NIMA within their catalytic domains. Neks have cell cycle-related functions and were recently described as related to pathologies, particularly cancer, consisting in potential chemotherapeutic targets. Human Nek6, -7 and -9 are involved in the control of mitotic spindle formation, acting together in a mitotic kinase cascade, but their mechanism of regulation remain elusive.

Results: In this study we performed a biophysical and structural characterization of human Nek6 with the aim of obtaining its low resolution and homology models. SAXS experiments showed that hNek6 is a monomer of a mostly globular, though slightly elongated shape. Comparative molecular modeling together with disorder prediction analysis also revealed a flexible disordered N-terminal domain for hNek6, which we found to be important to mediate interactions with diverse partners. SEC-MALS experiments showed that hNek6 conformation is dependent on its activation/phosphorylation status, a higher phosphorylation degree corresponding to a bigger Stokes radius. Circular dichroism spectroscopy confirmed our *in silico* predictions of secondary structure content and thermal stability shift assays revealed a slightly higher stability of wild-type hNek6 compared to the activation loop mutant hNek6(S206A).

Conclusions: Our data present the first low resolution 3D structure of hNek6 protein in solution. SAXS, comparative modeling and SEC-MALS analysis revealed that hNek6 is a monomeric kinase of slightly elongated shape and a short unfolded N-terminal domain.

Background

Mitotic progression and assembly of the bipolar mitotic spindle are regulated by several serine/threonine protein kinases, including members of the cyclin-dependent kinase (Cdk), Polo-like kinase (Plk), Aurora, and NIMA-related kinase (Nek) families [1–4]. The founding member of Nek family, the NIMA kinase of *Aspergillus nidulans*, contributes to multiple aspects of mitotic progression including the timing of mitotic entry, chromatin condensation, spindle organization and cytokinesis. Mammals contain a large family of eleven Neks, the catalytic domain of which is evolutionarily related to that of NIMA [4]. Nek2 has a central role in centrosome maturation and disjunction [5], whereas Nek1 and Nek8 have been proposed to contribute

to ciliary function [6,7]. Besides Nek2, Nek1, -6, -7 and -9 were also described to participate in centrosomal regulation [7–11]. Nek6, Nek7 [9] and Nek9 [12] are involved in the control of mitotic spindle formation, acting together in a mitotic kinase cascade, with Nek9 being upstream of Nek6 and Nek7 [13]. Nek kinases are also described as related to pathologies, particularly cancer, presenting thereby interesting potential chemotherapeutic targets [14–20]. Recently, hNek6 was described to have its transcript, protein, and/or kinase activity levels highly elevated in a number of tumors and human cancer cell lines, indicating an important role for hNek6 in tumorigenesis [21–24].

Structurally, Neks in general are characterized by having a conserved N-terminal catalytic domain, followed by a nonconserved C-terminal regulatory domain that varies in size and structure. However, Nek6 and Nek7 are significant exceptions to this, in that they are the

* Correspondence: jorg.kobarg@lnbio.org.br

¹Laboratório Nacional de Biotecnologia, Centro Nacional de Pesquisa em Energia e Materiais, Campinas, SP, Brazil

Full list of author information is available at the end of the article

smallest of the kinases and consist only of a catalytic domain with a relatively short N-terminal extension [4]. Although they share significant similarity with each other, being ~86% identical within their catalytic domains, the N-terminal extensions are not conserved, and it has been suggested that they may play a role in differential regulation of the kinases [25].

The mechanisms of regulation of hNek6, -7, and -9 kinases are currently unknown, and elucidating this pathway would provide relevant knowledge on early mitotic events as well as new hints for drug design and cancer therapy. However, hNek2 and hNek7 are the only NIMA-related kinases for which structures have been reported [26-28]. In this context, we present here the first low resolution three-dimensional structure of hNek6 protein in solution. SAXS experiments, together with SEC-MALS and comparative molecular modeling revealed a monomeric mostly globular, though slightly elongated conformation for hNek6, with a flexible disordered N-terminal domain.

Results and Discussion

Human Nek6 is predicted to be phosphorylated at various sites and has an unfolded short N-terminal domain

Human Nek6 amino acid sequence was analyzed considering its secondary structure, disordered regions, conserved motifs and putative phosphorylation sites by upstream kinases, resulting in a linear representation of its main structure predictions (Figure 1A). These analyses were also performed for hNek7, for which the crystallographic structure was recently determined [28], in order to validate our results (Figure 1B).

Our consensus of secondary structure was scored by the number of times (one to five times) the predicted secondary structure element (α -helices, β -strands or coils) scored positive from five predictions using different databases: **PredictProtein/Prof** [29], **PSIPRED** [30], **SSpro** [31], **SOPMA** [32] and **GOR4** [33]. In summary, the secondary structure analysis suggested that hNek6 was composed of approximately 34% α -helices, 12% β -strands and 54% coils. Our hNek7 consensus of predicted secondary structure is 80% identical to the author-approved secondary structure in PDB (2WQM) (Figure 1B).

In the case of the disordered regions predictions, our consensus was obtained following the same criteria as for the secondary structure predictions, except that we used here nine different databases: **FoldIndex** [34], **GlobPlot Russell/Linding** [35], **PONDR VL-XT** [36], **DISpro** [37], **IUPred** [38], **DisEMBL Hot-loops**, **DisEMBL Remark-465**, **DisEMBL Loops/coils** [39], and **VSL2B** [40]. From this analysis, we were able to identify

a short high scored segment of disorder covering the majority of hNek6 N-terminal extension before its catalytic domain, which we are calling here the regulatory domain. This characteristic is also present in our hNek7 consensus of disorder predictions and in its crystal structure [28], where amino acids 1-19 are missing residues (due to a flexible region) and amino acids 20-23 are coils. Notably, we found that hNek6 unfolded short N-terminal region is important to mediate interactions with diverse partners [41] and, since hNek6 and hNek7 are similar in their catalytic domain sequences (~86% identity), but different in their N-terminal extensions (~20% identity) (Figure 1C), it is possible that both proteins depend on their disordered N-terminal domain to regulate the interactions with specific/different partners.

For phosphorylation analysis, NetPhosK [42] and NetPhos [43] databases were used to predict phosphorylation sites (Table 1), and together with *in vitro* and *in vivo* phosphorylation data [13], they were used to assign tyrosine, threonine and serine residues as putative phosphorylation sites for hNek6 and hNek7 (Figure 1). This analysis shows a variety of high score phosphorylation predictions for hNek6. Interestingly, there are four predicted sites localized in hNek6 N-terminal domain (serine residues 13, 14, 37 and 41), and one of them (Ser³⁷) also described to be phosphorylated *in vivo* [13], suggesting that this is an important phosphorylation-regulated region.

Secondary structure analysis

The secondary structure content of hNek6 was analyzed by Circular Dichroism (CD) spectroscopy. Figure 2 shows the CD spectra of recombinant wild-type hNek6 fused to a 6xHis-tag recorded at 4°C. Purified protein presents negative ellipticity in the far-UV, with minima at 208 (-15567 deg cm² dmol⁻¹) and 222 nm (-12053 deg cm² dmol⁻¹). This spectrum is typical of many globular proteins [44] and suggests a high content of α -helices, since this secondary structure is characterized by minima around 208 and 222 nm. Deconvolution of the CD spectrum using the CDNN software [45] indicated approximately 41.7% of α -helices, 13.2% of β -strands, 15.7% of beta-turns and 25.8% of random coils. Deconvolution using another software, K2d [46], indicated a similar amount of secondary structure elements: approximately 41% of α -helices, 17% of β -strands and 42% of coils. We also estimated the quantity of α -helix structure by the evaluation of the CD spectrum signal at 222 nm, according to Corrêa and Ramos, 2009 [47], resulting in 38.6% of α -helices. Compared to our predictions, wild-type hNek6 showed a very similar content of α -helices (~34%), β -strands (12%) and coils (54%). In conclusion, both the *in silico* prediction and the experimentally derived data

Table 1 Prediction of putative phosphorylation sites in human Nek6

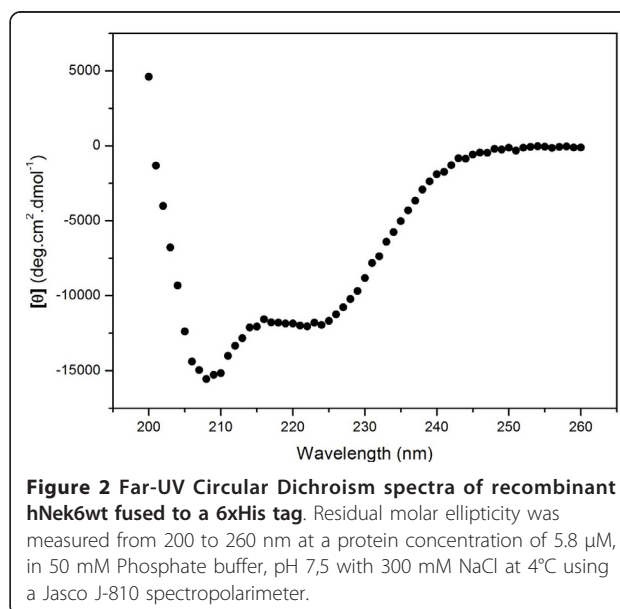
Residue ^a	Putative Upstream Kinase ^b	Predictor (Score)
S ¹³	PKA	NetPhosK (0.63)
S ¹⁴	PKA	NetPhosK (0.52)
S ¹⁴	Cdc2	NetPhosK (0.53)
S ³⁷	PKC	NetPhosK (0.82)
S ⁴¹	PKC	NetPhosK (0.56)/NetPhos (0.72)
S ⁴¹	PKA	NetPhosK (0.65)/NetPhos (0.72)
T ⁷⁰	PKC	NetPhosK (0.79)
S ¹¹¹	CKII	NetPhosK (0.64)
S ¹³¹	DNAPK	NetPhosK (0.62)
S ¹³¹	ATM	NetPhosK (0.68)
S ¹⁵⁸	CKII	NetPhosK (0.53)
S ¹⁵⁸	Cdc2	NetPhosK (0.51)
T ¹⁸³	PKC	NetPhosK (0.65)
S ¹⁹⁸	PKA	NetPhosK (0.56)/NetPhos (0.79)
S ¹⁹⁸	Cdc2	NetPhosK (0.50)/NetPhos (0.79)
S ¹⁹⁹	CKII	NetPhosK (0.50)
S ¹⁹⁹	Cdc2	NetPhosK (0.55)
T ²⁰¹	PKC	NetPhosK (0.73)
S ²⁰⁶	CKI	NetPhosK (0.53)/NetPhos (0.99)
T ²¹⁰	GSK3	NetPhosK (0.51)
T ²¹⁰	CDK5	NetPhosK (0.55)
S ²¹⁵	GSK3	NetPhosK (0.50)/NetPhos (0.99)
S ²¹⁵	Cdk5	NetPhosK (0.59)/NetPhos (0.99)
Y ²²⁴	EGFR	NetPhosK (0.55)/NetPhos (0.72)
S ²³²	PKA	NetPhosK (0.67)
S ²⁴⁵	p38MAPK	NetPhosK (0.50)
S ²⁴⁵	Cdk5	NetPhosK (0.55)
S ²⁵⁶	CKI	NetPhosK (0.54)
S ²⁵⁶	PKC	NetPhosK (0.50)
S ²⁷⁵	CKII	NetPhosK (0.52)
S ³¹¹	PKC	NetPhosK (0.66)

^a Putative phosphorylated residues predicted with the highest scores by NetPhosK, which may additionally be predicted by NetPhos server.

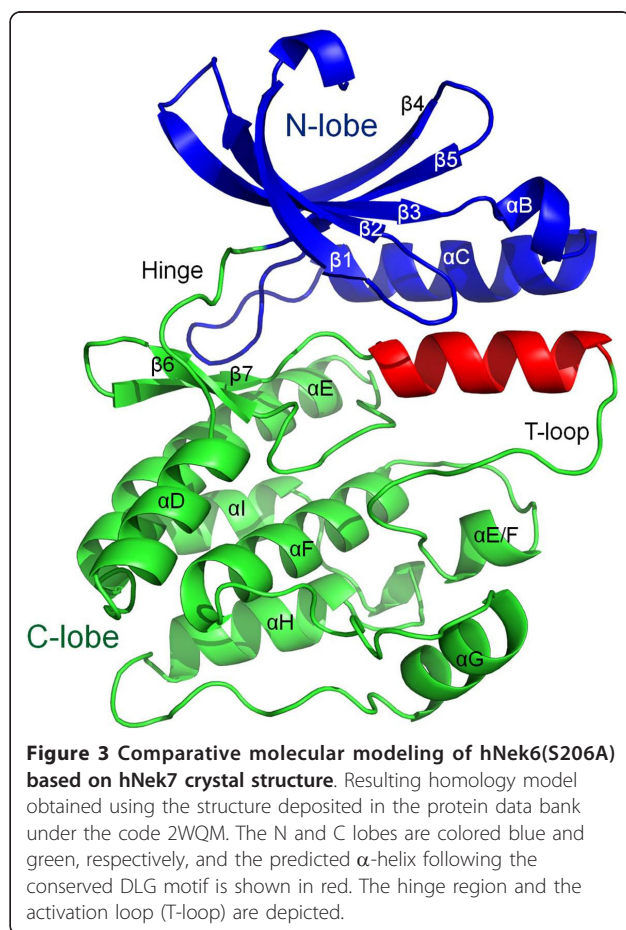
^b Kinases as predicted by NetPhosK to phosphorylate the corresponded residue in hNek6 sequence [Protein Kinase A, C or G (PKA, PKC and PKG); Cell division cycle 2 (Cdc2); Casein Kinase I or II (CKI and CKII); DNA-dependent Protein Kinase (DNAPK); Ataxia Telangiectasia Mutated (ATM); Cyclin-dependent kinase 5 (Cdk5); Glycogen synthase kinase 3 (GSK3); Epidermal Growth Factor Receptor (EGFR); Mitogen-Activated Protein Kinase p38 (p38MAPK)].

increase in the activation status of the kinase [13,41]. The activation loop has the capacity to undergo large conformational changes when the kinase switches between inactive and active states, adopting distinct conformations in different kinases when they are inactive (unphosphorylated activation loop), a fact that has recently been exploited to great medical benefit [49] and which makes our hNek6 mutant an interesting target to be studied.

To obtain a homology model of the hNek6 protein, the crystallographic structure of hNek7, available in the Protein Data Bank (PDB: 2WQM) [28], was used as a



template. Both proteins share about 77% identity in primary sequence alignment, being ~86% identical in their catalytic domain sequences (Figure 1C). Several homology/comparative modeling tools were used as described in the “Methods” section of this article. In order to choose the best predicted model, stereochemistry quality analyses were done to check for ϕ and ψ torsion angles using the Ramachandran plots. A comparison of the results indicated that the model generated by SWISS-MODEL [50] is more acceptable than those generated by the other programs (more amino acids in the most favourable regions and less in the disallowed regions). The SWISS-MODEL homology model is shown in Figure 3. The Ramachandran plot (Additional file 1, Figure S1A) showed 86.6% residues in the most favourable regions, 12.1% in additional allowed regions, 0.8% in generously allowed regions and 0.4% (only 1 amino acid) in a disallowed region. As compared to the 2WQM template, these values were 90.8%, 8.8%, 0.4% and 0.0%, respectively. It is important to keep in mind that the template has relatively long regions (one of them consists of 18 amino acids) where the phases could not be solved by X-ray crystallography. Consequently, the homology modeling may not be so accurate in these regions, although the high identity of the target-template sequences makes the whole model plausible. The results revealed that the majority of the amino acids are in a ϕ - ψ distribution consistent with right handed α -helix and reliable to be a good quality model (Additional file 1, Figure S1A). More details of the validation of the predicted structure results and its quality assessment using PROSA [51,52] are displayed in the Additional Material section (Additional file 1, Figure S1B and S1C). No abnormalities were observed



in the validation process, which indicated a good model for the protein.

Our hNek6(S206A) model generated by SWISS-MODEL [50] shows a short region of α -helix composed of twelve residues ($G^{192}LGRFFSSETTA^{203}$) following the conserved DLG motif, with high score (Figure 3). A helical structure following the DFG/DLG motif is also present in hNek2(T175A) structures (PDB: 2JAV, 2W5H and 2W5B) [26,27] and in other kinase families, such as inactive forms of both the EGFR kinase [53] and Src/Hck [54]. Therefore, although the activation loop is missing in the electron density map of hNek7, a short helical structure is possibly present in hNek6(S206A), which was predicted in the model generated by SWISS-MODEL [50].

Human Nek6 is a monomeric mostly globular, though slightly elongated protein in solution, as revealed by SAXS

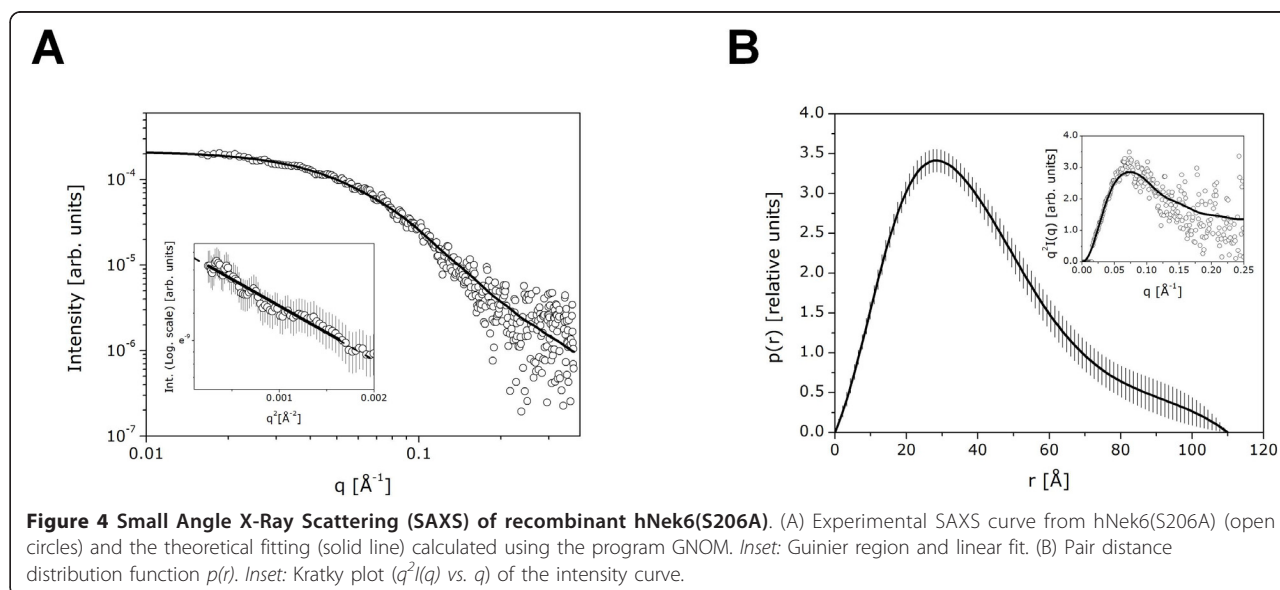
To study hNek6 molecular structure, in addition to our homology modeling, we also performed SAXS (Small Angle X-ray Scattering) experiments for the recombinant 6xHis-hNek6(S206A). SAXS is a very useful

technique for the determination of overall size, shape and oligomerization status of the macromolecules in solution [55-58]. Figure 4A shows the corrected and normalized experimental scattering curve and theoretical fitting of data by using the program GNOM [59]. The Guinier region providing an R_g value of $32.0 \pm 1.0 \text{ \AA}$ is shown in the inset. The $p(r)$ function resulting from these calculations is shown in Figure 4B, with an inset showing the Kratky representation of the intensity curve. The Kratky plot indicates a slightly globular conformation for 6xHis-hNek6(S206A) in solution, although, as expected, the same plot also indicated the presence of flexible regions in the structure, possibly the N-terminal region and the activation loop. The $p(r)$ function shows that the protein conformation is slightly elongated. The maximum dimension (D_{max}) value obtained was approximately 110 \AA and the R_g value calculated from the $p(r)$ function was $32.4 \pm 0.8 \text{ \AA}$, in close agreement with that calculated from the Guinier approximation. Using BSA as a standard sample, the molecular mass of 6xHis-hNek6(S206A) estimated from the SAXS data was $\sim 42 \text{ kDa}$. This value indicates that the protein is a monomer in solution, since the theoretically calculated molecular mass of the monomer was $\sim 38 \text{ kDa}$ (calculated from the amino acid sequence using ProtParam tool [60]). The molecular mass and consequently the monomeric nature were also confirmed by analytical size-exclusion chromatography coupled to multi-angle light scattering (SEC-MALS).

The low-resolution models obtained from the SAXS data by the combination of *ab initio* calculation and rigid body modeling methods are presented in Figure 5. The calculated homology model of the mutant hNek6(S206A) was used in the rigid body calculation. We displayed two typical models of the set of results (Figure 5A and 5B) and a superposition of all 10 models (Figure 5C) obtained in different and independent runs of the program BUNCH [61]. In spite of the flexibility of the N-terminal region, the NSD values of the pairwise comparison of the models obtained ranged from 0.96 to 1.20, which shows the stability of the independent calculations. In order to further compare the resulting models with the information contained in the SAXS curve, we also calculated one average molecular envelope of the 10 models (Figure 5D) and compared with the filtered average models obtained from the two sets of 10 purely *ab initio* model calculations (Figure 5E and 5F).

Analytical size-exclusion chromatography reveals variations in human Nek6 conformation dependent on its phosphorylation status

Analytical Size-Exclusion Chromatography (SEC) was performed for five variants of recombinant hNek6 fused to a 6xHis tag: wild-type hNek6 (6xHis-hNek6wt),



activation loop mutant hNek6(S206A) (6xHis-hNek6(S206A), kinase domain of wild-type hNek6 (6xHis-hNek6(Δ 1-44)), and dephosphorylated wild-type and mutant hNek6 (6xHis-hNek6wtD and 6xHis-hNek6(S206A)D). Interestingly, the dephosphorylated wild-type and mutant proteins, which were co-expressed with lambda phosphatase, were eluted at equal elution volumes (Figure 6A), showing the same Stokes radius of ~ 2.1 nm, while the more phosphorylated wild-type hNek6 showed a larger radius of ~ 2.6 nm and the partially phosphorylated mutant hNek6(S206A) showed an intermediate radius of ~ 2.4 nm (Figure 6B, Table 2). As expected, 6xHis-hNek6(Δ 1-44) showed the smallest radius of ~ 1.8 nm. Wild-type hNek6 elution curve also showed a smaller peak corresponding to a population of higher molecular weight, possibly due to aggregates. It is interesting to compare the Stokes radius estimated by SEC for 6xHis-hNek6(S206A) (~ 2.4 nm) with the radius of gyration determined by SAXS (~ 3.2 nm). The resulting ratio R_g/R_s for this protein is ~ 1.3 and, as R_g/R_s ratios are reported to vary from 0.78 for homogeneous spheres, up to values nearing 2 for extended coils and prolate ellipsoids [62]. This reinforces our results that hNek6 has a slightly elongated conformation, with a flexible unfolded N-terminal domain contributing to this shape.

SEC was also coupled to MALS (Multi-Angle Light Scattering), which is an useful technique to measure the weight average molecular masses (M_w) of the eluted proteins, as described in the Methods section. As expected, wild-type and mutant hNek6, dephosphorylated or not, showed a M_w of ~ 38 kDa, while the kinase domain showed a M_w of ~ 33 kDa (Table 3, Additional file 1, Figure S2). This corroborates our experimental

data from SAXS for 6xHis-hNek6(S206A) and the theoretically calculated molecular masses for all hNek6 variants, showing that hNek6 is a monomer in solution.

These results suggest that, although having the same molecular mass of ~ 38 kDa, wild-type hNek6 is purified from bacteria more phosphorylated than its mutant variant, mainly because of their different activation/autophosphorylation status, as described by Meirelles et al. [41], and these different phosphorylation degrees may cause changes in protein conformation and compactness, resulting in changes in their Stokes radii. This was better visualized for both proteins when dephosphorylated by lambda phosphatase, which promoted smaller radii and, possibly, more compact or less hydrated conformations. It seems that an increase in phosphorylation induces a structural change that increases the apparent size or shape of hNek6. In fact, in most kinases, the activation loop is phosphorylated when the kinase is active, which stabilizes it in an open and extended conformation that is permissive for substrate binding [49]. This phosphorylated extended conformation may therefore contribute to the increase in hNek6 Stokes radius. All hNek6 variants were submitted to SEC-MALS twice, using two different buffers (the same one used for SAXS and another one containing 600 mM NaCl in order to avoid any unspecific binding to the gel filtration column resin), and the same Stokes radii for each protein were obtained in both measurements. Figure 6 shows the results from SEC-MALS using the buffer containing 600 mM NaCl, and Tables 2 and 3 show all the results obtained from both measurements.

Thermal denaturation shift assays were also performed for the five recombinant hNek6 variants described above. The results revealed a slightly higher stability of

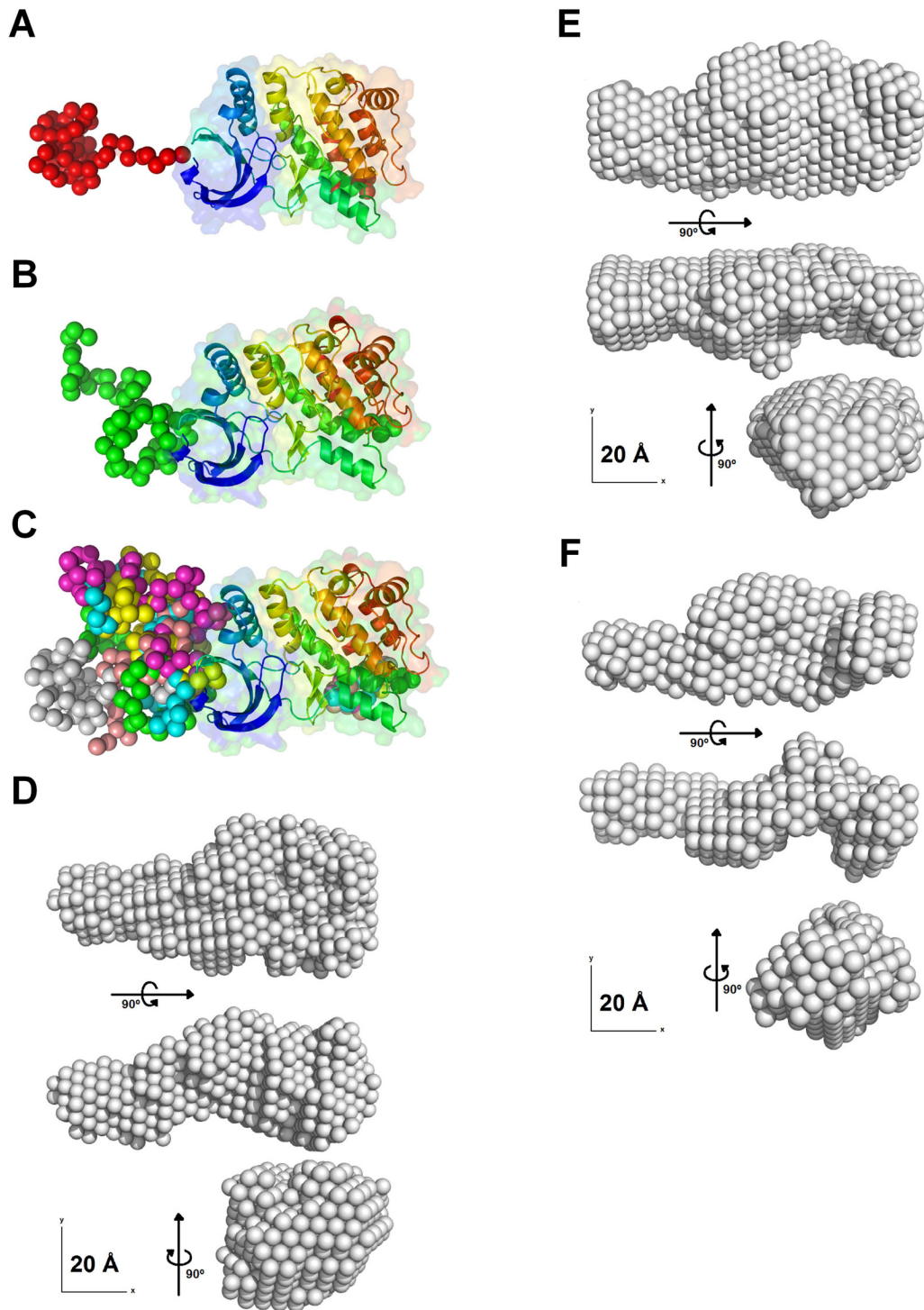
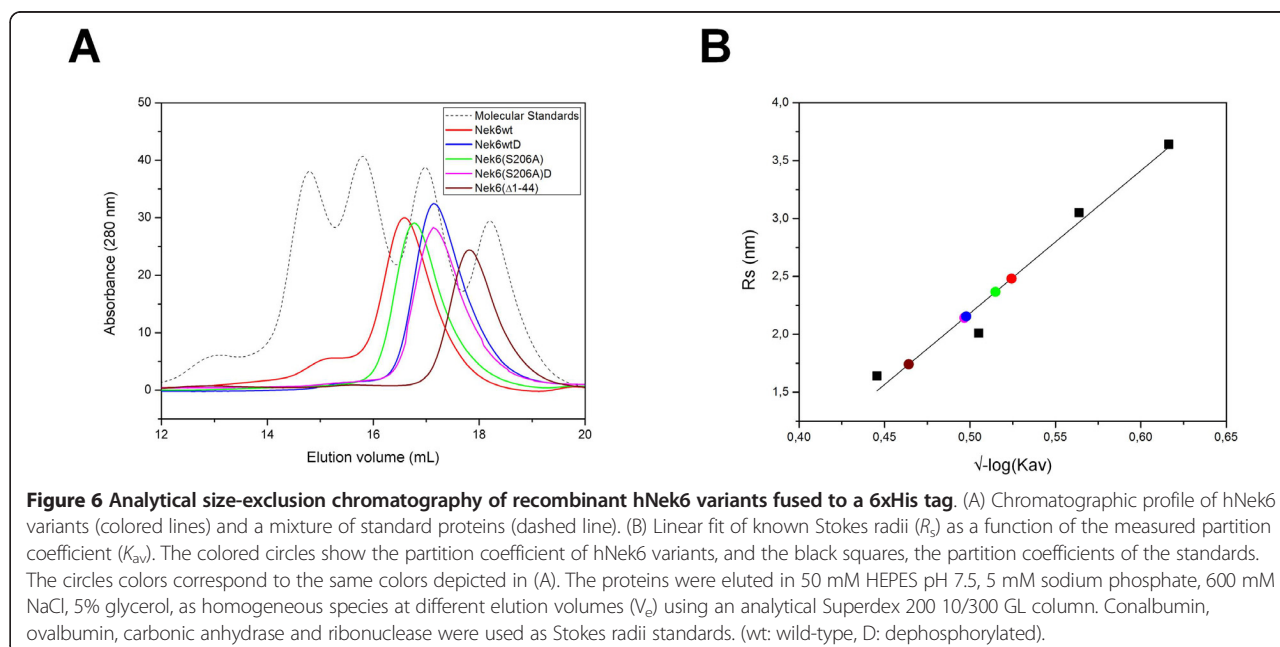


Figure 5 Low-resolution models of hNek6(S206A) obtained from the SAXS data using a combination of *ab initio* calculations and rigid body modeling. (A and B) Two typical models selected from the set of 10 resulting models. (C) Superposition of all 10 models obtained in different and independent runs of the program BUNCH. (D) Three orthogonal views of the average molecular envelope of the 10 low resolution BUNCH models. (E) Three orthogonal views of the *ab initio* dummy atoms model. (F) Three orthogonal views of the *ab initio* dummy residues model.



wild-type hNek6 compared to the activation loop mutant (Figure 7, Table 3). This may be explained by the fact that, in many kinases, like PKA, phosphorylation of the activation loop cause global stabilization of the active site [63], and molecular dynamics simulation of Cdk2 has demonstrated a decrease of B-factors throughout the molecule upon phosphorylation [64]. A model was proposed that dephosphorylation of the activation loop leads to mutual repulsion of the positive charges that were bound to the phosphate, which leads to the destabilization of the magnesium-binding loop, movement of the α C-helix out of the active site, disturbance of the hydrophobic spine, and loosening of the N-lobe, thereby providing an explanation of the protein kinase stabilization induced by phosphorylation [48]. This may therefore also reflect a higher stability for the wild-type hNek6 compared to its activation loop mutant in thermal melting measurements.

Table 2 Recombinant hNek6 Stokes radii (R_s) determined by analytical size-exclusion chromatography

Protein	R_s (nm)	V_e (mL) ^a	Apparent R_s (nm) ^a
Conalbumin	3.6	14.9 ± 0.1	3.5 ± 0.2
Ovalbumin	3.0	15.8 ± 0.1	2.9 ± 0.0
Carbonic Anhydrase	2.0	16.9 ± 0.1	2.2 ± 0.0
Ribonuclease	1.6	18.2 ± 0.0	1.4 ± 0.1
Nek6wt		16.4 ± 0.3	2.6 ± 0.1
Nek6wtD		17.1 ± 0.0	2.1 ± 0.0
Nek6(S206A)		16.7 ± 0.2	2.4 ± 0.0
Nek6(S206A)D		17.1 ± 0.0	2.1 ± 0.0
Nek6(Δ 1-44)		17.6 ± 0.3	1.8 ± 0.1

^a S.E. of two measurements at different buffers.

Conclusions

Our data presents the first low resolution 3D structure of hNek6 protein in solution. SAXS experiments show that hNek6 is a monomer of a mostly globular, though slightly elongated shape, which was also confirmed by analytical SEC-MALS experiments. These also showed that hNek6 conformation is dependent on its activation/phosphorylation status, a higher phosphorylation degree corresponding to a bigger Stokes radius. Thermal denaturation shift assays revealed a slightly higher stability of wild-type hNek6 compared to the activation loop mutant hNek6(S206A).

Methods

In silico sequence analysis

Human Nek6 and Nek7 amino acid sequences were used as queries in five different secondary structure prediction databases: PredictProtein/Prof [29], PSIPRED [30], SSpro [31], SOPMA [32] and GOR4 [33]. Comparison of their outputs resulted in a consensus of predicted secondary

Table 3 Recombinant hNek6 weight average molecular masses (M_w) determined by SEC-MALS and melting temperatures (T_m) during thermal shift denaturation

Protein	Pred. M (kDa) ^a	M_w (kDa) ^b	Apparent T_m (°C) ^c
Nek6wt	37.7	38.4 ± 0.6	39.5 ± 0.1
Nek6wtD	37.7	37.8 ± 2.2	40.8 ± 0.1
Nek6(S206A)	37.7	38.1 ± 2.1	38.0 ± 0.1
Nek6(S206A)D	37.7	38.4 ± 3.3	36.8 ± 0.3
Nek6(Δ 1-44)	33.2	33.3 ± 1.6	41.0 ± 0.2

^a Molecular masses predicted by ProtParam tool [60].

^b S.E. of two measurements at different buffers.

^c S.E. of three measurements.

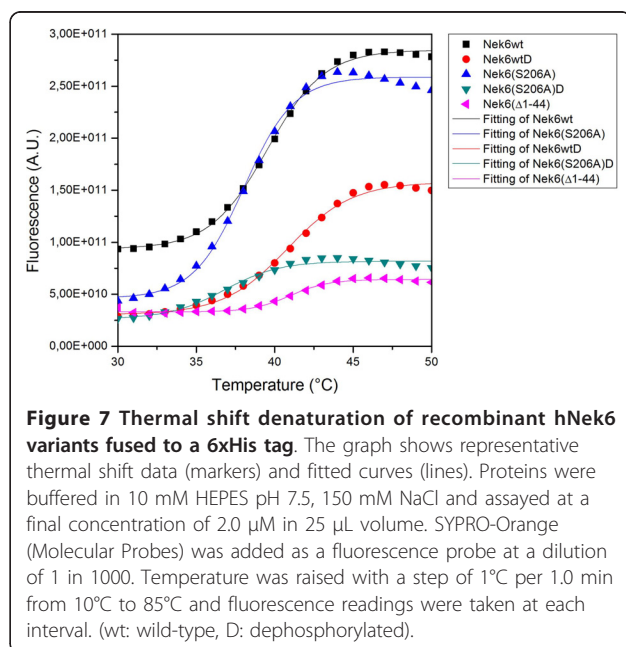


Figure 7 Thermal shift denaturation of recombinant hNek6 variants fused to a 6xHis tag. The graph shows representative thermal shift data (markers) and fitted curves (lines). Proteins were buffered in 10 mM HEPES pH 7.5, 150 mM NaCl and assayed at a final concentration of 2.0 μ M in 25 μ L volume. SYPRO-Orange (Molecular Probes) was added as a fluorescence probe at a dilution of 1 in 1000. Temperature was raised with a step of 1°C per 1.0 min from 10°C to 85°C and fluorescence readings were taken at each interval. (wt: wild-type, D: dephosphorylated).

structure, where each amino acid was assigned a score ranging from 1 to 5. Our Nek7 consensus of predicted secondary structure was compared to the author-approved secondary structure in PDB (2WQM) as a measure to validate our analysis. We also performed disordered regions analysis for both protein sequences using nine different predictors: FoldIndex [34], GlobPlot Russell/Linding [35], PONDR VL-XT [36], DISpro [37], IUPred [38], DisEMBL Hot-loops, DisEMBL Remark-465, DisEMBL Loops/coils [39], and VSL2B [40]. From this, a consensus of predicted disordered regions was generated with a consensus score ranging from 0 to 9, where a score above 4 represents disorder. Additionally, NetPhosK [42] and NetPhos [43] databases were used to predict phosphorylation sites for human Nek6 and Nek7. The conserved glycine-rich sequence, the HRD and DLG motifs, the conserved residues K⁷⁴ (β 3 strand) and E⁹³ (α C helix), the putative nuclear export signal LGDLGL based on la Cour et al., 2004 [65], the putative WW domain binding motifs PY and pSP based on Ingham et al., 2005 [66], as long as the PPLP motif, experimentally described for hNek6 by Lee et al., 2007 [67], were also assigned to both protein sequences.

Plasmid Constructions

All plasmid constructions were developed accordingly to Meirelles et al., 2010 [41].

Site-directed Mutagenesis

The hNek6 activation loop mutation S206A was introduced by PCR-based mutagenesis accordingly to Meirelles et al., 2010 [41].

Protein Expression and Purification

Soluble full-length hNek6 wild-type - 6xHis-hNek6wt - and mutant - 6xHis-hNek6(S206A) - or truncated hNek6 wild-type kinase domain - 6xHis-hNek6(Δ 1-44) - fused to a 6xHis tag were expressed and purified accordingly to Meirelles et al., 2010 [41].

Protein Dephosphorylation

In order to obtain dephosphorylated wild-type and mutant hNek6, plasmids encoding either 6xHis-hNek6wt or 6xHis-hNek6(S206A) and λ phosphatase were transformed into *E. coli* BL21 (DE3/pRARE) cells that were induced and purified as described by Meirelles et al., 2010 [41]. Lambda phosphatase cloned into pCDF-Duet (Novagen) was kindly provided by Dr. Richard Bayliss (Section of Structural Biology, Institute of Cancer Research, London, UK).

Circular dichroism

Circular dichroism (CD) spectra were recorded in a JASCO model J-810 CD spectropolarimeter equipped with Peltier-type system PFD 425S. Data were collected from 260 to 200 nm at 4°C using a quartz cuvette of 1 mm pathlength. Thirty-two spectra of purified 6xHis-hNek6wt at 5.8 μ M, in 50 mM Phosphate buffer pH 7.5, 300 mM NaCl, were averaged and corrected from the baseline for buffer solvent contribution. Experimental data were analyzed using CDNN [45] and K2d [46] softwares.

Comparative/Homology Molecular Modeling

The comparative/homology molecular modeling and model validation were performed in a similar way to that described in Bodade et al., 2010 [68]. Briefly, several comparative/homology modeling tools were used: I-TASSER [69-71], Geno3D [72], 3D-JIGSAW [73-75], SWISS-MODEL [50] and MODELLER 9v8 [76]. The NCBI Basic Local Alignment Search Tool (BLAST, <http://www.ncbi.nlm.nih.gov/BLAST/>) was used to search the crystal structure of the closest homologue available in the Protein Data Bank (PDB, <http://www.rcsb.org/pdb/>). The input was the amino acid sequence of hNek6(S206A). The NCBI results revealed that the structure of hNek7, deposited under the code 2WQM in the PDB, was a very suitable template (identity score of 81% and E-value 3×10^{-141}). This structure was used as a single template for the modeling approach. The overall stereochemical quality of the models was assessed by PROCHECK software [77]. The quality of the models was also evaluated by PROSA [51,52] and by the standard validation procedures included in the automated mode of the SWISS-MODEL server [50].

Small Angle X-Ray Scattering Analysis

The sample was first inspected by dynamic light scattering (DLS) to test for its monodispersity and then ultracentrifuged at $200.000 \times g$ for 40 min at 4°C to remove any possible aggregates. The SAXS experiments were performed at the D02A-SAXS2 beam line at the LNLS, and data treatment and analyses were done following standard procedures similar to those described in Trindade et al., 2009 [57]. Briefly, the measurements were performed at 4°C and the sample-to-detector distance was 902 mm, covering a scattering vector range of $0.015 \text{ \AA}^{-1} < q < 0.25 \text{ \AA}^{-1}$ (q is the magnitude of the \mathbf{q} -vector defined by $q = (4\pi/\lambda)\sin\theta$ and 2θ is the scattering angle) using a wavelength of $\lambda = 1.488 \text{ \AA}$. The measurements were performed using two different protein concentrations in HEPES buffer (50 mM HEPES pH 7.5, 5 mM sodium phosphate, 300 mM NaCl, 5% glycerol, 200 mM imidazole): 0.5 and 1.0 mg/mL. A 8 mg/ml BSA (66 kDa) solution in the same sample buffer was used as a standard sample to estimate the molecular mass of 6xHis-hNek6(S206A) making use of the ratio of the extrapolated values of the intensity at the origin, $I(0)$ [78,79]. The radius of gyration (R_g) was calculated from the Guinier approximation (valid for $qR_g < 1.3$) [80-82] and also from the pair distance distribution function, $p(r)$, which was obtained using the program GNOM [56]. The maximum dimension (D_{\max}) of the molecule was obtained from the $p(r)$ function. The Kratky plot ($q^2I(q)$ vs. q) [81,82] was used to analyze the compactness of the protein conformation.

Low resolution SAXS-based modeling

The low resolution model of 6xHis-hNek6(S206A) was obtained from the SAXS data using a combination of *ab initio* calculation and rigid body modeling methods. Taking advantage of the homology model obtained, we used the program BUNCH [61] to model the protein. No symmetry restraints were used in the calculation. We would like to mention that no unique solution can be obtained from these calculations. For this reason, 10 independent calculations were run for each sample data. The multiple solutions were analyzed and the reliability and stability of the set of models were estimated. A pairwise comparison and the normalized spatial discrepancy (NSD) evaluation was performed using the DAMAVER program suite [83] complemented by the SUPCOMB [84] routine. Analyzing the NSD values (which describe the dissimilarity between pairs of models of the several calculations), the models with common features led to the selection of a representative, low resolution conformation for hNek6(S206A) protein. Models were displayed by the PyMOL program [85].

For comparison purposes, two other low resolution models were also obtained by using two different

ab initio approaches: the *dummy atoms* method implemented in the program DAMMIN [86] and the *dummy residues* method implemented in GASBOR [87]. The procedures were similar to those described in Trindade et al. [57].

SEC-MALS Analysis

We used Analytical Size-Exclusion Chromatography coupled to Multi-Angle Light Scattering (SEC-MALS) to estimate the hydrodynamic or Stokes radii (R_s) of recombinant hNek6wt, hNek6(S206A), hNek6(Δ 1-44) and dephosphorylated hNek6wt and hNek6(S206A), all fused to a 6xHis tag. SEC was performed with an analytical Superdex 200 10/300 GL column using an ÄKTA FPLC system (GE Healthcare) equilibrated with two column volumes of 50 mM HEPES pH 7.5, 5 mM sodium phosphate, 600 mM NaCl, 5% glycerol, at a flow rate of 0.5 ml/min, at 20°C . Recombinant hNek6 variants at concentrations ranging from 0.2 to 0.7 mg/ml and a mixture of standard proteins with known Stokes radii (conalbumin: 3.64 nm, 3.2 mg/ml; ovalbumin: 3.05 nm, 4.2 mg/ml; carbonic anhydrase: 2.30 nm, 3.0 mg/ml; and ribonuclease: 1.64 nm, 3.4 mg/ml) (Sigma) were loaded onto the column and their elution profiles were monitored by absorbance at 280 nm. The Stokes radius of each hNek6 variant was estimated by a linear fit of the Stokes radii of the standard proteins versus the partition coefficient K_{av} [88,89] as described by the equation: $K_{\text{av}} = V_e - V_o/V_t - V_o$, where V_e is the elution volume of the protein, V_o the void volume and V_t is the total volume of the column. The SEC was also coupled to a DAWN TREOS™ MALS instrument (Wyatt Technology). The on-line measurement of the intensity of the Rayleigh scattering as a function of the angle of the eluting peaks in SEC was used to determine the weight average molecular masses (M_w) of the eluted proteins [90], using the ASTRA™ (Wyatt Technologies) software. SEC-MALS measurements were performed using two different buffers: the first one described above for SEC and a second one also used in SAXS experiments (50 mM HEPES pH 7.5, 5 mM sodium phosphate, 300 mM NaCl, 5% glycerol, 200 mM imidazole). The chromatographic profile of the recombinant hNek6 variants were the same in both measurements and the mean and standard errors of their M_w and M_n were calculated.

Thermal Shift Assays

Thermal shift assays were performed based on a protocol devised by the Structural Genomics Consortium [91] using a real time PCR machine 7300 (Applied Biosystems). Proteins were buffered in 10 mM HEPES pH 7.5, 150 mM NaCl and assayed at a final concentration of 2.0 μM in 25 μL volume. SYPRO-Orange (Molecular Probes) was added as a fluorescence probe at a dilution

of 1 in 1000. The emission filter for the SYPRO-Orange dye was set to 580 nm. Temperature was raised with a step of 1°C per 1.0 min from 10°C to 85°C and fluorescence readings were taken at each interval. OriginPro 8 software was used to fit data to the Boltzmann equation, $y = LL + (UL - LL) / (1 + \exp((T_m - x) / a))$, where LL and UL are the slopes of the native and denatured baselines, T_m is the apparent melting temperature and a describes the slope of the denaturation. T_m values were calculated by determination of the maximum of the first derivative.

Additional material

Additional file 1: Supplemental Figures S1 and S2, PROCHECK and PROSA analysis results of the validation procedures of the hNek6 (S206A) homology/comparative model and Analytical SEC-MALS of the five recombinant protein variants of Nek6. Figure S1: PROCHECK and PROSA analysis results of the validation procedures of the hNek6 (S206A) homology/comparative model. (A) Ramachandran Plot calculated using the program PROCHECK. (B) Plot of the residue score showing the local model quality by plotting energies as a function of the residue sequence position using PROSA. In general, positive values correspond to problematic or erroneous parts of the structure. Here, the plots were smoothed by calculation of the average energy over 10- and 40-residues. This average is needed because of the large fluctuation in a plot of single residue energies. (C) The Z-score indicated overall model quality using PROSA. The Z-score of the hNek6(S206A) model was -7.14 (black point). The plot contains the Z-scores of all experimentally determined protein chains in the current PDB. The structure determined by X-ray and NMR are distinguished by different colors. Figure S2: Analytical SEC-MALS of recombinant (A) hNek6wt, (B) hNek6wtD, (C) hNek6(S206A), (D) hNek6(S206A)D and (E) hNek6(Δ 1-44). The Mw determined by MALS correspond to a monomer in all five cases.

Acknowledgements

Financially supported by: Fundação de Amparo à Pesquisa do Estado São Paulo, the Conselho Nacional de Pesquisa e Desenvolvimento and the LNLs. We thank Maria Eugenia R. Camargo for technical assistance, Rodrigo Martinez for the technical support at the SAXS2 beamline, and Dr. Richard Bayliss (Section of Structural Biology, Institute of Cancer Research, London, UK) for providing the pCDF-Duet lambda phosphatase construct.

Author details

¹Laboratório Nacional de Biociências, Centro Nacional de Pesquisa em Energia e Materiais, Campinas, SP, Brazil. ²Departamento de Bioquímica-Programa de Pós-graduação em Biologia Funcional e Molecular, Instituto de Biologia, Universidade Estadual de Campinas, 13083-970 Campinas, SP, Brazil. ³Instituto de Química, Universidade Estadual de Campinas, Campinas, SP, Brazil. ⁴Laboratório Nacional de Luz Síncrotron, Centro Nacional de Pesquisa em Energia e Materiais, Campinas, SP, Brazil. ⁵Instituto de Física "Gleb Wataghin", Universidade Estadual de Campinas, Campinas, SP, Brazil.

Authors' contributions

GVM and JK conceived and designed the experiments, analyzed the data and wrote the manuscript. GVM performed the experiments. JCS performed comparative molecular modeling and SAXS experiments and interpreted them together with ICLT. YAM helped in SEC-MALS and CD experiments which were analyzed together with CHIR. JK supervised the project. All authors read and approved the final version of the manuscript.

Received: 10 September 2010 Accepted: 14 February 2011
Published: 14 February 2011

References

1. Barr FA, Sillje HH, Nigg EA: Polo-like kinases and the orchestration of cell division. *Nat Rev Mol Cell Biol* 2004, **5**:429-440.
2. Carmena M, Earnshaw WC: The cellular geography of aurora kinases. *Nat Rev Mol Cell Biol* 2003, **4**:842-854.
3. Nigg EA: Mitotic kinases as regulators of cell division and its checkpoints. *Nat Rev Mol Cell Biol* 2001, **2**:21-32.
4. O'Regan L, Blot J, Fry AM: Mitotic regulation by NIMA-related kinases. *Cell Div* 2007, **2**:25.
5. Fry AM: The Nek2 protein kinase: a novel regulator of centrosome structure. *Oncogene* 2002, **21**(40):6184-94.
6. Quarmby LM, Mahjoub MR: Caught Nek-ing: cilia and centrioles. *J Cell Sci* 2005, **118**:5161-5169.
7. White MC, Quarmby LM: The NIMA-family kinase, Nek1 affects the stability of centrosomes and ciliogenesis. *BMC Cell Biol* 2008, **9**:29.
8. Lanza DC, Meirelles GV, Alborghetti MR, Abrile CH, Lenz G, Kobarg J: FEZ1 interacts with CLASP2 and NEK1 through coiled-coil regions and their cellular colocalization suggests centrosomal functions and regulation by PKC. *Mol Cell Biochem* 2010, **338**(1-2):35-45.
9. O'Regan L, Fry AM: The Nek6 and Nek7 protein kinases are required for robust mitotic spindle formation and cytokinesis. *Mol Cell Biol* 2009, **29**:3975-3990.
10. Yissachar N, Salem H, Tennenbaum T, Motro B: Nek7 kinase is enriched at the centrosome, and is required for proper spindle assembly and mitotic progression. *FEBS Lett* 2006, **580**(27):6489-95.
11. Roig J, Groen A, Caldwell J, Avruch J: Active Nerc1 protein kinase concentrates at centrosomes early in mitosis and is necessary for proper spindle assembly. *Mol Biol Cell* 2005, **16**(10):4827-40.
12. Roig J, Mikhailov A, Belham C, Avruch J: Nerc1, a mammalian NIMAfamily kinase, binds the Ran GTPase and regulates mitotic progression. *Genes Dev* 2002, **16**:1640-1658.
13. Belham C, Roig J, Caldwell JA, Aoyama Y, Kemp BE, Comb M, Avruch J: A mitotic cascade of NIMA family kinases. Nerc1/Nek9 activates the Nek6 and Nek7 kinases. *J Biol Chem* 2003, **278**:34897-34909.
14. Upadhy P, Birkenmeier EH, Birkenmeier CS, Barker JE: Mutations in a NIMA-related kinase gene, Nek1, cause pleiotropic effects including a progressive polycystic kidney disease in mice. *Proc Natl Acad Sci* 2000, **97**(1):217-21.
15. Liu S, Lu W, Obara T, Kuida S, Lehoczy J, et al: A defect in a novel Nek-family kinase causes cystic kidney disease in the mouse and in zebrafish. *Development* 2002, **129**(24):5839-46.
16. Surpili MJ, Delben TM, Kobarg J: Identification of proteins that interact with the central coiled-coil region of the human protein kinase NEK1. *Biochemistry* 2003, **42**:15369-15376.
17. Tsunoda N, Kokuryo T, Oda K, Senga T, Yokoyama Y, et al: Nek2 as a novel molecular target for the treatment of breast carcinoma. *Cancer Sci* 2009, **100**(1):111-6.
18. McHale K, Tomaszewski JE, Puthiyaveetil R, Livolsi VA, Clevenger CV: Altered expression of prolactin receptor-associated signaling proteins in human breast carcinoma. *Mod Pathol* 2008, **21**(5):565-71.
19. Bowers AJ, Boylan JF: Nek8, a NIMA family kinase member, is overexpressed in primary human breast tumors. *Gene* 2004, **328**:135-42.
20. Ahmed S, Thomas G, Ghossaini M, Healey CS, Humphreys MK, et al: Newly discovered breast cancer susceptibility loci on 3p24 and 17q23.2. *Nat Genet* 2009, **41**(5):585-90.
21. Chen J, Li L, Zhang Y, Yang H, Wei Y, et al: Interaction of Pin1 with Nek6 and characterization of their expression correlation in Chinese hepatocellular carcinoma patients. *Biochem Biophys Res Commun* 2006, **341**(4):1059-65.
22. Capra M, Nuciforo PG, Confalonieri S, Quarto M, Bianchi M, et al: Frequent alterations in the expression of serine/threonine kinases in human cancers. *Cancer Res* 2006, **66**(16):8147-54.
23. Takeno A, Takemasa I, Doki Y, Yamasaki M, Miyata H, et al: Integrative approach for differentially overexpressed genes in gastric cancer by combining large-scale gene expression profiling and network analysis. *Br J Cancer* 2008, **99**(8):1307-15.
24. Nassirpour R, Shao L, Flanagan P, Abrams T, Jallal B, Smeal T, Yin MJ: Nek6 Mediates Human Cancer Cell Transformation and Is a Potential Cancer Therapeutic Target. *Mol Cancer Res* 2010, **8**(5):717-28.

25. Minoguchi S, Minoguchi M, Yoshimura A: **Differential control of the NIMA-related kinases, Nek6 and Nek7, by serum stimulation.** *Biochem Biophys Res Commun* 2003, **301**:899-906.
26. Rellos P, Ivins FJ, Baxter JE, Pike A, Nott TJ, Parkinson DM, Das S, Howell S, Fedorov O, Shen QY, Fry AM, Knapp S, Smerdon SJ: **Structure and regulation of the human Nek2 centrosomal kinase.** *J Biol Chem* 2007, **282**(9):6833-42.
27. Westwood I, Cheary DM, Baxter JE, Richards MW, van Montfort RL, Fry AM, Bayliss R: **Insights into the conformational variability and regulation of human Nek2 kinase.** *J Mol Biol* 2009, **386**(2):476-85.
28. Richards MW, O'Regan L, Mas-Droux C, Blot JM, Cheung J, Hoelder S, Fry AM, Bayliss R: **An autoinhibitory tyrosine motif in the cell-cycle-regulated Nek7 kinase is released through binding of Nek9.** *Mol Cell* 2009, **36**(4):560-70.
29. Rost B, Yachdav G, Liu J: **The PredictProtein server.** *Nucleic Acids Res* 2004, **32**:W321-W326.
30. Bryson K, McGuffin LJ, Marsden RL, Ward JJ, Sodhi JS, Jones DT: **Protein structure prediction servers at University College London.** *Nucleic Acids Res* 2005, **33**:W36-W38.
31. Cheng J, Randall AZ, Sweredoski MJ, Baldi P: **SCRATCH: a protein structure and structural feature prediction server.** *Nucleic Acids Res* 2005, **33**:W72-W76.
32. Geourjon C, Deleage G: **SOPMA: significant improvements in protein secondary structure prediction by consensus prediction from multiple alignments.** *Comput Appl Biosci* 1995, **11**:681-684.
33. Garnier J, Gibrat J-F, Robson B: **GOR secondary structure prediction method version IV.** *Met Enzymol* 1996, **266**:540-553.
34. Prilusky J, Felder CE, Zeev-Ben-Mordehai T, Rydberg EH, Man O, Beckmann JS, Silman I, Sussman JL: **FoldIndex: a simple tool to predict whether a given protein sequence is intrinsically unfolded.** *Bioinformatics* 2005, **21**(16):3435-8.
35. Linding R, Russell RB, Neduva V, Gibson TJ: **GlobPlot: Exploring protein sequences for globularity and disorder.** *Nucleic Acids Res* 2003, **31**(13):3701-8.
36. Romero P, Obradovic Z, Li X, Garner EC, Brown CJ, Dunker AK: **Sequence complexity of disordered protein.** *Proteins* 2001, **42**(1):38-48.
37. Cheng J, Sweredoski M, Baldi P: **Accurate Prediction of Protein Disordered Regions by Mining Protein Structure Data.** *Data Mining and Knowledge Discovery* 2005, **11**(3):213-222.
38. Dosztanyi Z, Csizmek V, Tompa P, Simon I: **IUPred: web server for the prediction of intrinsically unstructured regions of proteins based on estimated energy content.** *Bioinformatics* 2005, **21**(16):3433-4.
39. Linding R, Jensen LJ, Diella F, Bork P, Gibson TJ, Russell RB: **Protein disorder prediction: implications for structural proteomics.** *Structure* 2003, **11**(11):1453-9.
40. Obradovic Z, Peng K, Vucetic S, Radivojac P, Dunker AK: **Exploiting heterogeneous sequence properties improves prediction of protein disorder.** *Proteins* 2005, **61**(7):176-82.
41. Meirelles GV, Lanza DCF, Silva JC, Bernachi JS, Leme AFP, Kobarg J: **Characterization of hNek6 Interactome Reveals an Important Role for Its Short N-Terminal Domain and Colocalization with Proteins at the Centrosome.** *J Proteome Res* 2010, **9**(12):6298-316.
42. Blom N, Sicheritz-Ponten T, Gupta R, Gammeltoft S, Brunak S: **Protein disorder prediction: implications for structural proteomics.** *Proteomics* 2004, **4**(6):1633-49.
43. Blom N, Gammeltoft S, Brunak S: **Sequence- and structure-based prediction of eukaryotic protein phosphorylation sites.** *J Mol Biol* 1999, **294**(5):1351-1362.
44. Chen YH, Yang JT, Martinez HM: **Determination of the secondary structures of proteins by circular dichroism and optical rotatory dispersion.** *Biochemistry* 1972, **11**:4120-4131.
45. Bohm G, Muhr R, Jaenicke R: **Quantitative analyses of protein far UV circular dichroism spectra by neural networks.** *Protein Engineering* 1992, **5**:191-195.
46. Andrade MA, Chacón P, Merelo JJ, Morán F: **Evaluation of secondary structure of proteins from UV circular dichroism using an unsupervised learning neural network.** *Prot Eng* 1993, **6**:383-390.
47. Correa DHA, Ramos CHI: **The use of circular dichroism spectroscopy to study protein folding, form and function.** *African J Biochem Res* 2009, **3**(5):164-173.
48. Kornev AP, Haste NM, Taylor SS, Eyck LF: **Surface comparison of active and inactive protein kinases identifies a conserved activation mechanism.** *Proc Natl Acad Sci USA* 2006, **103**(47):17783-8.
49. Huse M, Kuriyan J: **The conformational plasticity of protein kinases.** *Cell* 2002, **109**(3):275-82.
50. Schwede T, Kopp J, Guex N, Peitsch MC: **SWISS-MODEL: An automated protein homology-modeling server.** *Nucleic Acids Res* 2003, **31**(13):3381-3385.
51. Wiederstein M, Sippl MJ: **ProSA-web: interactive web service for the recognition of errors in three-dimensional structures of proteins.** *Nucleic Acids Res* 2007, **35**:W407-10.
52. Sippl MJ: **Recognition of Errors in Three-Dimensional Structures of Proteins.** *Proteins* 1993, **17**:355-362.
53. Zhang X, Gureasko J, Shen K, Cole PA, Kuriyan J: **An allosteric mechanism for activation of the kinase domain of epidermal growth factor receptor.** *Cell* 2006, **125**:1137-1149.
54. Sicheri F, Kuriyan J: **Structures of Src-family tyrosine kinases.** *Curr Opin Struct Biol* 1997, **7**:777-785.
55. Bressan GC, Silva JC, Borges JC, Dos Passos DO, Ramos CH, Torriani IL, Kobarg J: **Human regulatory protein Ki-1/57 has characteristics of an intrinsically unstructured protein.** *J Proteome Res* 2008, **7**(10):4465-74.
56. Lanza DC, Silva JC, Assmann EM, Quaresma AJ, Bressan GC, Torriani IL, Kobarg J: **Human FEZ1 has characteristics of a natively unfolded protein and dimerizes in solution.** *Proteins* 2009, **74**:104-21.
57. Trindade DM, Silva JC, Navarro MS, Torriani IC, Kobarg J: **Low-resolution structural studies of human Stanniocalcin-1.** *BMC Struct Biol* 2009, **9**:57.
58. Gonçalves KA, Borges JC, Silva JC, Papa PF, Bressan GC, Torriani IL, Kobarg J: **Solution structure of the human signaling protein RACK1.** *BMC Struct Biol* 2010, **10**:15.
59. Svergun DI: **Determination of the regularization parameter in indirect-transform methods using perceptual criteria.** *J Appl Cryst* 1992, **25**:495-503.
60. Gasteiger E, Gattiker A, Hoogland C, Ivanyi I, Appel RD, Bairoch A: **ExpASY: The proteomics server for in-depth protein knowledge and analysis.** *Nucleic Acids Res* 2003, **31**:3784-3788.
61. Volkov VV, Svergun DI: **Uniqueness of ab initio shape determination in small-angle scattering.** *J Appl Crystallogr* 2003, **36**:860-864.
62. Rizos AK, Tsikalas I, Morikis D, Galanakis P, Spyroulias GA, Krambovitis E: **Characterization of the interaction between peptides derived from the gp120/V3 domain of HIV-1 and the amino terminal of the chemokine receptor CCR5 by NMR spectroscopy and light scattering.** *J Non-Cryst Solids* 2006, **352**:4451-4458.
63. Iyer GH, Garrod S, Woods VL Jr, Taylor SS: **Catalytic independent functions of a protein kinase as revealed by a kinase-dead mutant: study of the Lys72His mutant of cAMP-dependent kinase.** *J Mol Biol* 2005, **351**(5):1110-22.
64. Barrett CP, Noble ME: **Molecular motions of human cyclin-dependent kinase 2.** *J Biol Chem* 2005, **280**(14):13993-4005.
65. la Cour T, Kiemer L, Mølgaard A, Gupta R, Skriver K, Brunak S: **Analysis and prediction of leucine-rich nuclear export signals.** *Protein Eng Des Sel* 2004, **17**(6):527-36.
66. Ingham RJ, Colwill K, Howard C, Dettwiler S, Lim CS, Yu J, Hersi K, Raaijmakers J, Gish G, Mbamalu G, Taylor L, Yeung B, Vassilovski G, Amin M, Chen F, Matskova L, Winberg G, Ernberg I, Linding R, O'donnell P, Starostine A, Keller W, Metalnikov P, Stark C, Pawson T: **WW domains provide a platform for the assembly of multiprotein networks.** *Mol Cell Biol* 2005, **25**(16):7092-106.
67. Lee EJ, Hyun SH, Chun J, Kang SS: **Human NIMA-related kinase 6 is one of the Fe65 WW domain binding proteins.** *Biochem Biophys Res Commun* 2007, **358**(3):783-8.
68. Bodade RG, Beedkar SD, Manwar AV, Khobragade CN: **Homology modeling and docking study of xanthine oxidase of *Arthrobacter* sp. XL26.** *Int J Biol Macromol* 2010, **47**(2):298-303.
69. Roy A, Kucukural A, Zhang Y: **I-TASSER: a unified platform for automated protein structure and function prediction.** *Nat Protoc* 2003, **5**(4):725-38.
70. Zhang Y: **I-TASSER: Fully automated protein structure prediction in CASP8.** *Proteins* 2009, **77**S9:100-113.
71. Zhang Y: **I-TASSER server for protein 3D structure prediction.** *BMC Bioinformatics* 2008, **9**:40.

72. Combet C, Jambon M, Deléage G, Geourjon C: **Geno3D: Automatic comparative molecular modeling of protein.** *Bioinformatics* 2002, **18**:213-214.
73. Bates PA, Kelley LA, MacCallum RM, Sternberg MJE: **Enhancement of Protein Modeling by Human Intervention in Applying the Automatic Programs 3D-JIGSAW and 3D-PSSM.** *Proteins* 2001, **55**:39-46.
74. Bates PA, Sternberg MJE: **Model Building by Comparison at CASP3: Using Expert Knowledge and Computer Automation.** *Proteins* 1999, **53**:47-54.
75. Contreras-Moreira B, Bates PA: **Domain Fishing: a first step in protein comparative modeling.** *Bioinformatics* 1999, **18**:1141-1142.
76. Sali A, Blundell TL: **Comparative protein modeling by satisfaction of spatial restraints.** *J Mol Biol* 1993, **234**:779-815.
77. Laskowski RA, MacArthur MW, Moss DS, Thornton JM: **Procheck - a program to check the stereochemical quality of protein structures.** *J Appl Crystallogr* 1993, **26**:283-291.
78. Orthaber D, Bergmann A, Glatter O: **SAXS experiments on absolute scale with Kratky systems using water as a secondary standard.** *J Appl Crystallogr* 2000, **33**:218-255.
79. Mylonas E, Svergun DI: **Accuracy of molecular mass determination of proteins in solution by small-angle X-ray scattering.** *J Appl Crystallogr* 2001, **40**:245-249.
80. Guinier A, Fournet G: *Small angle scattering of X-rays* New York, John Wiley and Sons, Inc; 1955.
81. Glatter O, Kratky O: *Small angle X-ray scattering* New York, Academic Press; 1982.
82. Feigin LA, Svergun DI: *Structure analysis by small angle X-ray and neutron scattering* New York, Plenum Press; 1987.
83. Petoukhov MV, Svergun DI: **Global rigid body modeling of macromolecular complexes against small-angle scattering data.** *Biophys J* 2005, **89**:1237-1250.
84. Kozin PV, Svergun DI: **Automated matching of high- and low-resolution structural models.** *J Appl Crystallogr* 2001, **34**:33-41.
85. DeLano WL: **The PyMOL molecular graphics system.** 2002.
86. Svergun DI: **Restoring low resolution structure of biological macromolecules from solution scattering using simulated annealing.** *Biophys J* 1999, **76**:2879-2886.
87. Svergun DI, Petoukhov MV, Koch MH: **Determination of domain structure of proteins from X-ray solution scattering.** *Biophys J* 2001, **80**:2946-2953.
88. Le Maire M, Rivas E, Moller JV: **Use of gel chromatography for determination of size and molecular weight of proteins: Further caution.** *Analyt Biochem* 1980, **106**:12-21.
89. Siegel LM, Monty KJ: **Determination of molecular weights and frictional ratios of proteins in impure systems by use of gel filtration and density gradient centrifugation. Application to crude preparations of sulfite and hydroxylamine reductases.** *Biochim Biophys Acta* 1966, **112**:346-362.
90. Trathnigg B: **Determination of MWD and Chemical Composition of Polymers by Chromatographic Techniques.** *Prog Polym Sci* 1995, **20**:615-650.
91. Niesen FH, Berglund H, Vedadi M: **The use of differential scanning fluorimetry to detect ligand interactions that promote protein stability.** *Nat Protoc* 2007, **2**(9):2212-21.

doi:10.1186/1472-6807-11-12

Cite this article as: Meirelles et al.: Human Nek6 is a monomeric mostly globular kinase with an unfolded short N-terminal domain. *BMC Structural Biology* 2011 **11**:12.

Submit your next manuscript to BioMed Central and take full advantage of:

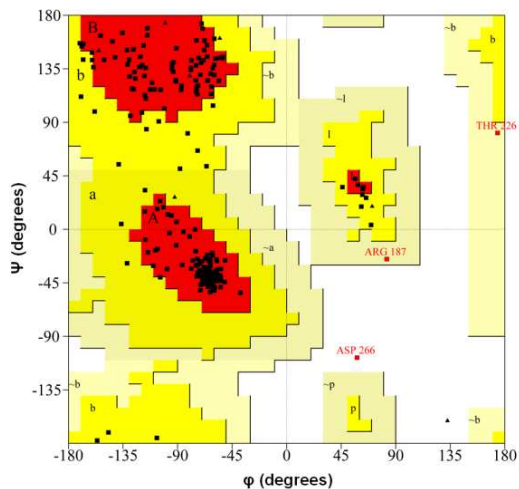
- Convenient online submission
- Thorough peer review
- No space constraints or color figure charges
- Immediate publication on acceptance
- Inclusion in PubMed, CAS, Scopus and Google Scholar
- Research which is freely available for redistribution

Submit your manuscript at
www.biomedcentral.com/submit



Additional file 1

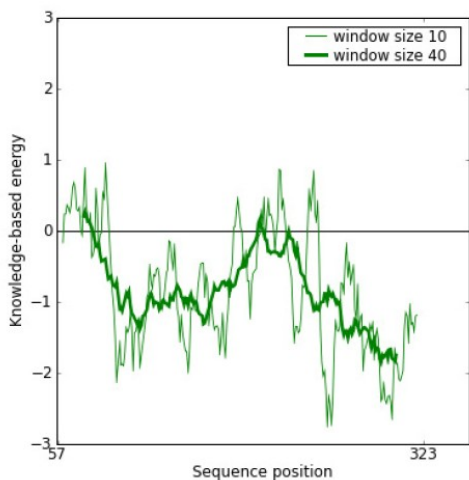
A



Ramachandran plot statistics

Residues in most favoured regions [A,B,L]	207	86.6%
Residues in additional allowed regions [a,b,l,p]	29	12.1%
Residues in generously allowed regions [~a,~b,~l,~p]	2	0.8%
Residues in disallowed regions	1	0.4%
<hr/>		
Number of non-glycine and non-proline residues	239	100%
Number of end-residues (excl. Gly and Pro)	2	
Number of glycine residues (shown as triangles)	14	
Number of proline residues	12	
<hr/>		
Total number of residues	267	

B



C

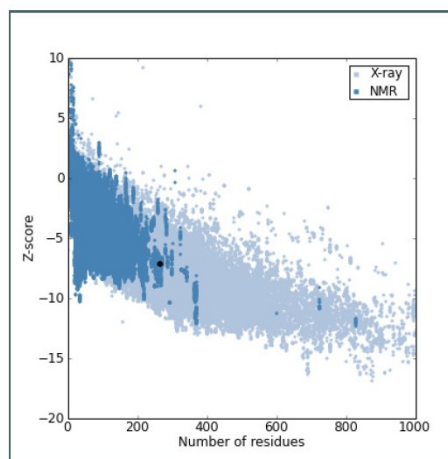


Figure S1. PROCHECK and PROSA analysis results of the validation procedures of the hNek6(S206A) comparative/homology model. (A) Ramachandran Plot calculated using the program PROCHECK. (B) Plot of the residue score showing the local model quality by plotting energies as a function of the residue sequence position using PROSA. In general, positive values correspond to problematic or erroneous parts of the structure. Here, the plots were smoothed by calculation of the average energy over 10- and 40-residues. This average is needed because of the large fluctuation in a plot of single residue energies. (C) The Z-score indicated overall model quality using PROSA. The Z-score of the hNek6(S206A) model was -7.14 (*black point*). The plot contains the Z-scores of all experimentally determined protein chains in the current PDB. The structures determined by X-ray and NMR are distinguished by different colors.

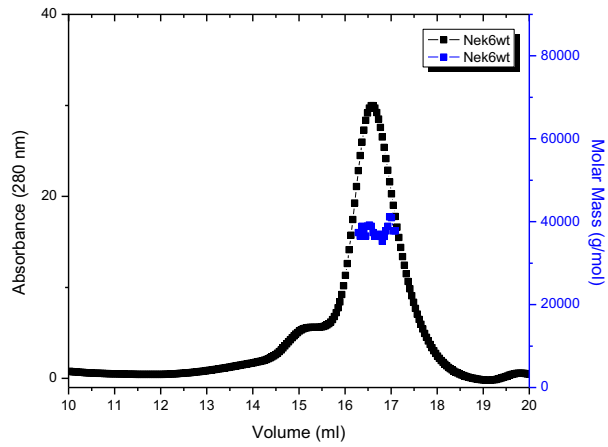
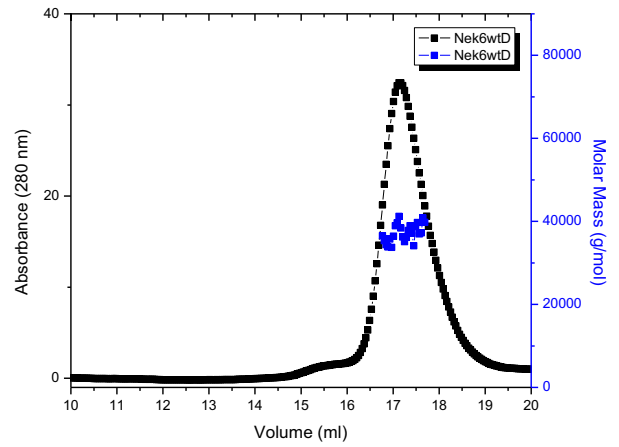
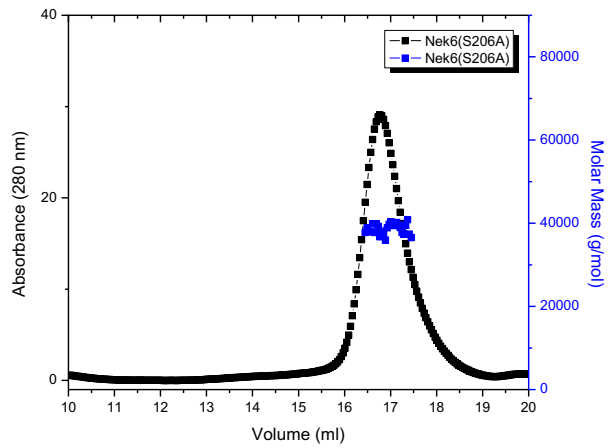
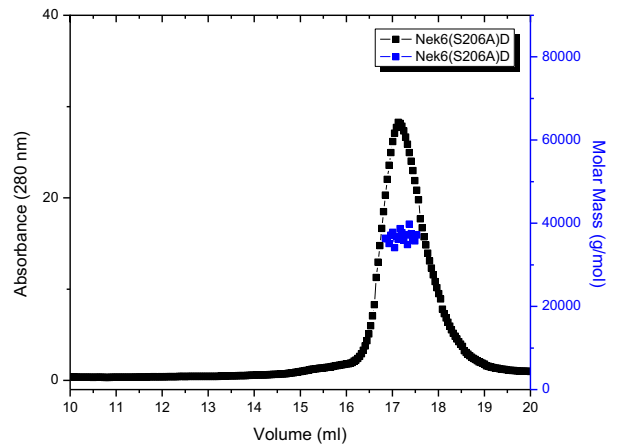
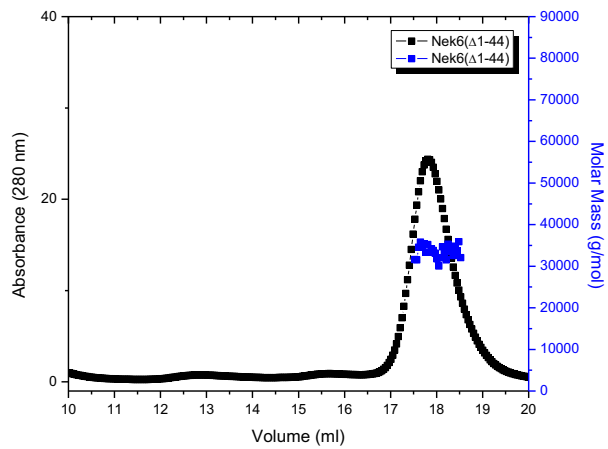
A**B****C****D****E**

Figure S2. Analytical SEC-MALS of recombinant (A) hNek6wt, (B) hNek6wtD, (C) hNek6(S206A), (D) hNek6(S206A)D and (E) hNek6(Δ 1-44). The M_w determined by MALS correspond to a monomer in all five cases.

3. Artigo III:

**FEZ1 INTERACTS WITH CLASP2 AND NEK1 THROUGH COILED-COIL
REGIONS AND THEIR CELLULAR COLOCALIZATION SUGGESTS
CENTROSOMAL FUNCTIONS AND REGULATION BY PKC**

DANIEL C. F. LANZA, GABRIELA V. MEIRELLES, MARCOS R.
ALBORGHETTI, CAMILA H. ABRILE, GUIDO LENZ, AND JÖRG KOBARG

MOLECULAR AND CELLULAR BIOCHEMISTRY, v. 338(1-2), p. 35-45, 2010.

(doi: 10.1007/s11010-009-0317-9)

FEZ1 interacts with CLASP2 and NEK1 through coiled-coil regions and their cellular colocalization suggests centrosomal functions and regulation by PKC

Daniel C. F. Lanza · Gabriela V. Meirelles ·
Marcos R. Alborghetti · Camila H. Abrile ·
Guido Lenz · Jörg Kobarg

Received: 29 June 2009 / Accepted: 3 November 2009 / Published online: 19 November 2009
© Springer Science+Business Media, LLC. 2009

Abstract FEZ1 was initially described as a neuronal protein that influences axonal development and cell polarization. CLASP2 and NEK1 proteins are present in a centrosomal complex and participate in cell cycle and cell division mechanisms, but their functions were always described individually. Here, we report that NEK1 and CLASP2 colocalize with FEZ1 in a perinuclear region in mammalian cells, and observed that coiled-coil interactions occur between FEZ1/CLASP2 and FEZ1/NEK1 in vitro. These three proteins colocalize and interact with endogenous γ -tubulin. Furthermore, we found that CLASP2 is phosphorylated and interacts with active PKC isoforms, and that FEZ1/CLASP2 colocalization is inhibited by PMA treatment. Our results provide evidence that these three proteins cooperate in centrosomal functions and open new directions for future studies.

Keywords NIMA · CLIP · Cytoskeleton · Tubulin

Electronic supplementary material The online version of this article (doi:10.1007/s11010-009-0317-9) contains supplementary material, which is available to authorized users.

D. C. F. Lanza · G. V. Meirelles · M. R. Alborghetti ·
C. H. Abrile · J. Kobarg (✉)
Centro de Biologia Molecular Estrutural, Associação Brasileira
de Tecnologia de Luz Síncrotron, Rua Giuseppe Máximo
Scolfaro 10.000, Campinas, C.P.6192, 13084-971, SP, Brazil
e-mail: jkobarg@lnls.br

D. C. F. Lanza · G. V. Meirelles · M. R. Alborghetti · J. Kobarg
Instituto de Biologia, Universidade Estadual de Campinas,
Campinas, SP, Brazil

G. Lenz
Departamento de Biofísica, Universidade Federal do Rio Grande
do Sul, Porto Alegre, RS, Brazil

Introduction

The protein FEZ1 (fasciculation and elongation protein zeta 1) was initially described as an orthologue of the UNC-76 protein, which performs important functions in the neuronal development of *C. elegans* [1]. Later, it was observed that FEZ1 interacts with cytoskeleton elements, mainly α -tubulin [2], and participates in microtubular transport mechanisms. FEZ1 associates physically with JIP1 and Kinesin-1, is indispensable for the formation of the cargo complex and participates in mitochondrial transport [3, 4]. Its interaction with PKC ζ is crucial for neuronal differentiation in PC12 cells [5]. Recently, it was observed that FEZ1 knockout mice presented hyperactivity, under novel social or stressful conditions as well as enhanced responsiveness to psychostimulants. These and other study confirm the importance of FEZ1 for the central nervous system development and in mechanisms causing schizophrenia [6]. Our group identified the interactions of FEZ1 with NEK1 (Nima-related kinase1) and CLASP2 (CLIP associated protein 2) in two independent yeast two-hybrid assays, using the NEK1 regulatory domain or the FEZ1 C-terminal region as baits, respectively [7, 8].

NEKs (NIMA-related kinases) represent a family of serine/threonine kinases implicated mainly in the control of the cell cycle at the G2/M checkpoint [9]. In mice, the mutations *kat* and *kat2J* of the NEK1 gene cause the polycystic kidney disease (PKD) [10, 11]. Murine NEK1 localizes to the centrosome in the interphase, and remains associated with the mitotic spindle during mitosis [12]. NEK1 interacts with proteins involved in the PKD, double-strand DNA break repair at the G2/M transition phase of the cell cycle, and neuronal cell development in vertebrates [7]. Some studies related that mNEK1 protein localizes to

the cilia basal body and participates in the cell cycle-associated ciliogenesis [13, 14].

The protein CLASP2 was initially described to be associated with CLIPs, linker proteins located mainly at the end of growing microtubules, where they function primarily as “anti-catastrophe” factors [15]. Recently, it was observed that glycogen synthase kinase 3 beta directly phosphorylates CLASPs at multiple sites in the domain required for MT plus end tracking [16]. CLASP2 has functions in mitotic spindle organization and kinetochore alignment during the cell division and participates in the formation of non-centrosomal microtubule organization centers [15–18].

We observed that FEZ1 dimerizes and shows an elongated shape, allowing its C-terminal coiled-coil regions to interact with other proteins [19]. We have also shown that FEZ1 interacts with tubulin and that its over-expression causes modifications in the microtubular organization that leads to the formation of “flower-like nuclei”, frequently observed in leukemic lymphocytes [20].

Here, we show the colocalization of FEZ1 with NEK1 and CLASP2(1192–1407) in mammalian cells and showed that these interactions occur through the coiled-coil regions of these proteins. Furthermore, we observe that PKC phosphorylates CLASP2, and that the addition of PMA inhibits its colocalization with FEZ1. Our data suggest a possible mutual function of these proteins in a centrosomal candidate region.

Materials and methods

Plasmid constructions

FEZ1(1–392) and truncated FEZ1(1–227) encoding nucleotide sequences were amplified by PCR and cloned into bacterial expression vector pET28a (Novagen/EMD Biosciences, San Diego, CA) as described [8]. FEZ1(229–269) was sub-cloned from 6xHis-FEZ1(1–392) into pET28a. Full-length FEZ1(1–392) and the fragments FEZ1(1–227) and FEZ1(221–392) were sub-cloned into pEGFPC2 vector (Clontech). Truncated CLASP2(1046–1407) was sub-cloned into pGEX-4T2 (GE Healthcare, Waukesha, WI) as described [8]. CLASP2(1192–1407) was sub-cloned into pDsRed-Monomer-C1 (Clontech) for expression of dsRED-CLASP2(1192–1407) fusion protein. Human full-length NEK1 cloned into pCMV5-FLAG vector was sub-cloned into pDsRed-Monomer-C1. Truncated GST-NEK1(441–621) and GST-NEK1(497–555) constructions were sub-cloned from the pDsRed-Monomer-C1 construction into pGEX-4T2 and a modified version of pET28a containing a GST-tag. All sequences were confirmed by DNA sequencing.

In vitro binding assays

GST-CLASP2(1046–1407), GST-NEK1(441–621) and GST-NEK1(497–555), or GST only (control) from bacterial lysate were allowed to bind to 50 μ L of glutathione sepharose beads in PBS for 1 h at 4°C. Experiments were performed as described previously [8].

Transient transfection

All transfections shown in this article were transient, and were performed using the calcium phosphate precipitation method. Adherent HEK293, HeLa, or COS-7 cells were cultivated in 24-well plates as described in [20]. For FLAG-NEK1 production, cells were cultivated in bottles and transfection was performed when the cells reached confluency of approximately 60%.

Fluorescence microscopy

HEK293, HeLa, or COS-7 cells previously transfected or not with GFP constructs were fixed as described [20]. The cells were blocked with 1% BSA in PBS for 1 h. For endogenous FEZ1 or NEK1 detection, the cells were incubated at room temperature for 1 h with 1% BSA in PBS containing antiserum that had been generated by four subsequent immunizations of rabbits with 6xHis-FEZ1(131–392) [20] or a NEK1 peptide (sequence: CMADGAYQEDNDE) coupled to KLH. For detection of endogenous CLASP2 in HeLa cells after incubation with 1% BSA, we used rabbit polyclonal anti-CLASP2 antibody (Santa Cruz Biotechnology). We also used a monoclonal anti- γ -tubulin antibody (1:5000, Sigma) in PBS containing 1% BSA (w/v). Subsequently, the cells were incubated at room temperature for 1 h with FITC or TRITC-conjugated secondary antibodies (Santa Cruz Biotechnology). Hoechst 33258 (1 μ g/ml) was used to stain nuclei. Cells were examined on a Nikon fluorescence microscope.

In vivo binding assays

HEK293 cells were harvested (approximately 1×10^7 cells), washed twice in PBS, re-suspended in 250 μ L of cold PBS and sonicated on ice. After centrifugation ($10,000 \times g$, 4°C) for 10 min, the supernatant was incubated for 2 h with Glutathione Sepharose beads containing GST-CLASP2(1046–1407) for γ -tubulin detection. Incubation was done for 24 h for the identification of activated PKC interactions. Next, beads were washed with PBS and the supernatant was subjected to SDS-PAGE and Western blotting (WB) with a monoclonal mouse anti- γ -tubulin, monoclonal anti-GST antibody 5.3.3 (hybridoma supernatant 1:5), anti-phospho PKC ζ (Thr410/403), or anti-phospho

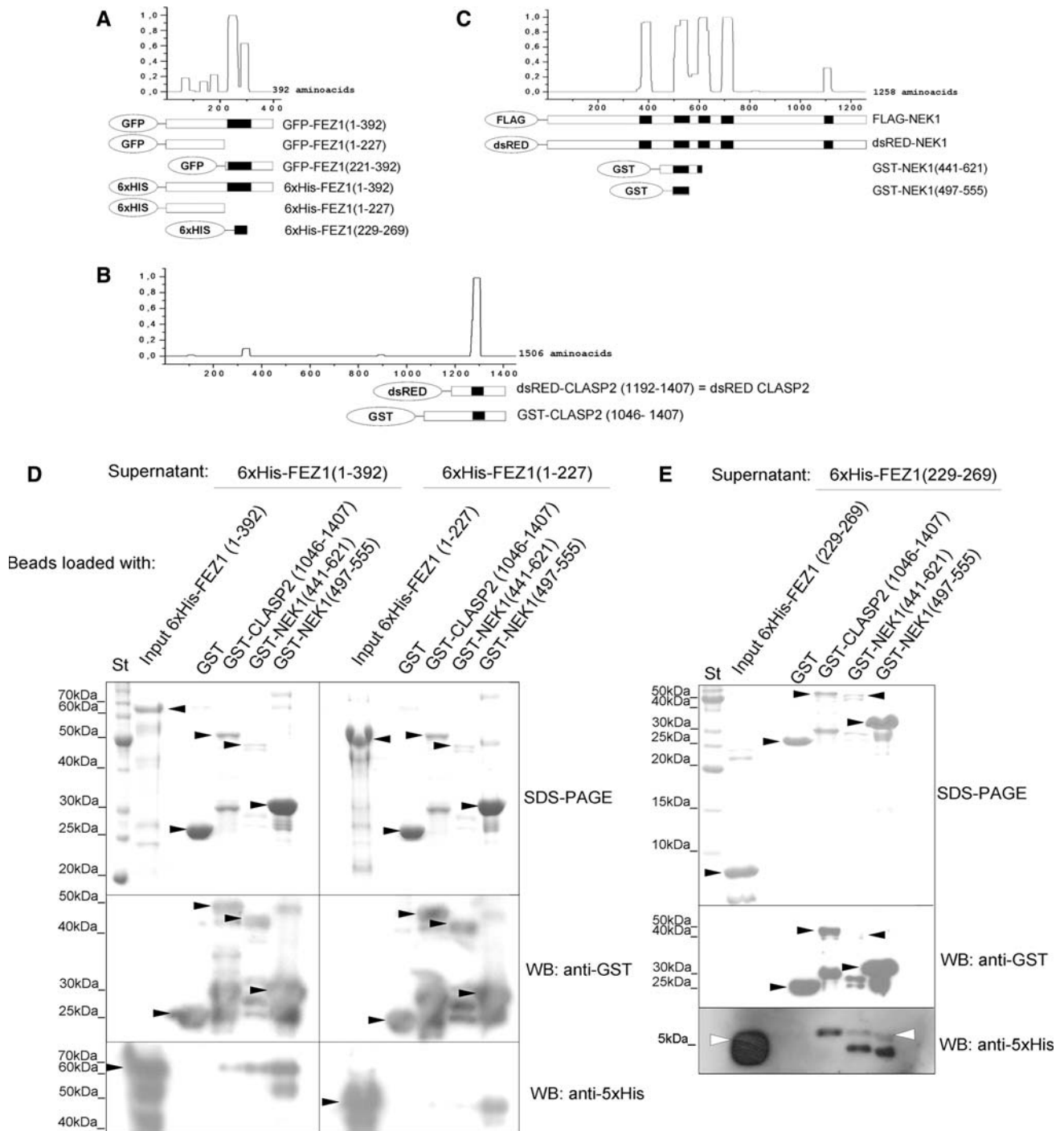


Fig. 1 GST-CLASP2(1046–1407) and GST-NEK1(441–621) interact with FEZ1 through defined coiled-coil regions. **a, b, c** Constructs of FEZ1, CLASP2, and NEK1 used in the experiments. The graphs above the construct indicate the coiled-coil prediction by COILS [22] for the complete primary sequences of all proteins. The *black regions* indicate the predicted coiled-coil regions. **d** Pull down assays showed that the interaction between 6xHis-FEZ1 and GST-CLASP2 (1046–1407) occurs mainly through the C-terminal region of the 6xHis-FEZ1. A supernatant containing 6xHis-FEZ1(1–392) or 6xHis-FEZ1(1–227) was added to glutathione sepharose beads containing GST-CLASP2(1046–1407), GST-NEK1 (441–621) and GST-NEK1

(497–555) or GST. **e** Pull down using 6xHis-FEZ1(229–269) in the supernatant confirms that the interactions of the FEZ1 with the indicated fusion proteins are mainly mediated through the coiled-coil region alone (229–269). The molecular weight and presence of GST and 6xHis-tagged proteins was confirmed by Coomassie-stained SDS-PAGE and WB. *Black arrowheads* indicate the positions of the GST fusion proteins in the WB and SDS-PAGE. *White arrowheads* indicate the position of 6xHis-FEZ1(229–269) in the WB anti-5xHis. The other bands in the same lane below the indicated bands are likely C-terminally degraded products, which maintain the same N-terminal fusion for detection. *St* molecular weight standard proteins

PKC α (Thr638/641) rabbit polyclonal antibodies (Cell Signaling) followed by HRP-coupled secondary antibodies. For immunoprecipitation of FLAG-NEK1, anti-FLAG monoclonal antibody was added to G Sepharose 4 fast flow beads (GE Healthcare) and then the beads were added to the lysate of transfected HEK293 cells. Next, beads were washed with PBS and then subjected to WB.

PMA treatment and in vitro phosphorylation

Approximately 1×10^4 cells growing in 24-well plates were incubated for 4 h with 200 ng/ml of PMA, 40 h after the transfection. Cells were fixed and submitted to immunocytochemistry as described above. For in vitro phosphorylation, 3 μ g of purified GST-CLASP2(1046–1407) were incubated in 25 μ L of the reaction mixture (20 mM Tris, 10 mM MgCl₂, 50 nM PMA; 20 mM ATP, pH 7.5) with 50 ng of PKC ζ -Pan (a mixture of predominantly classical PKC isoforms α , β I and β II, purified from the rat brain) or recombinant PKC ζ . For PKC ζ , we added 3.7 kBq of [γ -³²P]ATP (\sim 220 TBq/mMol). The mixture was incubated at 30°C for 30 min. Samples were analyzed by SDS-PAGE 10% and subsequent WB and autoradiography.

Results

The C-terminal coiled-coil region of FEZ1 is necessary for its interaction with CLASP2(1046–1407) and NEK1(441–621)

FEZ1, CLASP2, and NEK1 show coiled-coil regions, as predicted by the “Coils” software, using a score window 28 (http://www.ch.embnet.org/software/COILS_form.html) (Fig. 1a–c). We previously confirmed the presence of a major alpha helix content in the C-terminal region of FEZ1 (amino acids 221–392), using CD spectroscopy [19].

A pull down assay using full-length FEZ1 protein [6xHis-FEZ1(1–392)], or a truncated FEZ1 without the C-terminal region [6xHis-FEZ1(1–227)], showed that the interactions with both, GST-CLASP2(1046–1407) or GST-NEK1(441–621), but not GST, occur predominantly in dependence of the C-terminal region of FEZ1 (Fig. 1d). Interestingly, GST-NEK1(497–555), the second coiled-coil region of Nek1, interacts not only with full-length 6xHis-FEZ1(1–392) but also with the N-terminal construct 6xHis-FEZ1(1–227). This finding may suggest that GST-NEK1(497–555) interacts with other regions at the N-terminus of FEZ1. We speculate that this NEK1 region (from amino acid 497–555) may interact normally with other intramolecular coiled-coil or non-coiled-coil regions of NEK1. In other words, this NEK1 region may be involved in the structural organization of full-length NEK1.

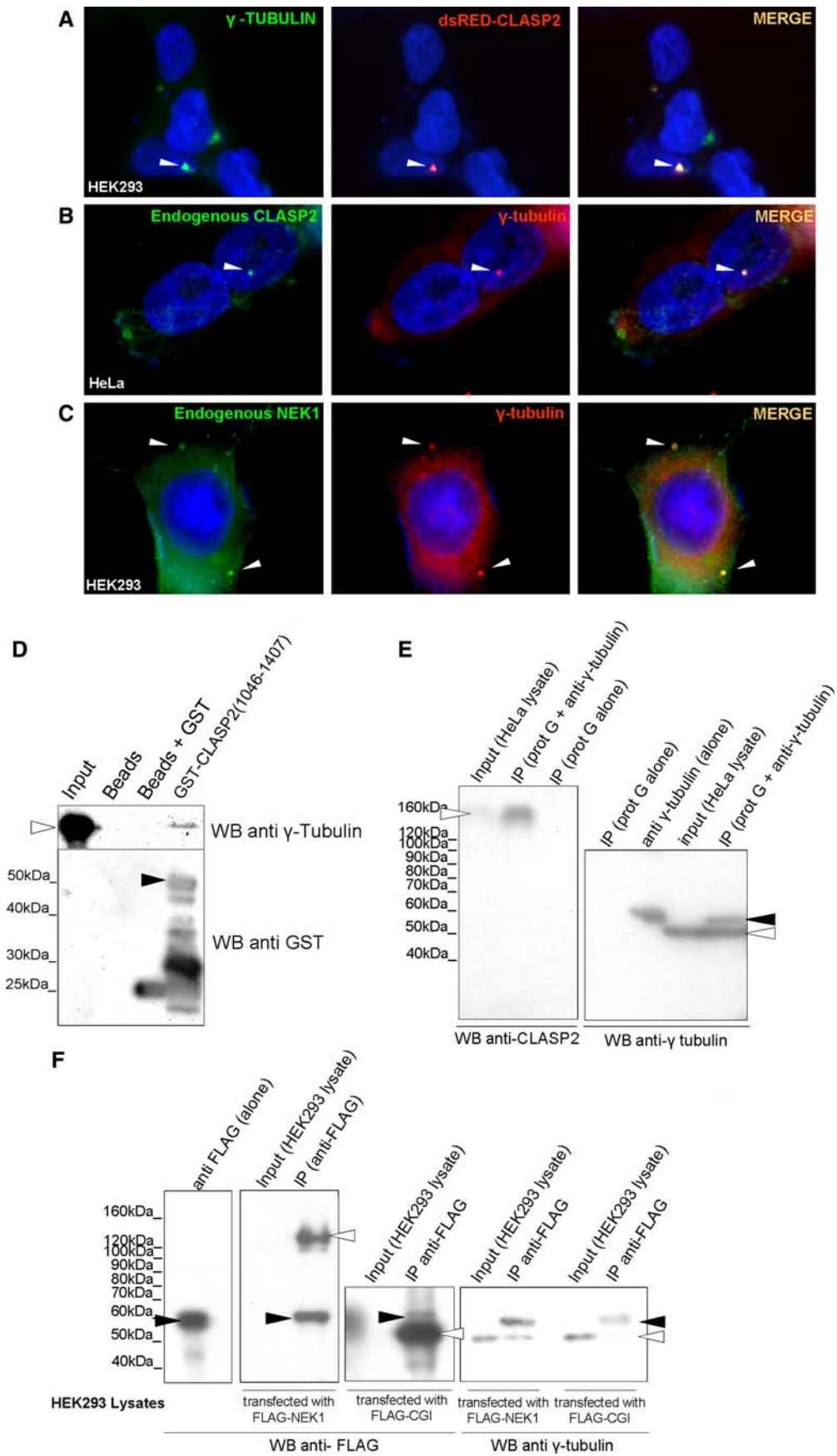
Fig. 2 dsRED-CLASP2, endogenous CLASP2 and NEK1 co-localize and interact with γ -tubulin. **a, b, c** The dsRED-CLASP2(1192–1407), endogenous CLASP2 and NEK1 all colocalize with endogenous γ -tubulin in HEK293 and HeLa cells (*white arrowheads*). The cell line used is indicated in left lower corner of the first panel. The DNA was counter-stained with Hoechst. **d** GST-CLASP2 (1046–1407) recombinant protein (*black arrowhead*) interacted with endogenous γ -tubulin (*white arrowhead*) from HEK293 cells lysate. The specificity of this interaction was controlled by unloaded and GST loaded beads. **e** *Left side* Endogenous CLASP2 is detected in γ -tubulin immunoprecipitate (IP) from HeLa cells (*white arrowheads*). Protein G sepharose alone was not able to bind to CLASP2. *Right side* Control of γ -tubulin IP The primary antibody heavy chain band (anti γ -tubulin, *black arrow*) was indicated. *White arrow head* γ -tubulin. **(f)** HEK293 cells were transfected with the FLAG-NEK1 or FLAG-CGI-55 constructions, as indicated below the panels. *Left side (anti-FLAG WB)* Demonstration of transfection with FLAG-NEK1 or FLAG-CGI. Only after IP were the specific protein bands be detected (*white arrow heads*). *Right side (anti- γ -tubulin WB)* endogenous γ -tubulin was detected in recombinant FLAG-NEK1 immunoprecipitate (IP) but not in recombinant FLAG-CGI-55 IP (*white arrows*). *Black arrow heads* primary antibody heavy chain band (of anti-FLAG antibody)

Therefore, when this fragment is employed alone it may also interact with the N-terminal region of FEZ1. Our hypothesis is in agreement with the observation that the N-terminal region of FEZ1 does not interact with the longer fragment GST-NEK1(441–621).

Using the region of amino acids 229–269 from FEZ1, we observed that this region alone is able to interact with GST-CLASP2(1046–1407), GST-NEK1(441–621) and GST-NEK1(497–555) (Fig. 1e). These results indicate that the coiled-coil domains alone can provide interaction between these proteins. In order to confirm the stability of the interaction of 6xHis FEZ1(229–269) with NEK1 (GST-NEK1-441–621 or 497–555), these proteins were coexpressed in bacteria (Supplementary Fig. S1). The copurification, revealed that the coiled-coil regions interact in a stable form, which is preserved after passage of the *E. coli* lysate through the GST-Trap column under stringent purification conditions. The helical-wheel analysis (Supplementary Fig. S2) shows the possibility of stable interactions of FEZ1 coiled-coil with CLASP2 and NEK1 coils, in agreement with the known versatility of the coiled-coil motifs for engaging in different protein–protein interactions [21].

The colocalization and interaction of CLASP2, NEK1, and FEZ1, with endogenous γ -tubulin suggest a concerted centrosomal function

Endogenous FEZ1 interacts and colocalizes with γ -tubulin in HEK293 cells [20, 22]. Here, we observed that dsRED-CLASP2(1129–1407) (called dsRED-CLAP2 from here) and endogenous CLASP2 and endogenous NEK1 colocalize with endogenous γ -tubulin in HEK293 and HeLa cells (Fig. 2a–c). Furthermore, recombinant GST-CLASP2 (1046–1407) coprecipitates with endogenous γ -tubulin



from HEK293 lysates (Fig. 2d) and in a reciprocal fashion endogenous CLASP2 also coimmunoprecipitates with γ -tubulin from HeLa cells (Fig. 2e). NEK1 is a large and somewhat unstable protein, maybe prone to rapid proteolysis. Its detection from cell lysates in Western blots is difficult, and frequently we did not observe it, even after over-expression. Immunoprecipitation of over-expressed FLAG-NEK1 from HEK293 also coprecipitated endogenous γ -tubulin (Fig. 2f). The reported interactions suggest a concerted centrosomal role for all three proteins, thereby shedding a new light on the previously reported, individual centrosomal roles of NEK1, CLASP2 [14, 16, 17], and FEZ1 [20].

dsRED-CLASP2 and endogenous CLASP2 have similar patterns of subcellular localization

GST-CLASP2(1046–1407) interacts with full-length 6xHis-FEZ1(1–392), but not with 6xHis FEZ1(1–227) in a pull down assay (Fig. 1d). This region of CLASP2 contains its major predicted coiled-coil region (Fig. 1b).

Three distinct phenotypes could be observed 48 h after transfection of HEK293 cells with the construction dsRED-CLASP2 (Fig. 3a). In the phenotypes called 1 and 2, which together make up $\sim 27.9\%$ of the transfected cells, a clear punctate perinuclear localization was observed, whereas the phenotype 3 shows only a diffuse red staining throughout the cell ($\sim 72.1\%$ of the transfected cells) (Fig. 3a). The colabelling with γ -tubulin (Fig. 2a) allowed us to propose that the punctate pattern of dsRED-CLASP2 in the phenotypes 1 and 2 represents most likely the centrosomal region. We further analyzed endogenous CLASP2 in HeLa cells and found a similar proportion of two similar phenotypes which we called 2E and 3E (Fig. 3b). The phenotype 2E corresponds to $\sim 14.6\%$ and the phenotype 3E to $\sim 85.4\%$ of the total analyzed cells (Fig. 3b, graphic). The defined punctate localization of endogenous CLASP2 (Fig. 3c), merges with that of the γ -tubulin staining (data not shown, Fig. 2b). The phenotypes observed are in agreement with previous localization analyses of endogenous CLASP2 in HeLa cells [15–17]. Probably, the phenotype 1 observed for recombinant dsRED-CLASP2 (Fig. 3a) is due to its over-expression, and therefore not observed for the endogenous protein (Figs. 3b–c, 2b).

Most interestingly, 4 h after addition of PMA, a PKC activator, the phenotypes 1 and 2, observed after the transfection of HEK293 cells with dsRED-CLASP2, practically disappeared, decreasing from 27.9% to only $\sim 3.06\%$ (Fig. 3a, graphic). In compensation, phenotype 3 increases from ~ 72.1 to $\sim 96.9\%$ of the transfected cells. This result suggests that the localization of CLASP2(1192–1407) to the centrosome candidate region may depend on PKC mediated phosphorylation.

FEZ1 colocalizes with endogenous NEK1 in a perinuclear region and its colocalization with dsRED-CLASP2 is decreased by PMA

Analysis of transfected COS-7 cells and HEK293 cells showed colocalization of GFP-FEZ1(1–392) and GFP-FEZ1(221–392) with both dsRED-NEK1 (data not show) or endogenous NEK1 in a perinuclear region (Fig. 4a, b). Full-length GFP-FEZ1(1–392) but especially the fragment FEZ1(221–392) showed a clearly localized pattern. The fragment GFP-FEZ1(221–392) contains the two major coiled-coil regions of FEZ1. The data shown above (Fig. 2c, f) together with data from the literature [12, 14, 20] allow us to suggest that the yellow stain seen in the merge panel of Fig. 4a, b includes the centrosome and that the coiled-coils are important for the FEZ1/NEK1 interaction at this site.

Furthermore, the dsRED-CLASP2 fragment colocalizes with endogenous FEZ1. This colocalization was observed in $\sim 15.45\%$ of the transfected cells, 48 h after transfection (Fig. 4c, graphic). Probably, the CLASP2 fragment is recruited to this site by the punctate localization of endogenous FEZ1, since we did not observe such perfect colocalization in other transfected cells that do not show FEZ1 in a punctate form. We further observed that in more than 60% of the cells that show endogenous FEZ1 in a punctate perinuclear form, as observed in Fig. 4c, this punctate region merges also with endogenous γ -tubulin localization (data not shown).

The colocalization of dsRED-CLASP2 in a punctate perinuclear region coincides with the localization of endogenous FEZ1 in HEK293 cells (15.5%), and this phenotype is significantly decreased (to 2.8%) after PMA treatment (Fig. 4c, d, graph). Likely, the colocalization of both proteins in a perinuclear region is influenced by their phosphorylation status. Our previous results showed that after in vitro phosphorylation by PKC, FEZ1 no longer interacts with CLASP2(1046–1407) [19]. Together, these data suggest that FEZ1 and CLASP2(1192–1407) colocalize in a centrosomal candidate region and this localization is decreased by PMA mediated activation of PKC.

CLASP2(1046–1407) interacts with endogenous active PKC isoforms and is phosphorylated by them in vitro

Using specific anti-phospho PKCs, we observed that GST-CLASP2(1046–1407) interacts with active endogenous PKC isoforms α/β and ζ from HEK293 cell lysates (Fig. 5a). The PMA addition to the cell cultures activated the classical and novel PKC isoforms. Although the PKC α/β band was not observed in the input after PMA activation, we observed that it interacts with GST-CLASP2(1046–1407). Possibly, activated PKC α/β remained mainly in the insoluble membrane

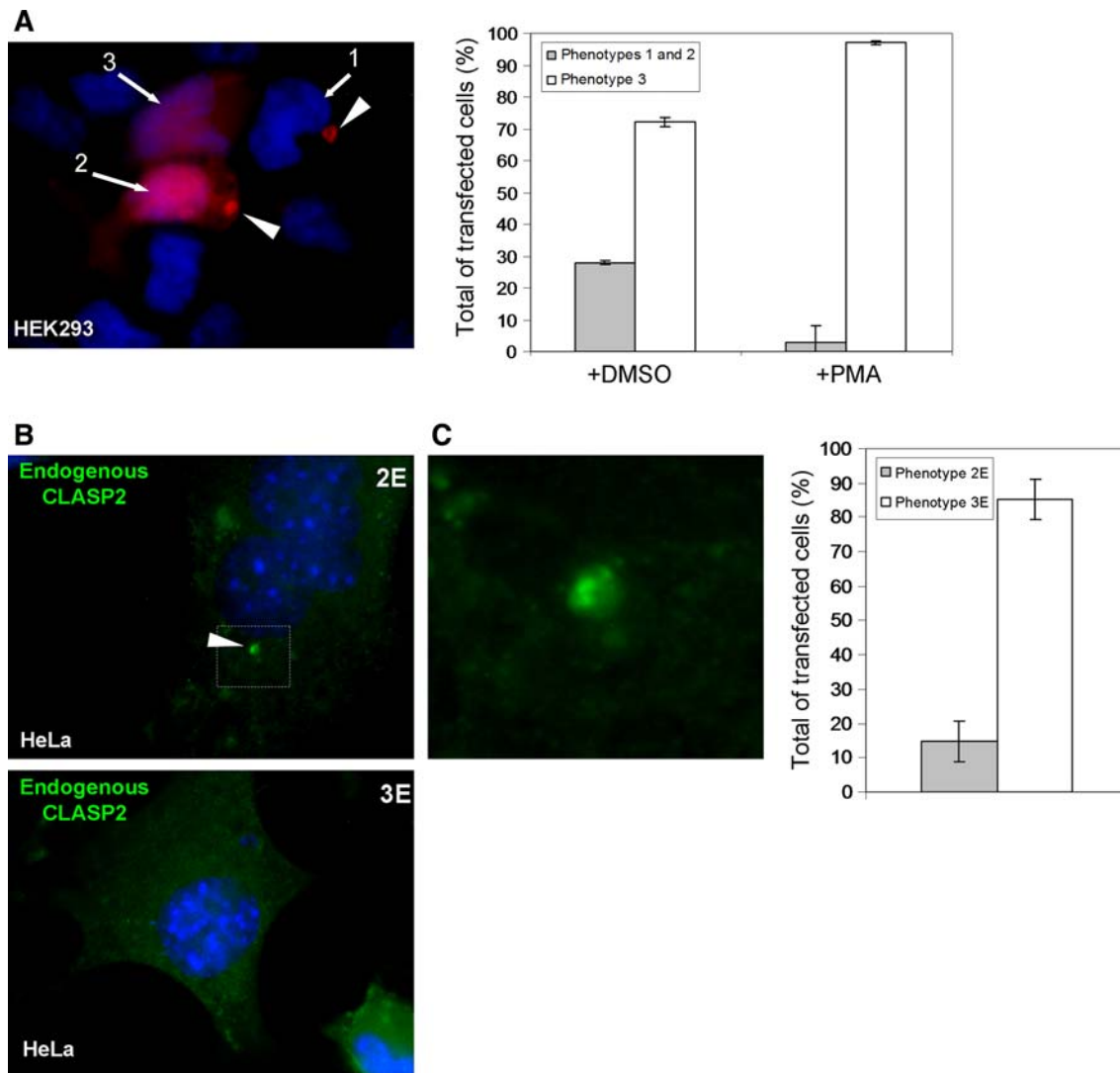


Fig. 3 dsRED-CLASP2 and endogenous CLASP2 have a similar sub-cellular localizations. **a** The over-expression of dsRED-CLASP2 (1192–1407) generates phenotypes 1–3, in transfected HEK293 cells. The addition of PMA affects the frequency of these phenotypes (graphic) in comparison to the absence of PMA (DMSO only). **b** Endogenous CLASP2 shows similar phenotypes in HeLa cells (named 2E and 3E, E for endogenous), comparable to the phenotypes

2 and 3 observed in HEK293 cells transfected with dsRED-CLASP2(1192–1407). The proportion of cells (HEK293 and HeLa) that showed these phenotypes was measured from three replicates, and is shown in the graphics accompanying the panels. The error bars represent the standard deviation of the mean. **c** Detail of the typical punctate, centrosomal CLASP2 localization in HeLa cells. The cell line used for each case is described in the left corner of each picture

fraction (pellet), but the interaction with GST-CLASP2 (1046–1407) concentrated PKC α/β to the IP beads. The PKC ζ was identified both, before and after the PMA addition, thereby confirming the known fact that the atypical PKCs are not activated by PMA. There is previous evidence in the literature that phosphorylation is important in the regulation of protein interactions with FEZ1. PKC ζ phosphorylation caused translocation of FEZ1 from de cell membrane to the cytoplasm [5]. We observed previously that PKC phosphorylates FEZ1 in vitro, and thereby inhibits its interaction with CLASP2(1192–1407) [19].

In order to investigate the phosphorylation of GST-CLASP2(1046–1407), we performed in vitro phosphorylation reactions using PKCpan, that contains isoforms activated by PMA, and PKC ζ , which was shown to phosphorylate FEZ1 in vivo [5]. Using anti-phospho-Ser and anti-phospho-Thr primary antibodies, we were able to detect a specific band in the Western Blot, that indicates that GST-CLASP2(1046–1407), but not GST, was phosphorylated in vitro by PKCpan (Fig. 5b).

When we used the isoform PKC ζ , which is not activated by PMA, we also observed a specific phosphorylation of

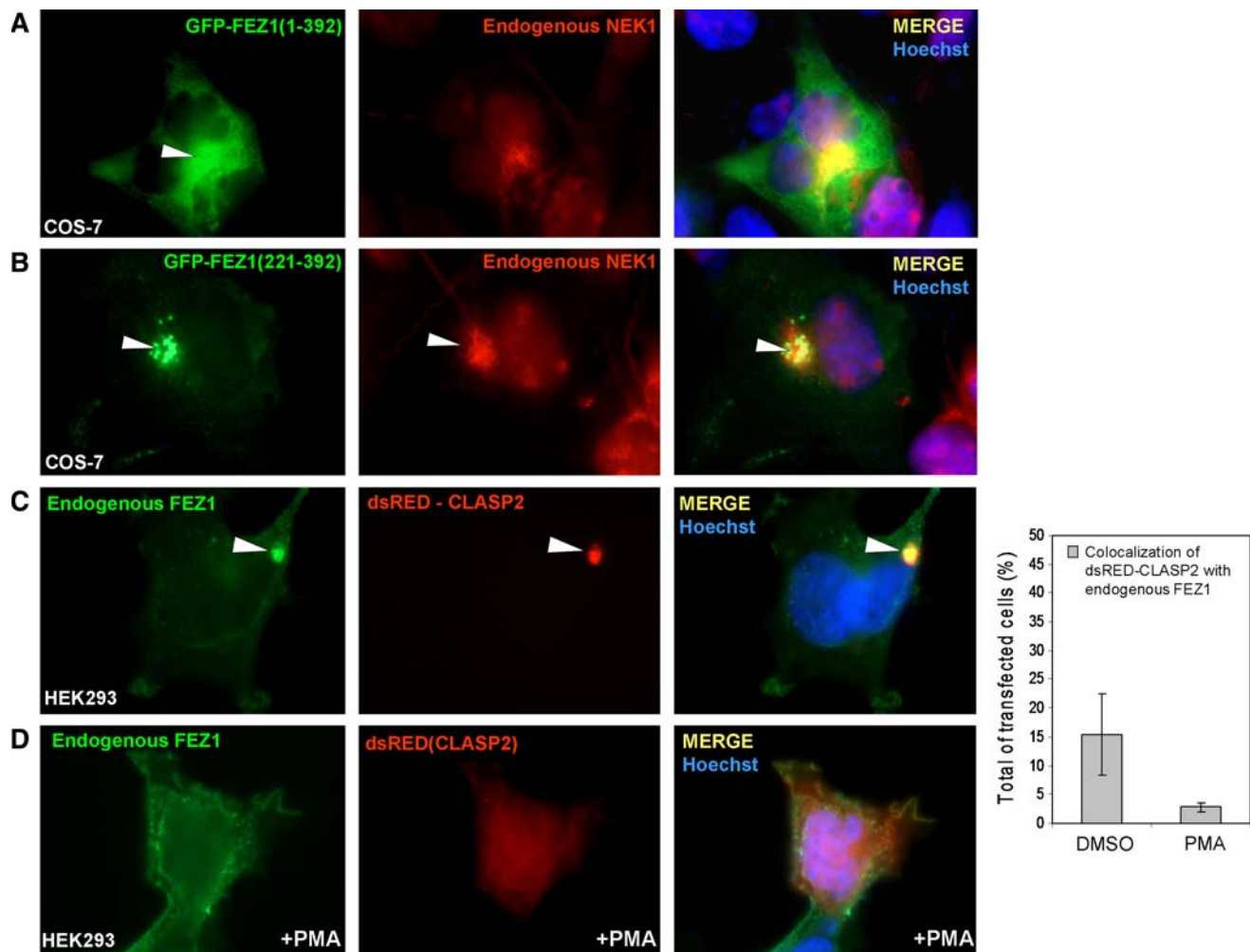


Fig. 4 FEZ1 colocalizes with endogenous NEK1 and with dsRED-CLASP2(1046–1407) in a punctate perinuclear region. **a, b** Different GFP-FEZ1 constructs colocalize with dsRED-NEK1 in a perinuclear fashion in COS-7 cells. A more intense merge region is observed when NEK1 is labeled in cells that also over-express GFP-FEZ1(221–392), which contains the major coiled-coil regions of FEZ1 (*white arrowheads*)

(b, c, d) Endogenous FEZ1 colocalizes with dsRED-CLASP2(1192–1407) in a punctate perinuclear region in HEK293 cells (*white arrowheads*), but the colocalization is abolished by addition of PMA. The proportion of cells that show colocalization was quantified, and represented in the graphic on the right. The cell line used for each case is described in the left corner of each picture

GST-CLASP2(1046–1407) and control protein 6xhis-FEZ1, but not of control protein GST-RAI (Fig. 5c). These results validate the hypothesis that FEZ1 and CLASP2 interact and suggest that its concerted functions may be regulated by phosphorylation by different members of the PKC family.

In conclusion, the same cellular localization of FEZ1, NEK1, CLASP2, and γ -tubulin, indicates that the function of these proteins may overlap in a temporal and spatial fashion at the centrosome. The centrosome is a very dynamic cellular structure, involved in various processes, principally during the cell division and in cellular polarization. The coiled-coil mediated, phosphorylation dependent interactions among FEZ1, NEK1, and CLASP2 reported here, demonstrate the complexity and dynamic of the interactions occurring at the centrosome.

Discussion

The functions of CLASP2 and NEK1 have not previously been reported to be connected. Here, we show that NEK1, CLASP2, and FEZ1 colocalize with endogenous γ -tubulin in mammalian cells and that NEK1 and CLASP2 colocalizes with FEZ1 in a centrosomal/perinuclear region.

Furthermore, our pull down experiments showed that NEK1 and CLASP2 interactions with FEZ1 occur through a specific coiled-coil region of FEZ1. The versatility of the coiled-coil interactions may allow specificity without the loss of dynamical rearrangements. In a recent study, we showed that FEZ1 has an elongated shape, and forms dimers in solution [19]. The dimerization occurs in the N-terminal region of FEZ1 and the two C-terminal coiled-coil regions of the dimer are free and exposed to the outside

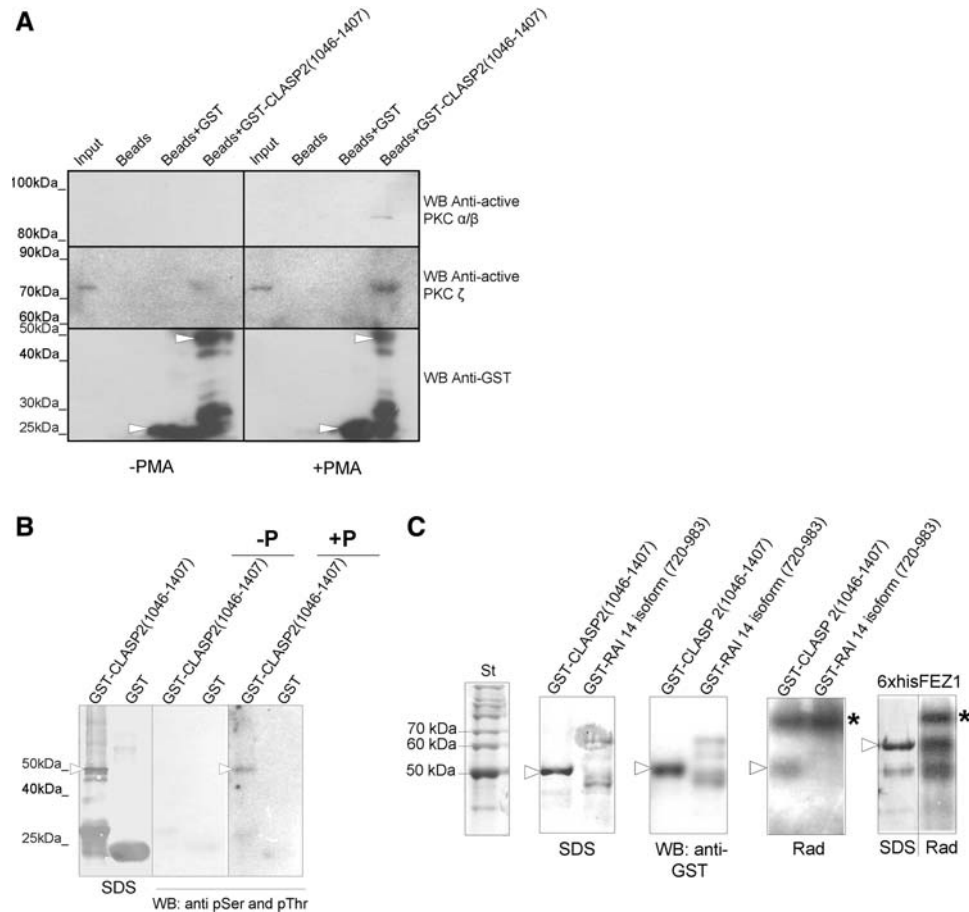


Fig. 5 CLASP2(1046–1407) is phosphorylated in vitro and interacts with endogenous active PKC isoforms. **a** Active PKCs from HEK293 lysates interact with recombinant GST-CLASP2(1046–1407) after incubation with HEK293 lysate. **b** GST-CLASP2(1046–1407) was (+P) or was not (–P) submitted to a phosphorylation reaction in vitro with PKC-Pan. Samples were analyzed by Coomassie-stained SDS-PAGE (left) and WB using anti-phospho-Ser/Thr antibodies (right, anti pSer and pThr). CLASP2(1046–1407) did not show unspecific phosphorylation when isolated in the bacteria (–P). **c** PKCζ

phosphorylates GST-CLASP2(1046–1407) in vitro. The indicated proteins were submitted to in vitro phosphorylation by PKCζ and were then analyzed by SDS-PAGE and autoradiography. The white arrowheads indicate phosphorylated GST-CLASP2(1046–1407). GST-RAI 14 isoform (720–983) served as a negative control protein. 6xHis-FEZ1(1–392) was used as a positive control protein. The asterisks (*) indicate PKCζ auto-phosphorylation. St molecular weight standard proteins

to mediate protein–protein interactions. The C-terminal region of FEZ1 (amino acids 221–392), which presents the major coiled-coil region, interacts with more than 40 different proteins, and presents several predicted phosphorylation sites, including PKC sites [19]. The results shown here allow us to speculate that the FEZ1 dimer may simultaneously interact with both NEK1 and CLASP2, through its two C-terminal coiled-coil regions.

Another interesting finding is the change in FEZ1 and dsRED-CLASP2(1192–12407) cellular colocalization promoted by PMA treatment. Subsequent coprecipitation and in vitro phosphorylation assays showed that CLASP2(1046–1407) is phosphorylated by different PKC isoforms. CLASP2 phosphorylation may therefore inhibit its localization to a centrosome candidate region, which may be mediated by binding to FEZ1. In support of this hypothesis, a

previous report showed that FEZ1 subcellular localization is altered by inhibition of PKCs in PC12 cells [5]. Here, we also observed that after PMA treatment the FEZ1/CLASP2 colocalization is decreased.

In a review, Bisgrove and Yost pointed out that there may be a functional link between the pathophysiology of the poly cystic kidney disease (PKD), the mechanosensory functions of the polycystins (Pkd1 and 2) and the intraflagellar transport in primary cilia [23]. This view is supported by the discovery of the concerted action of several proteins involved in these processes. The genes encoding these proteins may all be affected by mutations that can lead to the development of the PKD. These proteins include: Nek1, Nek8 (centrosome and cilia functions), Kif3a (transport), and Pkd1 and 2 (mechanosensors), among others [23]. Here, we add with FEZ1 (transport

adaptor) and CLASP2 (microtubular tip function) two new players to this scenario. Our findings may emphasize the view that the PKD may not only manifest itself in consequence of direct gene disruption of its key signaling components such as Pkd1 and 2, but also in an indirect fashion, through incorrect ciliary localization, function, or transport of its components. In this context, we now begin to understand the importance of the protein Kif3, which when missing also causes PKD [24] and also of FEZ1, which is intimately associated to microtubular transport processes and furthermore interacts directly with Nek1 [7] and Kif3 [3]. Future experiment will be directed at identifying the exact contribution and role of all individual components in this intricate protein network, which dysregulation leads through multiple pathways to the development of the PKD.

Our data suggest that the functions of FEZ1, NEK1, and CLASP2 should be analyzed together, in a context of cytoskeleton and centrosomal activities. The FEZ1 dimer mediates interactions principally through its C-terminal coiled-coil regions and our data suggest that FEZ1 may be a connecting point between the functions of NEK1 and CLASP2. The discovery of a concerted interaction of these proteins opens new avenues to the study of the highly dynamic centrosomal and microtubular functions.

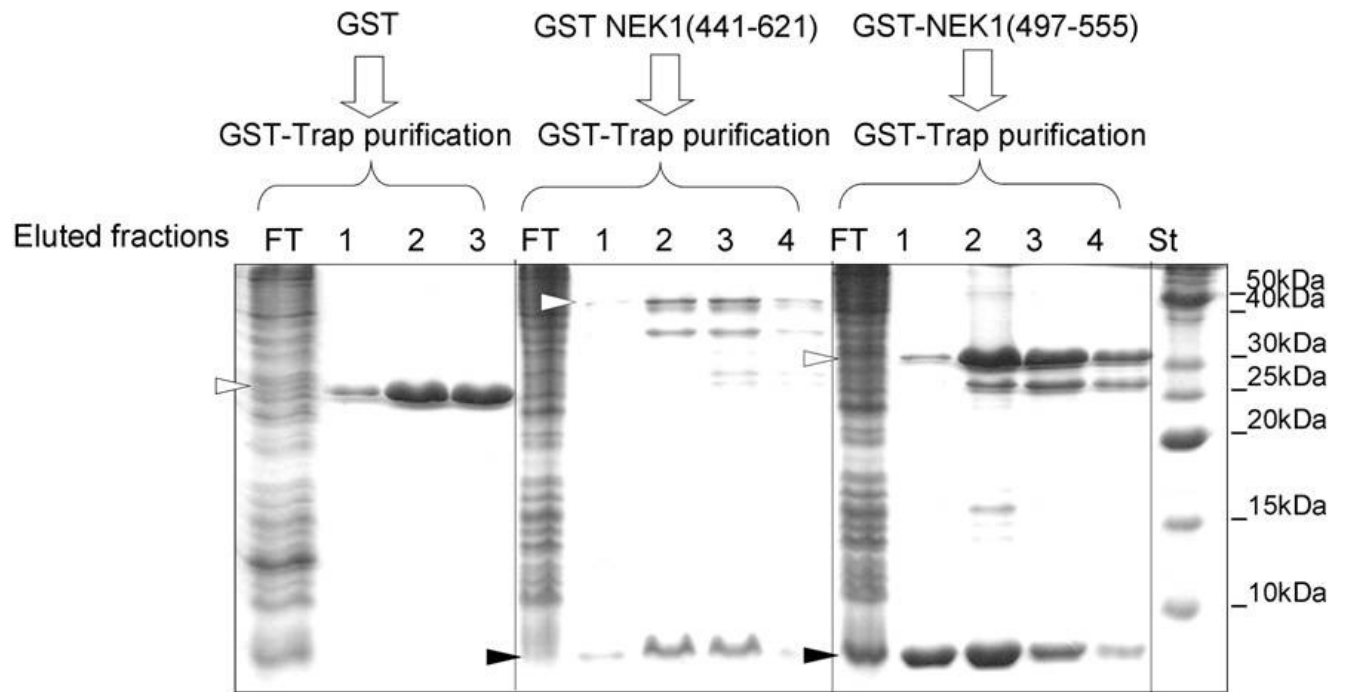
Acknowledgements Financially supported by: Fundação de Amparo à Pesquisa do Estado São Paulo, Conselho Nacional de Pesquisa e Desenvolvimento and LNLS. We thank Maria Eugenia Camargo and Jéssica Santana Bernachi for technical assistance. We are also grateful to Dr. Alexandre J. C. Quaresma for help in providing critical reagents.

References

- Bloom L, Horvitz HR (1997) The *Caenorhabditis elegans* gene *unc-76* and its human homologs define a new gene family involved in axonal outgrowth and fasciculation. *Proc Natl Acad Sci* 94:3414–3419
- Suzuki T, Okada Y, Semba S, Orba Y, Yamanouchi S, Endo S, Tanaka S, Fujita T, Kuroda S, Nagashima K, Sawa H (2005) Identification of FEZ1 as a protein that interacts with JC virus agnoprotein and microtubules. *J Biol Chem* 280:24948–24948–56
- Blasius TL, Cai D, Jih GT, Toret CP, Verhey KJ (2007) Two binding partners cooperate to activate the molecular motor Kinesin-1. *J Cell Biol* 176:11–17
- Ikuta J, Maturana A, Fujita T, Okajima T, Kenji T, Tanizawa K, Kuroda S (2007) Fasciculation and elongation protein zeta-1 (FEZ1) participates in the polarization of hippocampal neuron by controlling the mitochondrial motility. *Biochem Biophys Res Commun* 353:127–132
- Kuroda S, Nakagawa N, Tokunaga C, Tatematsu K, Tanizawa K (1999) Mammalian homologue of the *Caenorhabditis elegans* UNC-76 protein involved in axonal outgrowth is a protein kinase C zeta-interacting protein. *J Cell Biol* 114:403–411
- Sakae N, Yamasaki N, Kitaichi K, Fukuda T, Yamada M, Yoshikawa H, Hiranita T, Tatsumi Y, Kira JI, Yamamoto T, Miyakawa T, Nakayama KI (2008) Mice lacking the schizophrenia-associated protein FEZ1 manifest hyperactivity and enhanced responsiveness to psychostimulants. *Hum Mol Genet* 17:3191–3203
- Surpili MJ, Delben TM, Kobarg J (2003) Identification of proteins that interact with the central coiled-coil region of the human protein kinase NEK1 involved in the cell cycle regulation. *Biochemistry* 42:15369–15376
- Assmann EM, Alborghetti MR, Camargo ME, Kobarg J (2006) FEZ1 dimerization and interaction with transcription regulatory proteins involves its coiled-coil region. *J Biol Chem* 281:9869–9881
- O'Regan L, Blot J, Fry AM (2007) Mitotic regulation by NIMA-related kinases. *Cell Div* 29:2–25
- Vogler C, Homan S, Pung A, Thorpe C, Barker J, Birkenmeier EH, Upadhy P (1999) Clinical and pathologic findings in two new allelic murine models of polycystic kidney disease. *J Am Soc Nephrol* 12:2534–2539
- Upadhy P, Birkenmeier EH, Birkenmeier CS, Barker JE (2000) Mutations in a NIMA related kinase gene, *Nek1*, cause pleiotropic effects including a progressive polycystic kidney disease in mice. *Proc Natl Acad Sci USA* 97:217–221
- Mahjoub MR, Trapp ML, Quarmby LM (2005) NIMA-related kinases defective in murine models of polycystic kidney diseases localize to primary cilia and centrosomes. *J Am Soc Nephrol* 16:3485–3489
- Shalom O, Shalva N, Altschuler Y, Motro B (2008) The mammalian *Nek1* kinase is involved in primary cilium formation. *FEBS Lett* 582:1465–1470
- White MC, Quarmby LM (2008) The NIMA-family kinase, *Nek1* affects the stability of centrosomes and ciliogenesis. *BMC Cell Biol* 4:9–29
- Mimori-Kiyosue Y, Grigoriev I, Lansbergen G, Sasaki H, Matsui C, Severin F, Galjart N, Grosveld F, Vorobjev I, Tsukita S, Akhmanova A (2005) CLASP1 and CLASP2 bind to EB1 and regulate microtubule plus-end dynamics at the cell cortex. *J Cell Biol* 168:141–153
- Kumar P, Lyle KS, Gierke S, Matov A, Danuser G, Wittmann T (2009) GSK3beta phosphorylation modulates CLASP-microtubule association and lamella microtubule attachment. *J Cell Biol* 184:895–908
- Pereira AL, Pereira AJ, Maia AR, Drabek K, Sayas CL, Hergert PJ, Lince Faria M, Matos I, Duque C, Stepanova T, Rieder CL, Earnshaw WC, Galjart N, Maiato H (2006) Mammalian CLASP1 and CLASP2 cooperate to ensure mitotic fidelity by regulating spindle and kinetochore function. *Mol Biol Cell* 17:4526–4542
- Efimov A, Kharitonov A, Efimova N, Loncarek J, Miller PM, Andreyeva N, Gleeson P, Galjart N, Maia AR, McLeod IX, Yates JR, Maiato H, Khodjakov A, Akhmanova A, Kaverina I (2007) Asymmetric CLASP-dependent nucleation of noncentrosomal microtubules at the trans-Golgi network. *Dev Cell* 12:917–930
- Lanza DC, Silva JC, Assmann EM, Quaresma AJ, Bressan GC, Torriani IL, Kobarg J (2009) Human FEZ1 has characteristics of a natively unfolded protein and dimerizes in solution. *Proteins* 74:104–121
- Lanza DC, Trindade DM, Assmann EM, Kobarg J (2008) Overexpression of GFPFEZ1 causes generation of multi-lobulated nuclei mediated by microtubules in HEK293 cells. *Exp Cell Res* 314:2028–2039
- Lupas A, Van Dyke M, Stock J (1991) Predicting coiled-coils from protein sequences. *Science* 252:1162–1164
- Lee S, Walker CL, Karten B, Kuny SL, Tennese AA, O'Neill MA, Wevrick R (2005) Essential role for the Prader–Willi

- syndrome protein neccin in axonal outgrowth. *Hum Mol Genet* 14:627–637
23. Bisgrove BW, Yost HJ (2006) The roles of cilia in developmental disorders and disease. *Development* 133:4131–4143
24. Lin F, Hiesberger T, Cordes K, Sinclair AM, Goldstein LSB, Somlo S, Igarashi P (2003) Kidney-specific inactivation of the KIF3A subunit of kinesin-II inhibits renal ciliogenesis and produces polycystic kidney disease. *Proc Nat Acad Sci* 100:5286–5291

6xHis-FEZ1(229-269)



Supplementary figure 1

IV. CONCLUSÕES E PERSPECTIVAS

Artigo 1:

1. Os *screenings* de duplo-híbrido em levedura para a hNek6 resultaram na identificação de um amplo espectro de 66 prováveis parceiros de interação, classificados em 18 categorias funcionais baseadas no Gene Ontology (GO), refletindo uma elevada conectividade (grande número de interações) para a hNek6 e seu possível envolvimento em diversos processos biológicos.
2. Análises por espectrometria de massa identificaram peptídeos fosforilados nas proteínas recombinantes 6xHis-hNek6wt e 6xHis-hNek6(S206A) expressas em *E. coli*, mostrando sítios de provável autofosforilação e um padrão similar de peptídeos com relação à hNek6 expressa em células humanas, o que demonstra que a proteína humana expressa em sistema procarioto conserva características bastante similares à proteína humana expressa em células humanas.
3. Ensaios de *pull-down in vitro* confirmaram a interação entre a proteína recombinante 6xHis-hNek6wt e 12 dos 66 prováveis parceiros de interação, em fusão com GST.
4. Ensaios de *pull-down in vitro* utilizando-se a proteína recombinante 6xHis-hNek6(Δ 1-44) e 8 prováveis parceiros de interação (entre os 12 confirmados no *pull-down* com a proteína 6xHis-hNek6wt) mostraram que o N-terminal da hNek6 é essencial para mediar a interação com essas proteínas.
5. Ensaios de fosforilação *in vitro* para 7 prováveis parceiros de interação da hNek6 mostraram que 6 deles são também prováveis substratos da proteína recombinante 6xHis-hNek6wt, mas não do mutante 6xHis-hNek6(S206A).
6. Ensaios de imunocitoquímica demonstraram que a hNek6 endógena colocaliza com 10 prováveis parceiros de interação endógenos em células humanas (HEK293), possivelmente no centróssomo, o que valida tais

interações em uma região já descrita de grande atuação das Neks na formação do fuso mitótico e outras funções relacionadas ao ciclo celular.

7. Ensaio de imunoprecipitação em células humanas (THP1) com proteínas endógenas, mostrou que a hNek6 interage *in vivo* com o fator de transcrição RelB, confirmando assim seu possível papel na ativação da via do NF- κ B através de sua interação com o RelB.
8. A ligação à hNek6 dependente do seu domínio N-terminal e a colocalização no centrôssomo parecem corresponder a um fenômeno geral das interações da hNek6 identificadas em nosso estudo.
9. Análises *in silico* para os 66 prováveis parceiros de interação da hNek6 mostraram que eles apresentam características estruturais e funcionais similares, em relação à porcentagem de regiões desordenadas, à composição de domínios em suas sequências de aminoácidos, e aos processos biológicos e perfis de expressão gênica.
10. A construção de 5 diferentes redes de interação baseadas no banco de dados BioGRID e no software de visualização Osprey 1.2.0, juntamente com análises de conectividade dessas redes, mostraram que o quinoma humano é rico em proteínas com elevado grau de conectividade (hubs) e que a hNek6 é uma cinase hub.
11. Análise *in silico* utilizando-se o banco KOMP (*Knockout Mouse Project Repository*) mostrou que a maioria das cinases com elevados graus de conectividade apresentam fenótipos letais em camundongos nocauteados, sugerindo que possam consistir em genes essenciais também em humanos.
12. Em suma, os novos prováveis parceiros de interação da hNek6 conectam esta cinase a diferentes processos biológicos, fornecendo pistas de como ela poderia atuar em novas vias, como regulação do citoesqueleto de actina e sinalização Notch, ou como poderia regular vias previamente conhecidas, como ciclo celular, reparo de DNA e sinalização do NF- κ B (Figura 6).

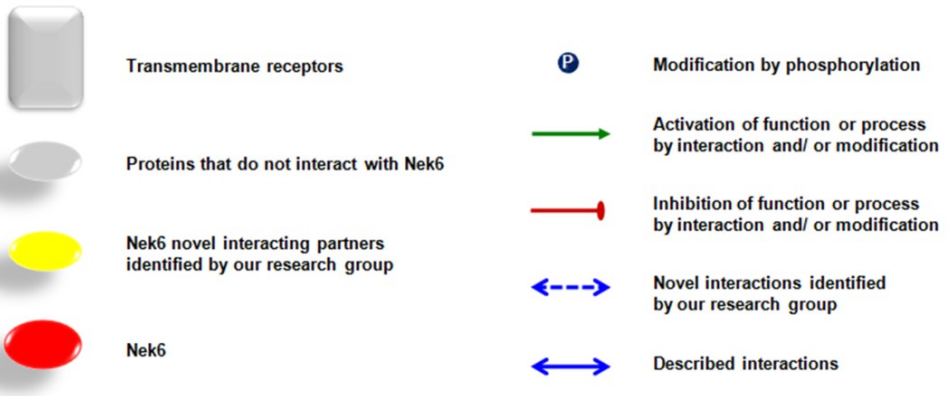
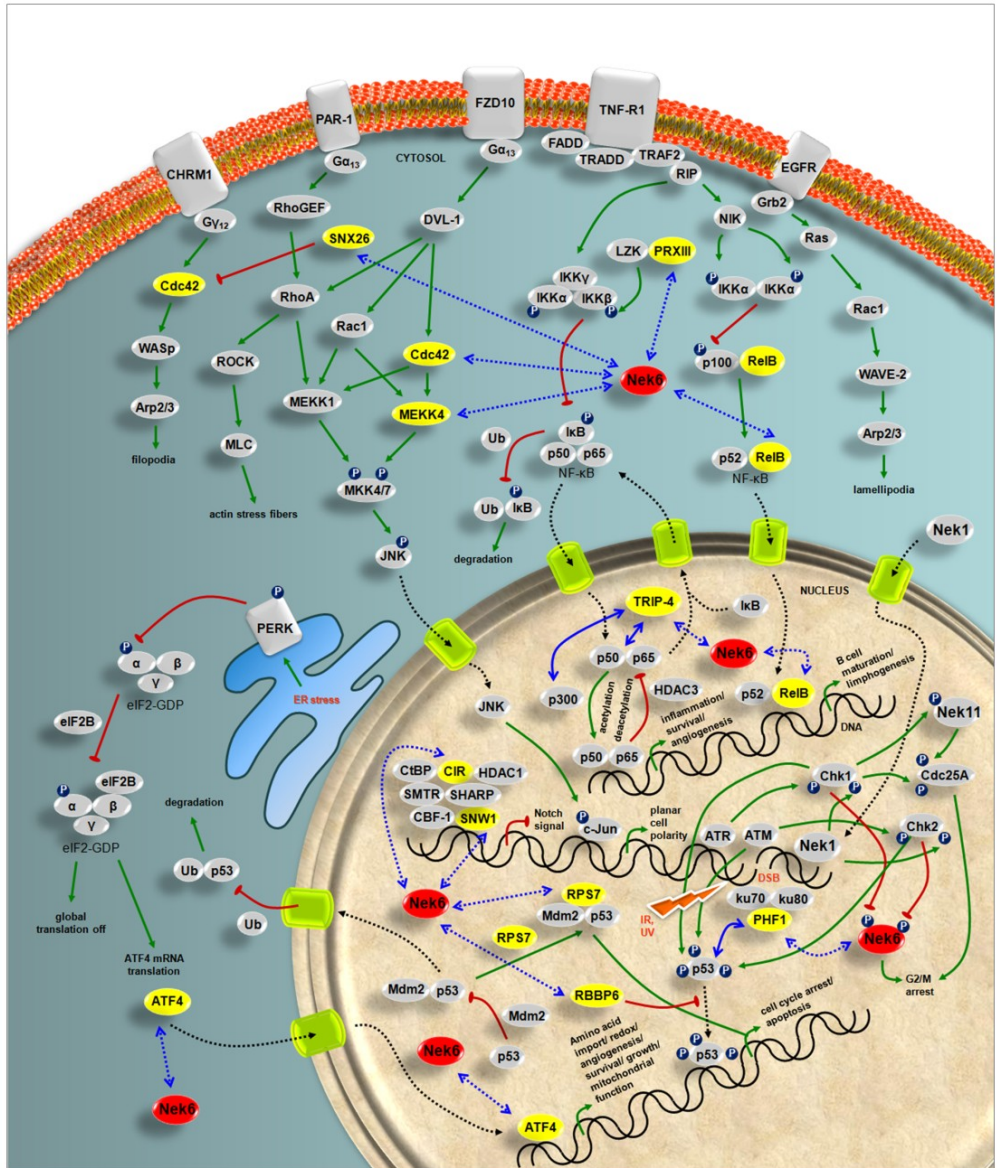


Figura 6. Possíveis vias de sinalização para a hNek6. Vias propostas com base nos novos parceiros de interação da hNek6 identificados em nossos *screenings* de duplo-híbrido em levedura.

Artigo 2:

1. Predições de estrutura secundária, desordem e sítios de fosforilação revelaram que a hNek6 é composta por, aproximadamente, 34% de α -hélices, 12% de fitas- β e 54% de *coils*, e apresenta uma curta região N-terminal desordenada e vários sítios prováveis de fosforilação por outras cinases.
2. Estudo de dicroísmo circular para a proteína recombinante 6xHis-hNek6wt resultou em um espectro típico de proteínas globulares, apresentando um alto conteúdo de α -hélices, estimado em torno de 38,6%, condizente à nossa predição *in silico*.
3. Estudos de SAXS combinados à modelagem molecular por homologia do mutante 6xHis-hNek6(S206A), utilizando-se a estrutura da hNek7 como molde, resultaram em um modelo de baixa resolução para a hNek6, indicando que trata-se de uma proteína monomérica, predominantemente globular, mas levemente alongada, com o domínio N-terminal flexível e desordenado contribuindo para essa conformação. Nesse sentido, e considerando as conclusões obtidas do Artigo 1, o N-terminal da hNek6 poderia funcionar como uma “vara de pesca”, consistindo numa região flexível responsável por mediar a interação da hNek6 com seus parceiros.
4. Ensaios de SEC-MALS analítica confirmaram o caráter monomérico da hNek6 e ainda revelaram variações na conformação da hNek6 dependentes de seu estado de fosforilação, apresentando maior raio de Stokes a variante mais fosforilada, o que sugere que um aumento na fosforilação induz uma mudança estrutural que leva ao aumento na forma ou tamanho aparente da hNek6. Em várias cinases, o *loop* de ativação encontra-se fosforilado em seu estado ativo, estabilizando-as numa conformação aberta e estendida que poderia ser responsável, portanto, por um aumento no raio de Stokes.
5. Ensaios de deslocamento térmico para a hNek6 mostraram uma estabilidade levemente maior para a hNek6 selvagem comparada ao mutante hNek6(S206A), o que pode ser explicado pelo fato de que, em

muitas cinases, a fosforilação do *loop* de ativação causa uma estabilização global da molécula.

Artigo 3:

1. Ensaios de *pull-down in vitro* e co-purificações mostraram que as proteínas Nek1 e Clasp2 interagem com a região C-terminal de Fez1 por meio de regiões *coiled-coil*.
2. Ensaios de imunocitoquímica em células humanas (HEK293) mostraram que Clasp2 (1192-1407) e Nek1 endógena colocalizam e interagem com γ -tubulina em uma região candidata ao centrossomo.
3. Ensaios de imunocitoquímica também mostraram que Fez1 colocaliza com Nek1 endógena e com Clasp2(1192-1407) em células humanas COS-7 e HEK293, respectivamente, de forma pontuada, em uma região perinuclear candidata ao centrossomo, que é uma região já descrita de grande atuação das Neks, e onde Nek6 também colocaliza com vários de seus parceiros de interação (Artigo 1).
4. Clasp2 (1046-1407) é fosforilada por diferentes isoformas de PKC *in vitro* e interage com diferentes isoformas de PKC ativa em nível endógeno, o que indica a fosforilação *in vivo*.

Este projeto direcionou-se, portanto, no sentido de desvendar as características estruturais e funcionais das hNeks 1 e 6, em especial da hNek6, onde buscamos retratar o seu perfil de interações inserido no contexto global do interactoma humano (Artigo 1), bem como caracterizar sua estrutura, quanto ao conteúdo de estrutura secundária, regiões desordenadas, forma tridimensional e estado de oligomerização (Artigo 2). No caso da hNek1, descrevemos sua interação com as proteínas Fez1 e Clasp2 através de seus motivos *coiled-coil*, e colocalização com as mesmas em uma região candidata ao centrossomo (Artigo 3).

Como perspectivas em relação à hNek6, futuros experimentos são necessários para compreender se a fosforilação é importante para os parceiros de interação se ligarem ou colocalizarem com a hNek6. Seria interessante desvendar o momento e a sequência de etapas pelas quais a hNek6 se liga a cada um dos parceiros de interação na célula (por exemplo, a proteína X se liga ao N-terminal da hNek6 no centrossomo,

sendo então fosforilada, e assim por diante). Além disso, dada a importância da hNek6 na regulação de uma variedade de funções celulares através da interação com diversas proteínas descritas neste trabalho, seria interessante determinar se tais interações são estimuladas ou perturbadas em células de câncer. Futuros estudos nesse sentido poderiam fornecer informações relevantes e possíveis implicações no desenho de drogas e em terapias anti-câncer. Além disso, uma busca por possíveis inibidores para a hNek6 encontra-se em andamento, uma vez que esta proteína apresenta um importante papel na tumorigênese (Nassirpour *et al.*, 2010). Ainda nesse contexto, estudos estruturais com resolução atômica são necessários para a hNek6 selvagem e mutante (S206A), na presença de possíveis inibidores e/ou domínios truncados de proteínas que interagem.

No caso da hNek1, nossos dados sugerem que esta cinase deve ser analisada, com maior profundidade, juntamente com Fez1 e Clasp2, no contexto de atividades relacionadas ao citoesqueleto e ao centrôssomo. Ao que tudo indica, Fez1 deve ser um ponto de conexão entre as funções de Nek1 e Clasp2, e a interação entre as três proteínas pode abrir novas possibilidades para o estudo da dinâmica dos microtúbulos e organização dos centrôssomos. Experimentos de fosforilação de Fez1 por Nek1, *in vitro* e *in vivo*, auxiliaria em uma melhor compreensão dos mecanismos de regulação de Fez1 na célula, em paralelo à sua regulação por PKC.

De modo geral, pretendemos nos anos seguintes realizar estudos relacionados à função e estrutura das Neks humanas, no contexto de uma Biologia de Sistemas (*Systems Biology*) aplicada, visando o desenvolvimento de modelos *in silico* para análise das redes de interação das Neks e de possíveis inibidores com potencial para testes pré-clínicos e clínicos. Realizaremos bioensaios *in vitro* e *in vivo* em larga escala, utilizando inibidores a partir de bibliotecas de compostos de origem diversa (comerciais, sintéticos e produtos naturais), além da implementação de uma plataforma de bioinformática e desenvolvimento de ferramentas computacionais fundamentais para integrar um extenso volume de dados (gerado a partir de ensaios de duplo-híbrido, imunoprecipitação de complexos e espectrometria de massa, microarranjo, *high content screening*, etc.), em modelos de redes regulatórias e de comportamento celular, que facilitem a validação de alvos terapêuticos e desenho de drogas.

V. REFERÊNCIAS BIBLIOGRÁFICAS

1. Ahmed S, Thomas G, Ghousaini M, Healey CS, Humphreys MK, Platte R, Morrison J, Maranian M, Pooley KA, Luben R, Eccles D, Evans DG, Fletcher O, Johnson N, dos Santos Silva I, Peto J, Stratton MR, Rahman N, Jacobs K, Prentice R, Anderson GL, Rajkovic A, Curb JD, Ziegler RG, Berg CD, Buys SS, McCarty CA, Feigelson HS, Calle EE, Thun MJ, Diver WR, Bojesen S, Nordestgaard BG, Flyger H, Dörk T, Schürmann P, Hillemanns P, Karstens JH, Bogdanova NV, Antonenkova NN, Zalutsky IV, Bermisheva M, Fedorova S, Khusnutdinova E; SEARCH, Kang D, Yoo KY, Noh DY, Ahn SH, Devilee P, van Asperen CJ, Tollenaar RA, Seynaeve C, Garcia-Closas M, Lissowska J, Brinton L, Peplonska B, Nevanlinna H, Heikkinen T, Aittomäki K, Blomqvist C, Hopper JL, Southey MC, Smith L, Spurdle AB, Schmidt MK, Broeks A, van Hien RR, Cornelissen S, Milne RL, Ribas G, González-Neira A, Benitez J, Schmutzler RK, Burwinkel B, Bartram CR, Meindl A, Brauch H, Justenhoven C, Hamann U; GENICA Consortium, Chang-Claude J, Hein R, Wang-Gohrke S, Lindblom A, Margolin S, Mannermaa A, Kosma VM, Kataja V, Olson JE, Wang X, Fredericksen Z, Giles GG, Severi G, Baglietto L, English DR, Hankinson SE, Cox DG, Kraft P, Vatten LJ, Hveem K, Kumle M, Sigurdson A, Doody M, Bhatti P, Alexander BH, Hooning MJ, van den Ouweland AM, Oldenburg RA, Schutte M, Hall P, Czene K, Liu J, Li Y, Cox A, Elliott G, Brock I, Reed MW, Shen CY, Yu JC, Hsu GC, Chen ST, Anton-Culver H, Ziogas A, Andrulis IL, Knight JA; kConFab; Australian Ovarian Cancer Study Group, Beesley J, Goode EL, Couch F, Chenevix-Trench G, Hoover RN, Ponder BA, Hunter DJ, Pharoah PD, Dunning AM, Chanock SJ, Easton DF. (2009)

- Newly discovered breast cancer susceptibility loci on 3p24 and 17q23.2. *Nat Genet.* 41(5): 585-90.
2. Barbagallo F, Paronetto MP, Franco R, Chieffi P, Dolci S, Fry AM, Geremia R, Sette C. (2009) Increased expression and nuclear localization of the centrosomal kinase Nek2 in human testicular seminomas. *J Pathol.* 217(3): 431-41.
 3. Barr FA, Sillje HH, Nigg EA. (2004) Polo-like kinases and the orchestration of cell division. *Nat Rev Mol Cell Biol.* 5: 429-440.
 4. Belham C, Roig J, Caldwell JA, Aoyama Y, Kemp BE, Comb M, Avruch J. (2003) A mitotic cascade of NIMA family kinases. Ncc1/Nek9 activates the Nek6 and Nek7 kinases. *J Biol Chem.* 278: 34897-34909.
 5. Bergen LG, Upshall A, Morris NR. (1984) S-phase, G2, and nuclear division mutants of *Aspergillus nidulans*. *J Bacteriol.* 159: 114-119.
 6. Bowers AJ, Boylan JF. (2004) Nek8, a NIMA family kinase member, is overexpressed in primary human breast tumors. *Gene.* 328: 135-42.
 7. Capra M, Nuciforo PG, Confalonieri S, Quarto M, Bianchi M, Nebuloni M, Boldorini R, Pallotti F, Viale G, Gishizky ML, Draetta GF, Di Fiore PP. (2006) Frequent alterations in the expression of serine/threonine kinases in human cancers. *Cancer Res.* 66(16): 8147-54.
 8. Carmena M, Earnshaw WC. (2003) The cellular geography of aurora kinases. *Nat Rev Mol Cell Biol.* 4: 842-854.
 9. Chen J, Li L, Zhang Y, Yang H, Wei Y, Zhang L, Liu X, Yu L. (2006) Interaction of Pin1 with Nek6 and characterization of their expression correlation in Chinese hepatocellular carcinoma patients. *Biochem Biophys Res Commun.* 341(4): 1059-65.

10. Chen Y, Riley DJ, Zheng L, Chen PL, Lee WH. (2002) Phosphorylation of the mitotic regulator protein Hec1 by Nek2 kinase is essential for faithful chromosome segregation. *J Biol Chem.* 277(51): 49408-16.
11. de Vos S, Hofmann WK, Grogan TM, Krug U, Schrage M, Miller TP, Braun JG, Wachsman W, Koeffler HP, Said JW. (2003) Gene expression profile of serial samples of transformed B-cell lymphomas. *Lab Invest.* 83(2): 271-85.
12. Fry AM, Schultz SJ, Bartek J, Nigg EA. (1995) Substrate specificity and cell cycle regulation of the Nek2 protein kinase, a potential human homolog of the mitotic regulator NIMA of *Aspergillus nidulans*. *J Biol Chem.* 270(21): 12899-905.
13. Fry AM, Arnaud L, Nigg EA. (1999) Activity of the human centrosomal kinase, Nek2, depends on an unusual leucine zipper dimerization motif. *J Biol Chem.* 274(23): 16304-10.
14. Fry AM. (2002) The Nek2 protein kinase: a novel regulator of centrosome structure. *Oncogene.* 21(40): 6184-94.
15. Greenman C, Stephens P, Smith R, Dalgliesh GL, Hunter C, Bignell G, Davies H, Teague J, Butler A, Stevens C, Edkins S, O'Meara S, Vastrik I, Schmidt EE, Avis T, Barthorpe S, Bhamra G, Buck G, Choudhury B, Clements J, Cole J, Dicks E, Forbes S, Gray K, Halliday K, Harrison R, Hills K, Hinton J, Jenkinson A, Jones D, Menzies A, Mironenko T, Perry J, Raine K, Richardson D, Shepherd R, Small A, Tofts C, Varian J, Webb T, West S, Widaa S, Yates A, Cahill DP, Louis DN, Goldstraw P, Nicholson AG, Brasseur F, Looijenga L, Weber BL, Chiew YE, DeFazio A, Greaves MF, Green AR, Campbell P, Birney E, Easton DF, Chenevix-Trench G, Tan MH, Khoo SK, Teh BT, Yuen ST,

- Leung SY, Wooster R, Futreal PA, Stratton MR. (2007) Patterns of somatic mutation in human cancer genomes. *Nature*. 446(7132): 153-8.
16. Hilton LK, White MC, Quarmby LM. (2009) The NIMA-related kinase NEK1 cycles through the nucleus. *Biochem Biophys Res Commun*. 389(1): 52-6.
17. Holland PM, Milne A, Garka K, Johnson RS, Willis C, Sims JE, Rauch CT, Bird TA, Virca GD. (2002) Purification, cloning and characterization of Nek8, a novel NIMA-related kinase, and its candidate substrate Bicd2. *J Biol Chem*. 277: 16229-16240.
18. Hubbard SR. (1997) Crystal structure of the activated insulin receptor tyrosine kinase in complex with peptide substrate and ATP analog. *EMBO J*. 16: 5572–5581.
19. Hubbard SR, Wei L, Ellis L, Hendrickson WA. (1994) Crystal structure of the tyrosine kinase domain of the human insulin receptor. *Nature*. 372: 746-754.
20. Huse M, Kuriyan J. (2002) The conformational plasticity of protein kinases. *Cell* 109(3): 275-82.
21. Jackman M, Lindon C, Nigg EA, Pines J. (2003) Active cyclin B1-Cdk1 first appears on centrosomes in prophase. *Nat Cell Biol*. 5(2): 143-148.
22. Kim S, Lee K, Rhee K. (2007) NEK7 is a centrosomal kinase critical for microtubule nucleation. *Biochem Biophys Res Commun*. 360(1): 56-62.
23. Kokuryo T, Senga T, Yokoyama Y, Nagino M, Nimura Y, Hamaguchi M. (2007) Nek2 as an effective target for inhibition of tumorigenic growth and peritoneal dissemination of cholangiocarcinoma. *Cancer Res*. 67(20): 9637-42.
24. Landi MT, Dracheva T, Rotunno M, Figueroa JD, Liu H, Dasgupta A, Mann FE, Fukuoka J, Hames M, Bergen AW, Murphy SE, Yang P, Pesatori AC, Consonni D, Bertazzi PA, Wacholder S, Shih JH, Caporaso NE, Jen J. (2008)

- Gene expression signature of cigarette smoking and its role in lung adenocarcinoma development and survival. *PLoS One*. 3(2): e1651.
25. Letwin K, Mizzen L, Motro B, Ben-David Y, Bernstein A, Pawson T. (1992) A mammalian dual specificity protein kinase, Nek1, is related to the NIMA cell cycle regulator and highly expressed in meiotic germ cells. *EMBO J*. 11: 3521-3531.
 26. Liu S, Lu W, Obara T, Kuida S, Lehoczky J, Dewar K, Drummond IA, Beier DR. (2002) A defect in a novel Nek-family kinase causes cystic kidney disease in the mouse and in zebrafish. *Development*. 129(24): 5839-46.
 27. Lu KP, Kemp BE, Means AR. (1994) Identification of substrate specificity determinants for the cell-cycle-regulated NIMA protein kinase. *J Biol Chem*. 269: 6603-6607.
 28. Lu KP, Hunter T. (1995) Evidence for a NIMA-like mitotic pathway in vertebrate cells. *Cell*. 81: 413-24.
 29. Malumbres M, Barbacid M. (2007) Cell cycle kinases in cancer. *Curr Opin Genet Dev*. 17: 60-65.
 30. McHale K, Tomaszewski JE, Puthiyaveetil R, Livolsi VA, Clevenger CV. (2008) Altered expression of prolactin receptor-associated signaling proteins in human breast carcinoma. *Mod Pathol*. 21(5): 565-71.
 31. Miller SL, DeMaria JE, Freier DO, Riegel AM, Clevenger CV. (2005) Novel association of Vav2 and Nek3 modulates signaling through the human prolactin receptor. *Mol Endocrinol*. 19(4): 939-49.
 32. Morris NR. (1975) Mitotic mutants of *Aspergillus nidulans*. *Genet Res*. 26(3): 237-254.

33. Nassirpour R, Shao L, Flanagan P, Abrams T, Jallal B, Smeal T, Yin MJ. (2010) Nek6 Mediates Human Cancer Cell Transformation and Is a Potential Cancer Therapeutic Target Mol Cancer Res. 8(5): 717-28.
34. Nigg EA. (2001) Mitotic kinases as regulators of cell division and its checkpoints. Nat Rev Mol Cell Biol. 2: 21-32.
35. Noble ME, Endicott JA, Johnson LN. (2004) Protein kinase inhibitors: insights into drug design from structure. Science. 303: 1800-1805.
36. Noguchi K, Fukazawa H, Murakami Y, Uehara Y. (2002) Nek11, a new member of the NIMA family of kinases, involved in DNA replication and genotoxic stress responses. J Biol Chem. 277(42): 39655-65.
37. Noguchi K, Fukazawa H, Murakami Y, Uehara Y. (2004) Nucleolar Nek11 is a novel target of Nek2A in G1/S-arrested cells. J Biol Chem. 279(31): 32716-27.
38. O'Connell MJ, Krien MJ, Hunter T. (2003) Never say never. The NIMA-related protein kinases in mitotic control. Trends Cell Biol. 13(5): 221-8.
39. O'regan L, Blot J, Fry AM. (2007) Mitotic regulation by NIMA-related kinases. Cell Div. 2: 25.
40. Osmani AH, McGuire SL, Osmani SA. (1991) Parallel activation of the NIMA and p34^{cdc2} cell cycle-regulated protein kinases is required to initiate mitosis in *A. nidulans*. Cell J. 67: 283-291.
41. Osmani SA, May GS, Morris NR. (1987) Regulation of the mRNA levels of nimA, a gene required for the G2-M transition in *Aspergillus nidulans*. J Cell Biol. 104: 1495-1504.
42. Osmani SA, Pu RT, Morris NR. (1988) Mitotic induction and maintenance by overexpression of a G2-specific gene that encodes a potential protein kinase. Cell. 53: 237-244.

43. Polci R, Peng A, Chen PL, Riley DJ, Chen Y. (2004) NIMA-Related protein kinase 1 is involved early in the ionizing radiation-induced DNA damage response. *Cancer Res.* 64: 8800-8803.
44. Pu RT, Osmani SA. (1995) Mitotic destruction of the cell cycle regulated NIMA protein kinase of *Aspergillus nidulans* is required for mitotic exit. *EMBO J.* 14: 995-1003.
45. Quarmby LM, Mahjoub MR. (2005) Caught Nek-ing: cilia and centrioles. *J Cell Sci.* 118: 5161-9.
46. Rapley J, Baxter JE, Blot J, Wattam SL, Casenghi M, Meraldi P, Nigg EA, Fry AM. (2005) Coordinate regulation of the mother centriole component nlp by nek2 and plk1 protein kinases. *Mol Cell Biol.* 25(4): 1309-24.
47. Rellos P, Ivins FJ, Baxter JE, Pike A, Nott TJ, Parkinson DM, Das S, Howell S, Fedorov O, Shen QY, Fry AM, Knapp S, Smerdon SJ. (2007) Structure and regulation of the human Nek2 centrosomal kinase. *J Biol Chem.* 282: 6833-6842.
48. Richards MW, O'Regan L, Mas-Droux C, Blot JM, Cheung J, Hoelder S, Fry AM, Bayliss R. (2009) An autoinhibitory tyrosine motif in the cell-cycle-regulated Nek7 kinase is released through binding of Nek9. *Mol Cell.* 36(4): 560-70.
49. Roig J, Mikhailov A, Belham C, Avruch J. (2002) Nercc1, a mammalian NIMA-family kinase, binds the Ran GTPase and regulates mitotic progression. *Genes & Dev.* 16: 1640-1658.
50. Roig J, Groen A, Caldwell J, Avruch J. (2005) Active Nercc1 protein kinase concentrates at centrosomes early in mitosis and is necessary for proper spindle assembly. *Mol Biol Cell.* 16: 4827-4840.

51. Schindler T, Bornmann W, Pellicena P, Miller WT, Clarkson B, Kuriyan J. (2000) Structural mechanism for STI-571 inhibition of Abelson tyrosine kinase. *Science*. 289: 1938-1942.
52. Sohara E, Luo Y, Zhang J, Manning DK, Beier DR, Zhou J. (2008) Nek8 regulates the expression and localization of polycystin-1 and polycystin-2. *J Am Soc Nephrol*. 19(3): 469-76.
53. Songyang Z, Lu KP, Kwon YT, Tsai LH, Filhol O, Cochet C, Brickey DA, Soderling TR, Bartleson C, Graves DJ, DeMaggio AJ, Hoekstra MF, Blenis J, Hunter T, Cantley LC. (1996) A structural basis for substrate specificities of protein ser/thr kinases: primary sequence preference of casein kinase I and II, NIMA, phosphorylase kinase, calmodulin dependent kinase II, cdk5 and erk1. *Mol Cell Biol*. 16: 6486-6493.
54. Surpili MJ, Delben TM, Kobarg J. (2003) *Biochemistry* 42: 15369-15376.
55. Takeno A, Takemasa I, Doki Y, Yamasaki M, Miyata H, Takiguchi S, Fujiwara Y, Matsubara K, Monden M. (2008) Integrative approach for differentially overexpressed genes in gastric cancer by combining large-scale gene expression profiling and network analysis. *Br J Cancer*. 99(8): 1307-15.
56. Tan BC, Lee SC. (2004) Nek9, a novel FACT-associated protein, modulates interphase progression. *J Biol Chem*. 279(10): 9321-30.
57. Tsunoda N, Kokuryo T, Oda K, Senga T, Yokoyama Y, Nagino M, Nimura Y, Hamaguchi M. (2009) Nek2 as a novel molecular target for the treatment of breast carcinoma. *Cancer Sci*. 100(1): 111-6.
58. Upadhyya P, Birkenmeier EH, Birkenmeier CS, Barker JE. (2000) Mutations in a NIMA-related kinase gene, Nek1, cause pleiotropic effects including a

- progressive polycystic kidney disease in mice. *Proc Natl Acad Sci USA*. 97(1): 217-21.
59. Vieth M, Higgs RE, Robertson DH, Shapiro M, Gragg EA, Hemmerle H. (2003) Kinomics-structural biology and chemogenomics of kinase inhibitors and targets. *BBA*. 1697(1-2): 243-57.
60. Vieth M, Sutherland JJ, Robertson DH, Campbell RM. (2005) Kinomics: characterizing the therapeutically validated kinase space. *Drug Discovery Today* 10: 839-846.
61. Wai DH, Schaefer KL, Schramm A, Korsching E, Van Valen F, Ozaki T, Boecker W, Schweigerer L, Dockhorn-Dworniczak B, Poremba C. (2002) Expression analysis of pediatric solid tumor cell lines using oligonucleotide microarrays. *Int J Oncol*. 20(3): 441-51.
62. Westwood I, Cheary DM, Baxter JE, Richards MW, van Montfort RL, Fry AM, Bayliss R. (2009) Insights into the conformational variability and regulation of human Nek2 kinase. *J Mol Biol*. 386: 476-485.
63. White MC, Quarmby LM. (2008) The NIMA-family kinase, Nek1 affects the stability of centrosomes and ciliogenesis. *BMC Cell Biol*. 9: 29.
64. Wu L, Osmani SA, Mirabito PM. (1998) A role for NIMA in the nuclearlocalization of cyclin B in *Aspergillus nidulans*. *J Cell Biol*. 141: 1575-1587.
65. Yissachar N, Salem H, Tennenbaum T, Motro B. (2006) Nek7 kinase is enriched at the centrosome, and is required for proper spindle assembly and mitotic progression. *FEBS Lett*. 580(27): 6489-6495.
66. Ye XS, Xu G, Pu RT, Fincher RR, McGuire SL, Osmani AH, Osmani SA. (1995). The NIMA protein kinase is hyperphosphorylated and activated

downstream of p34cdc2/cyclin B: coordination of two mitosis promoting kinases. *EMBO J.* 14(5): 986-994.

67. Yin MJ, Shao L, Voehringer D, Smeal T, Jallal B. (2003) The serine/threonine kinase Nek6 is required for cell cycle progression through mitosis. *J Biol Chem.* 278(52): 52454-60.

68. Zheng J, Knighton DR, TenEyck LF, Karlsson R, Xuong NH, Taylor SS, Sowadski JM. (1993) Crystal structure of the catalytic subunit of c-AMP-dependent protein kinase complexed with Mg/ATP and peptide inhibitor. *Biochemistry.* 32: 2154–2161.

DECLARAÇÃO

Declaro para os devidos fins que o conteúdo de minha dissertação/tese de Mestrado/Doutorado intitulada Estudos estruturais e funcionais das proteínas cinases humanas Nek1 e Nek6

() não se enquadra no § 3º do Artigo 1º da Informação CCPG 01/08, referente a bioética e biossegurança.

(X) tem autorização da(s) seguinte(s) Comissão(ões) de Bioética ou Biossegurança*:

CIBio (Comissão Interna de Biossegurança da ABTLvS), sob Protocolo(s) nº JK 04.01

* Caso a Comissão seja externa ao IB/UNICAMP, anexar o comprovante de autorização dada ao trabalho. Se a autorização não tiver sido dada diretamente ao trabalho de tese ou dissertação, deverá ser anexado também um comprovante do vínculo do trabalho do aluno com o que constar no documento de autorização apresentado.

Gabriela Vaz Meirelles

Aluno: Gabriela Vaz Meirelles

Jörg Kobarg

Orientador: Jörg Kobarg

Para uso da Comissão ou Comitê pertinente:

() Deferido () Indeferido

Nome:
Função:


Prof. Dr. MARCELO LANCELOTTI
Presidente da Comissão Interna de Biossegurança
Instituto de Biologia - UNICAMP

Formulário de encaminhamento de projetos de pesquisa para análise pela CIBio - Comissão Interna de Biossegurança da ABTLuS – Associação Brasileira de Tecnologia de Luz Síncrotron

Título do projeto: Expressão das proteínas cinases humanas Nek1 e Nek6 para estudos estruturais e funcionais

Pesquisador responsável: Jörg Kobarg

Experimentador: Gabriela Vaz Meirelles

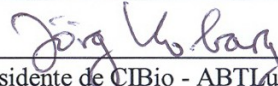
Nível do treinamento do experimentador: []-Iniciação científica, []-mestrado, []-doutorado, [x]-doutorado direto, []-pós-doutorado, []-nível técnico, []-outro, especifique: _____

Resumo do projeto:

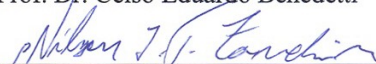
A proteína NIMA (*never in mitosis, gene A*) foi identificada e caracterizada funcionalmente em *Aspergillus nidulans* como sendo uma serina/treonina cinase crítica para a progressão do ciclo celular. Mutações no gene da Nek1, membro humano da família de NIMA cinases, levam ao desenvolvimento da doença renal policística (PKD) e ao aparecimento de diversos efeitos pleiotrópicos, sugerindo sua participação em vias reguladoras de diversos processos celulares. Estudos anteriores do nosso grupo, utilizando o sistema duplo-híbrido, resultaram na identificação de três grupos de proteínas que interagem com o domínio regulatório de Nek1: proteínas envolvidas no reparo de quebras de fita dupla de DNA durante a fase G2/M do ciclo celular, no desenvolvimento do sistema nervoso, e na etiologia da PKD. Em células humanas submetidas à radiação ionizante, Nek1 desloca-se para o núcleo e co-localiza-se com proteínas conhecidas por atuarem no reparo de DNA. Isso sugere seu envolvimento direto na resposta a danos de DNA. Neste projeto, pretendemos realizar a expressão e purificação de Nek1 e Nek6 em larga escala para ensaios biofísicos e de cristalização, visando análises estruturais. Em paralelo, serão realizados estudos funcionais envolvendo o silenciamento (iRNA) da expressão de Nek1 e sua superexpressão em células humanas e a identificação de proteínas que interagem intracelularmente com Nek1 ativada/fosforilada através de espectrometria de massa.

A CIBio analisou este projeto em reunião realizada no dia: 16.4.2007 .

Parecer final: [x]-projeto aprovado, []-projeto recusado, []-projeto com deficiências, favor comentários abaixo:


 Presidente de CIBio - ABTLuS
 Prof. Dr. Jörg Kobarg


 Membro da CIBio - ABTLuS
 Prof. Dr. Celso Eduardo Benedetti


 Membro da CIBio - ABTLuS
 Prof. Dr. Nilson Ivo Tonin Zanchin